ABSTRACT

TAMBE, NISARG MAHESH. Interfacial Phenomena in Glass Fiber Composites. (Under the direction of Dr. Russell E. Gorga and Dr. Jon P. Rust).

Surface interactions between fibers and polymer matrix are known to affect the properties of the composite materials. Glass reinforced polymer composite materials have long been used in the industry for making roofing shingles. The interfacial properties of these composites are governed by the chemical nature and physical compatibility between glass fibers and polymer matrix. There are different surface modification techniques applied to the glass fiber surfaces which aid processing and achieving of optimum composite properties. In this study, we enhanced our understanding of these complex surface interactions by elucidating the effect of different surface modification techniques used on glass fibers during processing and their effect on composite properties.

The effect of different sizing components on the interfacial properties of glass fibers has been studied by varying the ɣ-aminopropyltrimethoxysilane and 1-hydroxyethyl-2-cocoimidazoline concentrations in the sizing to form sized glass fibers containing different amounts of silane and imidazoline components and their corresponding glass composite properties are also studied. We found that the sizing chemistry has a strong influence on the mechanical performance of these composites. The isoelectric point, the pH where the zeta potential of the surface is zero, is useful in predicting the dispersion properties of sized glass fibers in polyelectrolyte. The imidazoline component changes the isoelectric point to neutral pH which is good for fiber dispersion and leads to good composite structure making imidazoline a key component contributing to the mechanical performance. The silane

component changes the isoelectric point to high basic pH which leads to poor fiber dispersion and leads to decrease in the mechanical performance. The silane component distributes uniformly on the sized glass fiber interface while the imidazoline component shows non-uniform distribution with agglomeration at specific locations. Increasing homogeneity of the imidazoline component distribution is a desired outcome that was not recognized.

We also explored the effect of sizing, polyelectrolyte and binder surface treatments on the surface properties of glass fibers and their synergistic interactions. It was observed that the polyelectrolyte treatment covers the sizing chemistry and the corresponding binder treatment covers the polyelectrolyte treatment. The water dynamic contact angle of sized, polyelectrolyte and binder treated glass fibers shows that the sized and binder treated glass fibers show slightly hydrophilic interactions while the polyelectrolyte treated glass fibers show hydrophobic interactions. We also demonstrated that the polyelectrolyte solution wets the sized glass fiber surface during dispersion and the polyelectrolyte completely covers the sized glass surface by non-specific physical adsorption after multiple wetting cycles.

The distribution of urea-formaldehyde modified acrylic polymeric binders on glass mats was also studied. We found out that the binder deposits at the cross points between the glass fibers as well as coats on the single glass fiber surface. The binder deposition is non-uniform throughout the mat surface with little control on the distribution. Also, the binder by itself is hydrophilic in nature but the glass mat coated with binder shows hydrophobic interactions due to the mat structure. With time, wetting of the water droplet on the glass mat demonstrates the hydrophilic nature of the binder present on glass mat.

Interfacial Phenomena in Glass Fiber Composites

by
Nisarg Mahesh Tambe

A dissertation submitted to the Graduate Faculty of
North Carolina State University
in partial fulfillment of the
requirements for the degree of
Doctor of Philosophy

Fiber and Polymer Science

Raleigh, North Carolina

2014

APPROVED BY:

_____	_____
Russell E. Gorga Committee Co-Chair	Jon P. Rust Committee Co-Chair
_____	_____
Julie A. Willoughby	Orlando Rojas

DEDICATION

I dedicate this dissertation to god as well as my parents, grandparents and my wife who have all supported me through everything.

BIOGRAPHY

Nisarg Tambe was born on 16th July, 1987 in India and has lived for 22 years in Mumbai. His parents continue to live in Mumbai and he is married to Rachita Salaria who works as a Speech Pathologist in Raleigh area. He received his Bachelor of Technology (B. Tech) in Fiber and Textile Processing Technology in May 2009 from Institute of Chemical Technology Mumbai, India (formerly known as UDCT). In pursuit of further studies, he joined North Carolina State University in August 2009 for a Master's program in Textile Chemistry. He completed his MS Textile Chemistry in August 2011 under the guidance of Dr. Martin W. King working on his thesis titled "Surface modification techniques for polymeric biomaterials for use as tissue engineering scaffolds". He immediately commenced his PhD program in Fiber and Polymer Science in August 2011. He joined Willoughby research group in the Spring semester 2012 and has since worked on his doctoral dissertation focused on interfacial phenomena in glass fiber composites. Upon completion of his PhD Fiber and Polymer Science, he plans to work in the industry and continue his passion for surface science, biomaterials and polymers.

ACKNOWLEDGMENTS

This dissertation work would not have been completed without the help and support of many people who have been acknowledged here.

First and foremost, I would like to express my sincere gratitude and appreciation to Dr. Julie Willoughby for giving me a chance to join her research group. Her guidance and encouragement throughout my PhD has been invaluable and I greatly appreciate that. Her insights in my research, guidance on experimental work, help in improving my presentation and writing skills are some of the precious assets. Also, I am really grateful to both Dr. Russell Gorga and Dr. Jon Rust who agreed to guide me for the past one year. They have been positively critical while correcting my mistakes and the discussions with them have been amazing. Their smart opinions on my research work have played a huge part in shaping the project. All three of them have been great mentors to me and consider myself fortunate that I could work with them. I also wish to address special thanks to Dr. Orlando Rojas for agreeing to be on my committee and has given valuable suggestions during my preliminary examination for improving my research work.

A heartfelt and sincere thanks goes to GAF Materials Corporation for supporting my project. I have thoroughly enjoyed working with the company and learning about the corporate culture. My special thanks to Thomas Taylor with whom I have had several amazing research discussions and has been an excellent role model. Also, Avi Desai has been very supportive towards me and encouraged me like a mentor. Also, Sami Abounassif and Emily Tenney have been very helpful in providing materials as well as giving insights in my project. Dan

Boss has also been very supportive of the project. The plant visits, research meetings with GAF have provided me valuable industrial experience while working on my dissertation.

I also would want to extend great appreciation to Dr. Martin W. King for being a constant support for the past 5 years. Ever since I have been in Raleigh, he has been a mentor and like a family member for me.

From the Analytical Instrumentation Facility on campus, I would like to thank Dr. Chuanzhen Zhou (Elaine) for her efforts in helping me in analysis and get acclimatized with TOF-SIMS technique. Her experience has helped in solving many research problems. I also want to thank Chuck Mooney and Fred Stevie for their help in SEM and XPS respectively.

I would also like to thank Vinod Radhakrishnan and Gerd Lagenbucher of Anton Paar for helping me setup SurPASS electrokinetic analyzer in our lab as well as for allowing me to use their facility when the analyzer was under repair. I would also like to thank Spencer and Paul at DataPhysics for their help with data analysis, contact angle measurements and solving problems with the instrument. I would also like to thank Chris Dunkley for helping setup and train me on Confocal microscope in our lab. Also, thanks to Judy Elson for helping with lab inventory.

I extend deep appreciation to all my lab mates for helping during the journey and moments we have all shared together - Jing Cao, Kewei Xu, Amsarani Ramamoorthy, Hasan Shahariar, Lu Liu, Farzad Rezaei. Also, thanks to other graduate students in College of Textiles who have helped me and with whom I have shared thoughts on graduate life and future. Special thanks to all TECS faculty members whose courses I have taken which have helped me. I want to acknowledge all the staff members of TECS, especially Traci Figura,

Vicki Stocksdale and Amanda Holbrook for all their help. My gratitude also extends towards all my lovely friends, here in Raleigh and back home in Mumbai, who have been such a big support and source of encouragement during the last 5 years. I have had superb roommates over the years with whom I have shared great moments and continue to have great rapport – Nakul, Tejas, Shreyas, Tejas, Nilya, Mohit, Sherry, Abhay, Abhinav. Also I would like to thank my best friend, Akshay Shukla, who has stood by me and believed in me for the last 16 years. Special thanks go to ETD editor, Erica Cutchins, who puts in lot of time and effort to make our dissertations perfect.

Most importantly, I would like to thank and express my sincere appreciation, love and gratitude to my parents and grandparents back in India, who continue to love, support and encourage me unconditionally throughout my life. Without their confidence and support in me over the years, I would not have made it this far. Also, I am very thankful to my lovely wife, Rachita who has been a pillar of support and love. We began our journey as a married couple in December 2013 and it has since been amazing. You have been and will always be very important to me.

I hope to continue working with passion, honesty, determination and hard work and make all of you proud of my achievements.

TABLE OF CONTENTS

LIST OF TABLES

LIST OF FIGURES

CHAPTER 1

Motivation and Overview

Fiber reinforced polymer composites have seen a rapid rise in the past two decades due to their high strengths, stiffness and light weight as compared to more traditional materials like metals, steel. The synergistic combination of two or more phases in these composites is an important parameter for their superior performance. The synergy is brought about by the interactions between fibers and the polymeric matrix[1]. As most interactions with materials occur at their surface or interface between two materials, an understanding of this behavior at a molecular, microscopic, and macroscopic level is critical to its ultimate end-use. Surface modification of materials allows the ability to tailor material interactions without changing the bulk properties. For instance, surface interactions between glass fibers and a polymer will affect the properties of subsequent composites made with the two components[2]. Depending on the desired application, these interactions may need to be modified from their original behavior. The use of glass fibers as a reinforcement agent in a resinous matrix has shown to improve the mechanical properties of the overall composite[3]. To increase tensile and tear strength of a fiber-polymer composite, it is believed that increasing interfacial adhesion between the fiber and the polymer will increase the composite tensile strength[4]. However, these interactions are complex, and depend on the fiber processing and specific chemistries used to 1) aid manufacture and 2) provide optimum composite properties for a given application.

The words “interphase” and “interface” have been alternatively employed to describe the region between bulk matrix and the fiber. The interphase is a region in which there is chemical and/or mechanical bonding between the fiber and the matrix phases[5]. The interphase dictates the response of a fiber/matrix system as it can form a diffusion zone, nucleation zone or chemical reaction zone or a combination of them. The interface term is used to refer to a two-dimensional border, which separates distinct phases from each other like fiber, matrix, and coating[6]. The interphase region is formed by different interactions like physical mixing of matrix and sizing and the nature of chemisorption at the fiber interface[7]. It also depends upon the physical or thermodynamic compatibility between the fiber and the matrix[8]. A bond formed between the fiber and polymeric matrix may be formed by the interdiffusion of atoms or molecules across the interface[9,10]. The interphase acts like a transition region where the properties vary between the fiber and the matrix[11]. The interphase properties like thickness and composition depend upon the fiber and matrix properties, as well as any treatments on the fiber surface or the matrix. The extent of interfacial bonding influences the material characteristics of the interphase[12]. However, a strong interfacial bonding improves the strength of the material but compromises the material toughness. Fibers are generally surface treated and modified to improve the interphase bond quality. The surface treatments, generally in form of a functional interlayer deposited between fiber and polymer matrix, can improve compatibility and improve the material strength and toughness simultaneously.

For around two decades, glass fiber and their composites have been used in various applications such as roofing materials, aerospace, circuit boards, light weight armor, wind

blades and filtration[13]. E-glass was originally patented by Owens Corning in 1943 for applications which required glass to possess high electrical resistivity[14]. Because of excellent mechanical properties and water durability, the range of applications have grown considerably making E-glass one of the most widely used glass fibers. In this study, we focus on the glass fiber composites used exclusively for roofing shingle application. As it is well known that the interfacial properties are governed by the chemical nature and physical compatibility between the fibers and the matrix, there are different surface modification techniques applied to the glass fiber surfaces to appropriately tune the interface. Silane chemistry has found abundant use in glass fiber processing to form thin films on its surface which has improved its bonding with the polymeric matrix material[15]. Recently, imidazoline chemistry has also been useful in improving the mechanical properties. These chemistries, also known as sizing, have long been utilized in the glass industry. These fibers are then reacted with stiff thermoset polymer matrix to bind them together and subsequently coated with asphalt to form roofing shingles.

This creates a complex surface for the reinforcement comprising glass, sizing and polymer matrix (which for our purposes will be referred to here forward as the "binder"). The interactions between these three surfaces with soft matrices are not very well understood. Also, the different chemistries and their interactions are not fully understood in terms of effects on the glass surface chemistry behavior, the sizing-glass-binder interface, the polymerized network-asphalt interface and subsequent interactions in downstream performance metrics. There is a *gap in the knowledge* with respect to these surface interactions preventing precise tuning of their chemistries for enhanced product performance.

As a result, there is a *critical need* to understand the behavior, stability, and effect of these interactions on composite properties. The *hypothesis* for studying this interfacial phenomenon in glass fiber – polymer composites is that by understanding the surface interactions on glass fibers, the glass-binder interface, the distribution of binder matrix, we can correspondingly tune and improve the processing and downstream properties of the composites. The *rationale* for studying the surface interactions of sizing chemistries and associated interfaces is to combine benefits imparted from each component and understand synergistic effects. Ultimately, this work will help bridge the gap in fundamental understanding of controlling glass-binder interfaces to improve end use applications.

Chapter 2 discusses the glass fiber processing, the sizing system application and the corresponding binder matrices in detail. Silane agents are applied to the glass surface as sizing along with other components to protect the glass fibers during processing and to act as coupling agents to improve adhesion with the binder. The nature and pretreatment of the substrate, the chemistry of silane and the silane layer thickness on the glass fiber are some of the parameters which define the effectiveness of this treatment are discussed along with thermoset resins which have found great popularity as binders in glass composite application.

The different surface interactions at the interface formed between the sizing and the glass fibers are studied in Chapter 3. The sizing contains silane coupling agent, a polymeric film former and imidazolines or fatty acids. The combined behavior of the sizing components is not well understood. The effect of two different components within the sizing formulation was studied to understand their individual effects on the interface properties. Four different silane levels and imidazoline levels were used to make different sizing formulations to study

the effect of the two components. The silane used in the formulation in this study was ɣ-aminopropyltriethoxysilane (known as A-1100) and the imidazoline used was hydroxyethyl imidazoline. We demonstrate that the change in the sizing chemistry causes changes in the interface properties of the glass fibers and each component has different effect of the surface properties of glass fibers. The silane and imidazoline chemistries also affect the mechanical performance of the composites.

Chapter 4 further explores the effects of sizing and polyelectrolyte treatments on the surface chemistry of glass fibers as well as the interactions between sized glass fibers and polyelectrolyte solution. We use Time-of-flight secondary ion mass spectrometry (TOF-SIMS) to compare the effect of different surface treatments on surface composition of glass fibers and identify particular ions for treatment. The surface interactions are studied by understanding the wetting properties of these individual glass fibers. The wettability of fiber surfaces towards a liquid is a critical parameter in determining their interaction during processing. The distribution of polymeric binder on the surface of glass fiber mats is studied in Chapter 5. The distribution of binder on surface of glass mats is an important factor in maintaining uniform mat properties during production. The control over binder deposition on the mat still invokes much debate within the industry. TOF-SIMS is an important surface characterization technique which provides useful information to identify binder adhesion and define binder distribution characteristics in glass mats. We found that the binder deposits at the cross points of fibers as well as a thin coating on the single glass fiber surface.

Our research work is a unique and transformative approach to understanding surface interactions occurring between three components: 1) sizing distribution on glass fibers, 2)

processing treatments for mat formation, and 3). distribution of binder on the surface of the glass mats. The expected outcomes will enable robust process chemistry for the glass composite industry by gaining control over the glass fiber surface and downstream properties of the composites. This project aims to determine the fundamental factors that dictate various properties which can help industry develop more robust process chemistry, design more cost-effective products with higher performance, and ultimately increase profits and quality.

References

1. Berg, J.; Jones, F. R. The role of sizing resins, coupling agents and their blends on the formation of the interphase in glass fibre composites. *Composites Part A: Applied Science and Manufacturing* **1998**, *29*, 1261-1272.

2. Tanoglu, M.; McKnight, S. H.; Palmese, G. R.; Gillespie Jr, J. W. The effects of glass-fiber sizings on the strength and energy absorption of the fiber/matrix interphase under high loading rates. *Composites Sci. Technol.* **2001**, *61*, 205-220.

3. Cech, V.; Prikryl, R.; Balkova, R.; Vanek, J.; Grycova, A. The influence of surface modifications of glass on glass fiber/polyester interphase properties. *Journal of Adhesion Science & Technology* **2003**, *17*, 1299.

4. Gao, S. L.; Mäder, E.; Plonka, R. Coatings for glass fibers in a cementitious matrix. *Acta Materialia* **2004**, *52*, 4745-4755.

5. Sharpe, L. H. The Interphase in Adhesion. *The Journal of Adhesion* **1972**, *4*, 51-64.

6. Swain, R. E.; Reifsnider, K. L.; Jayaraman, K.; El-Zein, M. Interface/Interphase Concepts in Composite Material Systems. *Journal of Thermoplastic Composite Materials* **1990**, *3*, 13-23.

7. Tripathi, D.; Chen, F.; Jones, F. In *In A pseudo-energy based method to predict fiber-matrix adhesion using a single filament composite;* Tenth International Conference on Composite Materials. VI. Microstructure, Degradation, and Design; 1995; , pp 689-696.

8. Rot, K.; Huskić, M.; Makarovič, M.; Ljubič Mlakar, T.; Žigon, M. Interfacial effects in glass fibre composites as a function of unsaturated polyester resin composition. *Composites Part A: Applied Science and Manufacturing* **2001**, *32*, 511-516.

9. Ishida, H.; Koenig, J. L. Fourier transform infrared spectroscopic study of the structure of silane coupling agent on E-glass fiber. *J. Colloid Interface Sci.* **1978**, *64*, 565-576.

10. Ishida, H.; Koenig, J. L. A fourier-transform infrared spectroscopic study of the hydrolytic stability of silane coupling agents on E-glass fibers. *Journal of Polymer Science: Polymer Physics Edition* **1980**, *18*, 1931-1943.

11. Feih, S.; Thraner, A.; Lilholt, H. Tensile strength and fracture surface characterisation of sized and unsized glass fibers. *J. Mater. Sci.* **2005**, *40*, 1615-1623.

12. Kim, J.; Sham, M.; Wu, J. Nanoscale characterisation of interphase in silane treated glass fibre composites. *Composites Part A: Applied Science and Manufacturing* **2001**, *32*, 607-618.

13. Stickel, J. M.; Nagarajan, M. Glass Fiber-Reinforced Composites: From Formulation to Application. *International Journal of Applied Glass Science* **2012**, *3*, 122-136.

14. Li, X.; Bhushan, B.; McGinnis, P. B. Nanoscale mechanical characterization of glass fibers. *Mater Lett* **1996**, *29*, 215-220.

15. Olmos, D.; González-Benito, J. Visualization of the morphology at the interphase of glass fibre reinforced epoxy-thermoplastic polymer composites. *European Polymer Journal* **2007**, *43*, 1487-1500.

CHAPTER 2

Interfacial properties in sized glass fiber and their role in polymer matrix adhesion

2.1. Glass composite processing

Glass fibers are among the most versatile industrial materials in application today. They can be easily produced from raw materials, which are available in abundant supply. They have valuable properties as a result of their geometric shape and uniqueness of the glass itself[1]. They exhibit useful bulk properties like hardness, transparency, stability, inertness, and resistance to chemicals. They also are a sustainable resource and exhibit desirable fiber properties like strength, stiffness, and flexibility. These properties have made them popular in a wide-range of special purpose products like structural composites, circuit boards, optical cables and other reinforcement applications[2]. Glass reinforced polymer composites are high volume, commodity materials which have a huge and an increasing demand[3]. Roofing shingles are of specific interest in this study for use of these glass fiber based composites.

Figure 2.1 shows the overall processing for asphalt roofing shingle, which are of prime importance in the present study. The production of asphalt shingles is a semi-continuous process in most companies. The glass manufacturing involves glass fiberization and sizing application. Some companies manufacture their own glass fibers while some of them directly buy sized glass fibers. These sized glass fibers are dispersed to form wet web and are further treated with binder to form glass mats. The mat formation is a continuous process and these

glass mats are taken to different plant/location for asphalt application to produce roofing shingles.

Figure 2.1. Glass Composite processing for roofing shingle application. Our focus for the proposed work is on the sized fibers, dispersion, mat formation and deposition of binder.

2.1.1. Glass fiberization

The glass fibers are made from a variety of different combinations of glass forming oxides such as silica (SiO_2), B_2O_3, P_2O_5, GeO_2. Most of the commercial glass fibers mainly comprise silica in combination with other oxides. Depending upon the type, amounts of glass forming and non-glass forming oxides added to silica, a range of different glasses are produced with different properties[4].

There are different types of glass fibers available in the market which can be broadly classified into general-purpose and special-purpose glass fibers. The general-purpose glass fibers are E-glass, which refers to low electrical conductivity and are commonly produced glasses for reinforcement applications. Due to environment restrictions and stringent government regulations, much of the commercial E-glass fibers are produced without boron in its oxides. The special purpose glass fibers have different letter designations assigned to

them having different meanings as shown in **Table 2.1**. The S-glass fiber is the pure silica fiber, which has the highest strength and stiffness properties for such applications as lightweight armors. The A-glass is a soda-lime-silica glass, which is similar to the common bottle glass and resists alkali while the C-glass is acid resistant and is used as battery plate separators.

Table 2.1. Commonly used glass fiber types in industry

Designation	Property or Characteristics
E	Low electrical conductivity
S	High strength
C	High chemical durability
M	High stiffness
A	High alkali or soda lime glass
D	Low dielectric constant

The glass manufacturing process is integral for understanding the processing of glass-reinforced composites. Glass fibers are manufactured by rapidly cooling the melt of different oxides such that there is no crystallization occurring thus forming an amorphous solid. If the melt is cooled slowly, crystallization can occur at a temperature known as the "Liquidus temperature (T_L)"[5,6]. The amorphous structure and the resistance of glass melt to crystallize allow the glass to be drawn into fibers. The glass forming ability of the melt can be

determined by the time-temperature-transformation (TTT) curve as shown in **Figure 2.2**. This curve helps to predict the formability and stability of glass formation[7,8]. To obtain an amorphous glass material, the liquid should be cooled fast enough to avoid intersecting the curve at a rate known as the minimum cooling rate (R_c). Thus, crystallization occurs between T_g and T_L and can be avoided by cooling the melt at a rate above R_c[9].

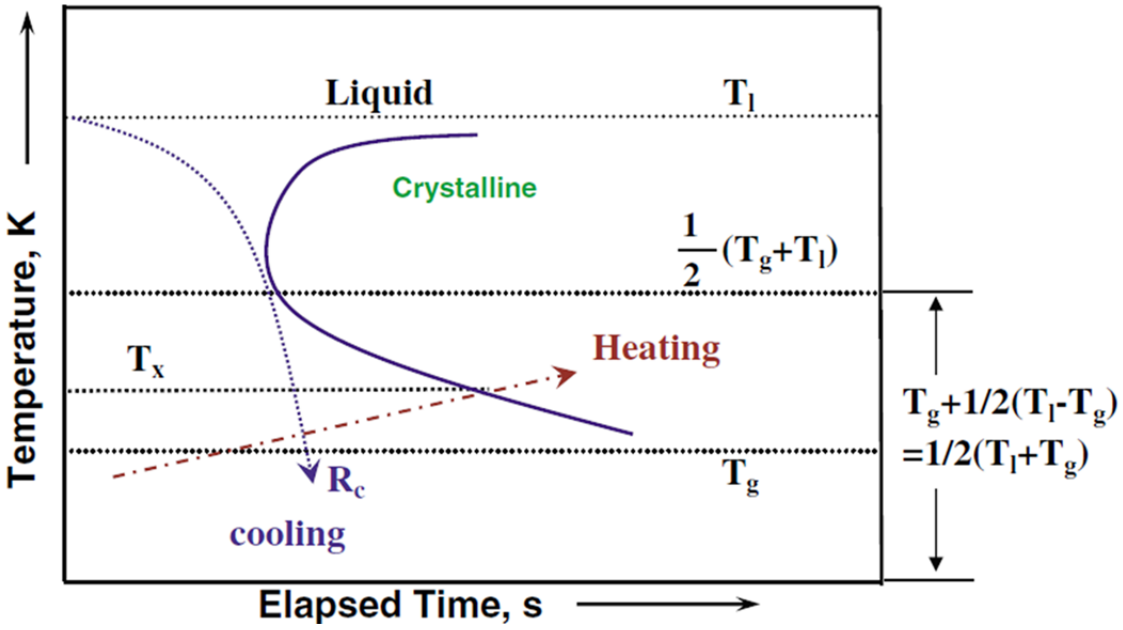

Figure 2. 2. Time-temperature-transformation curve for glass formation. Use of Rc cooling curve avoids formation of crystalline phase during glass formation[8]

The glass can be thought of as a network of silica and the other glass oxides aid in the melting and other fiber formation processes. The glass formation process is exhibited in **Figure 2.3**. The selected raw materials are weighed and blended together and are transported

to the furnace. The glass melt is formed in the furnace at high temperatures (generally around 1400^{o}C), the gaseous inclusions are removed and the melt is thoroughly homogenized. The temperatures in this process are governed by the type and amount of various oxides used for the glass fiber production. In addition, the melt viscosity of a specific glass formulation can vary; where process temperature can be adjusted to ensure consistent process melt viscosity. This homogenized melt is then passed through the refiner section where the temperature is lowered and passed into a forehearth for glass fiber formation. The glass-melt then flows through heated bushings with large number of holes. The fibers are then drawn and rapidly cooled on exiting the bushings. The cooling rate can dictate the glass network formation and the glass fiber properties[10,11].

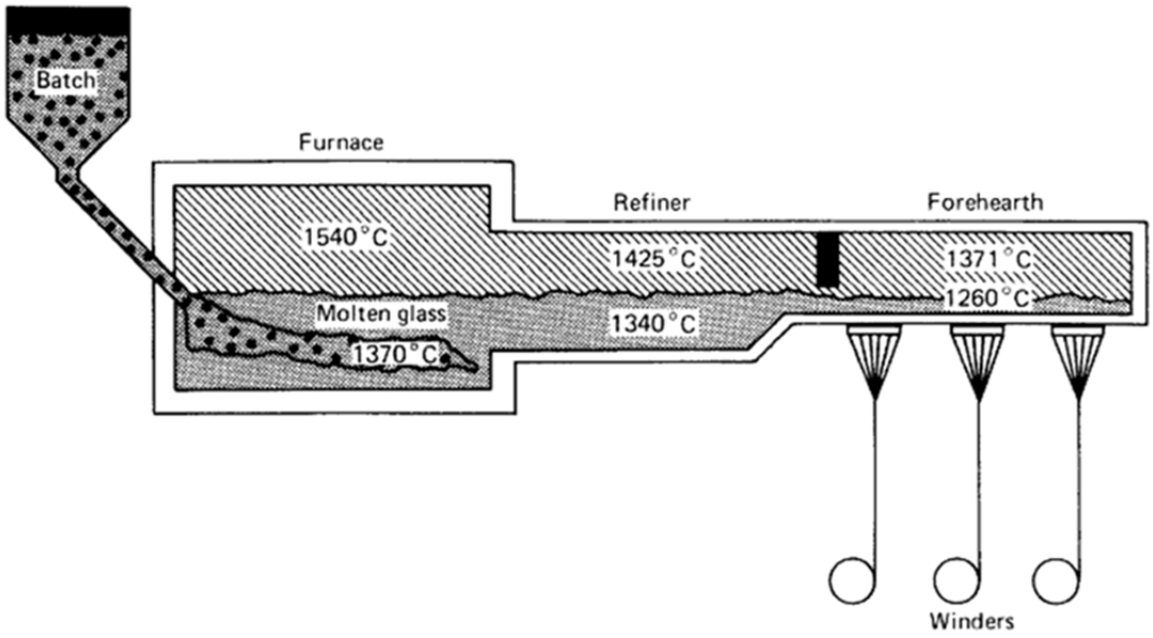

Figure 2. 3. Glass melting and fiber formation process

2.1.2. Sizing

Once the glass fibers are formed, they are passed through an applicator where a sizing is applied on their surface. The applicator rotates in the sizing bath to maintain a thin film formation of the size on the glass fiber surface. The sizing application improves the integrity and lubrication properties of the glass fibers as well as improves the resin compatibility and adhesion of glass fibers for the composite matrix. They also help protect the glass fibers from each other during processing and handling[12]. The sizing generally consists of silane coupling agent, imidazolines, film formers, and lubricants. The formulation depends on the type of bonding matrix used in the composite[13]. After the sizing application, the fibers are dried and can be wound together in different forms like strands, sliver, and rovings.

2.1.3. Glass mat formation

The glass fiber composites are predominantly based on E-glass fibers with a wide variety of fiber formats such as mats, fabrics, rovings; binder types and additives; and a wide range of processing techniques[14]. The glass fiber composites are also known as glass fiber mats where small bundles of glass fibers are bound by polymeric binder. Many methods are known for producing these glass mats for use in a variety of applications. The two well-known methods are wet-laid and dry-laid processing. The glass fibers in the form of strand or sliver or a rove are used here. In wet-laid processing, the glass fibers are chopped into required fiber length and are introduced into the slurry with agitation to disperse the fibers finely. The glass fibers are dispersed in slurry, which contains surfactants, polyelectrolytes, defoaming agents, and viscosity modifiers. The fibers along with the slurry are deposited along a moving screen to remove the excess water and form a web-like structure. The binder is then spray applied onto

this web and the resulting mat is then passed through drying and curing cycles to remove water and cure the binder respectively. The resulting glass mats exhibit uniform fiber distribution and consistent mat weight distribution. In a dry-laid process, the glass fibers are chopped and air-blown onto a conveyor belt and a binder is then applied to form a mat. This process forms mats with open porous structures with minimal glass fiber volume. However, they produce mats with non-uniform weight distribution and are also expensive to produce. They need separate steps for drying and packaging before the chopping step while in the wet-laid process the sized fibers are directly chopped[15]. Vaidya et. al[16] produced a nonwoven preform for composites using blends of glass and low melt polyester. They used hydroentanglement to form wet-lay webs, which acted as nonwoven preforms that were then compression molded to form composites. This decoupled the sheet formation from composite manufacture and provided additional strength and integrity to these wet-laid mats.

2.2. Glass – size interface properties

Silane agents are applied to the glass surface as sizing along with other components to protect the glass fibers during processing and to act as coupling agents to improve adhesion with the polymeric binder. An established view of the interfacial adhesion mechanism is interdiffusion and formation of an interpenetrating network at the interphase region[17]. The number of interactions between the silane and the glass fiber surface can complicate the interphase region. Jones suggested that the sizing components dissolve in the surrounding polymeric matrix and the silane migrates to the fiber surface. Depending upon the ability of the silane to interdiffuse and react with the bulk matrix, the thickness of the interphase changes[18]. This makes the selection of the silane and the polymer matrix crucial. Also, the

interphase properties dictate the overall mechanical behavior of the composite making it a region of great interest[19].

Organofunctional silanes are the most commonly used coupling agents in the glass composite industry. The nature and pretreatment of substrate, the chemistry of silane and the silane layer thickness on the glass fiber are some of the parameters which define the effectiveness of this treatment. A variety of different mechanisms have been proposed to explain the functioning of silanes at the interface[20]. The key factors from the data obtained for proposed mechanism are as follows[21]:

- The chemical reactivity of the organofunctional silanes to form covalent bonds with the polymer matrix
- The bond formation at the interface
- The ability of polymer matrix to diffuse in the siloxane interphase to form an interpenetrating polymer network

Among the organofunctional silanes, alkoxysilanes are one of the most widely used. The reactions and bonding mechanism of the alkoxysilanes is depicted in **Figure 2.4**. The reaction and bonding mechanisms of alkoxysilanes is well documented in the literature[22]. The silanes are hydrolyzed and are then condensed on the glass fiber surface. Ideally, hydrolysis and condensation lead to the formation of a thin siloxane layer on glass surface via hydrogen bonding. The hydrolysis is an acid catalyzed reaction while the condensation is base catalyzed reaction. The rate of the formation of the siloxane layer depends upon the rates of hydrolysis and condensation reactions. The functional group is available for reaction with the polymeric matrix. Ishida and Koeng[23] reported a reduction in the amount of silane

present on the glass fibers during soaking with hot water as a result of hydrolytic degradation of silane. The siloxane bonds which were formed due to hydrolysis of silane were reformed back to silanols.

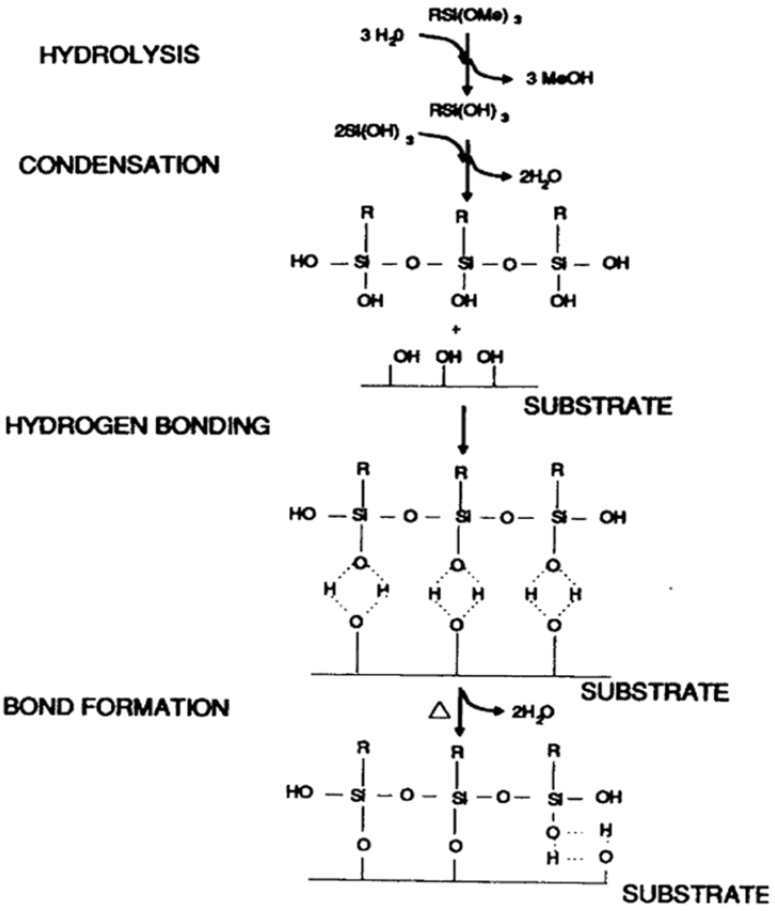

Figure 2. 4. Reaction and bonding of alkoxysilanes. Alkoxysilanes are initially hydrolyzed and condensed on the glass fiber surface to form a siloxane layer via hydrogen bonding mechanism[22].

The chemistry of silane coupling agents plays an important role in influencing the bonding mechanism and interface properties in glass fiber composites and is well documented in the literature. Aminofunctional silane coupling agents have shown unique solution properties and rapid hydrolyzation in water. Chiang et al.[24] showed that aminopropyltriethoxysilane (APTES) adsorbed on the e-glass fiber surface as a multilayer and predominantly formed a cyclic ring structure in the coupling agent interphase. Naviroj et al.[25] demonstrated the unique properties of the APTES adsorption on e-glass fiber depended on the pH of the solution and its structure in the solution. Ishida et al.[26] showed that the amine groups in APTES are mutually hydrogen bonded before hydrolyzation and are free or interacting with water molecules after condensation in aqueous solution. Laura et al.[27] studied the effect of silane chemistry on mechanical properties of glass fiber reinforced composites of Nylon 6 and its blends of maleated ethylene-propylene rubber (EPR-g-MA). When 20% EPR-g-MA was used in the blend for composite formation, the anhydride silane produced highest yield strength while amine silane produced the least because of the extent of adhesion between glass fibers and the matrix. The anhydride silane treated glass fibers appeared bound to the polymer matrix while most of the amine silane treated glass fibers were unbound. Park Soo-Jin et. al.[28] demonstrated the effect of silane chemistry on hydrogen bonding and interlaminar strength. They found that methacryloxypropyltrimethoxysilane treated glass fibers showed increased surface free energy and improved interlaminar strength of composite while glycidoxypropyltrimethoxysilane showed low surface free energy and strengths similar to untreated glass composites. The increase is surface energy was a resultant of increased

hydrogen bonding between glass fiber and silane coupling agent which leads to an increase in the bonding between fiber and polymer matrix.

The microscopic properties of the silane coupling agent at the interface have a profound effect on the performance of the composites. Shokoohi et. al.[29] have listed various theories developed for understand the bonding mechanism of the coupling agents – chemical bonding theory, deformable layer theory, friction coefficient theory, selective absorbance theory, restrained layer theory, interpenetrating network theory. Pape et al.[22] illustrated the concept of the polymer/siloxane/glass interphase where a monolayer of hydrogen bonds connects a rigid polymer and siloxane network as shown in **Figure 2.5**. The glass surface is connected by a monomolecular layer of hydrogen bonds to a rigid polymer/siloxane interphase of the order of 15 – 5000 Å.

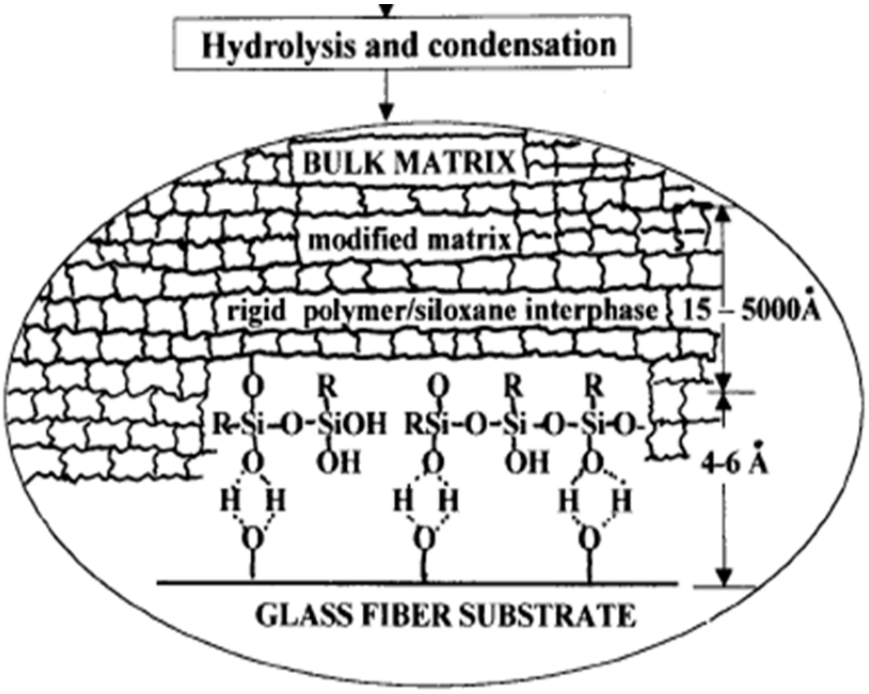

Figure 2. 5. Glass/Siloxane/Polymer Interphase formation[22]

The mechanical properties of the glass fiber reinforced composites are dependent upon the stability of the interfacial region between glass fibers and the polymeric binder. Since glass fibers are hygroscopic, durability is one of the prime concerns for roofing shingle manufacturers because environmental factors such as temperature, humidity, moisture can cause degradation in interfacial adhesion properties. Untreated glass fiber surfaces used in reinforced composites are susceptible to degradation of mechanical properties under wet conditions because of loss of interfacial adhesion and decrease in tensile strength of the fibers. Thus, the bonding properties at the sizing – glass interface are significant in controlling the mechanical properties of the composite[30]. The effects of certain silane coupling agents on composite properties for specific polymer binders have been well

documented in literature. Wu et al.[31] demonstrated that the flexural strength of the E-glass fiber reinforced polyester resin was directly proportional to the interfacial strength which is governed by the amount of aminopropyltriethoxysilane adsorbed on the glass fiber surface during sizing application as illustrated in **Figure 2.6**.

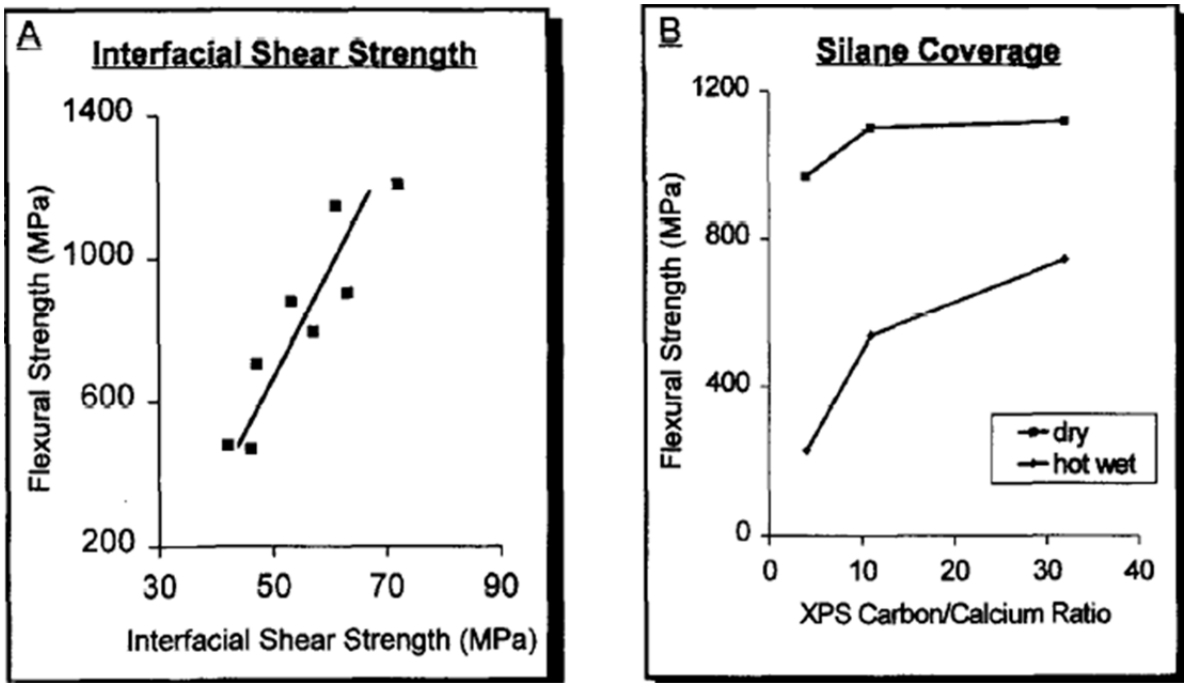

Figure 2. 6. Composite flexural strength, both dry and hot wet aged, is a function of interfacial strength which is in turn related to the amount of silane chemisorbed on e-glass fiber[31].

Di Benedetto et al.[32] showed that the interactions between coupling agent and resin binder in silane coated glass fibers reinforced in polyester resin creates an interphase zone which exhibit properties different than the bulk matrix. They also found that the interfacial adhesion

changed with different silane chemistry, film thickness and crosslinking density between silane and resin which affected the interfacial strength. Similar observations were made by Al-Moussawi et al.[33] where silane interaction with epoxy matrix produced interphase which exhibited properties different than the bulk matrix.

For thermosetting composites, theoretical and experimental studies have shown that the interphase region between fiber and the polymeric binder has distinct properties (Drown 1991). It is well known that a fraction of sizing dissolves into the binder on wetting of glass fibers with the resin binder while the rest of sizing remains bound to the surface[34]. Thomason[35] also argued that if soluble portion of the sizing remains bound to the glass fiber surface, then the interphase properties are affected by the soluble part of the sizing. Tanoglu et al.[36] illustrated a model to understand the structure and properties of the interpenetrating network formed by the diffusion of bound functionalized silane and reactive polymeric resin as shown in **Figure 2.7**. The wetting of silanized glass fibers by resin leads to interdiffusion into the interphase region. The thermodynamics of mixing and kinetics of diffusion govern the equilibrium concentration and diffusion rates. The chemical reaction between the compatible silane and polymer binder leads to formation of a strong interpenetrating network.

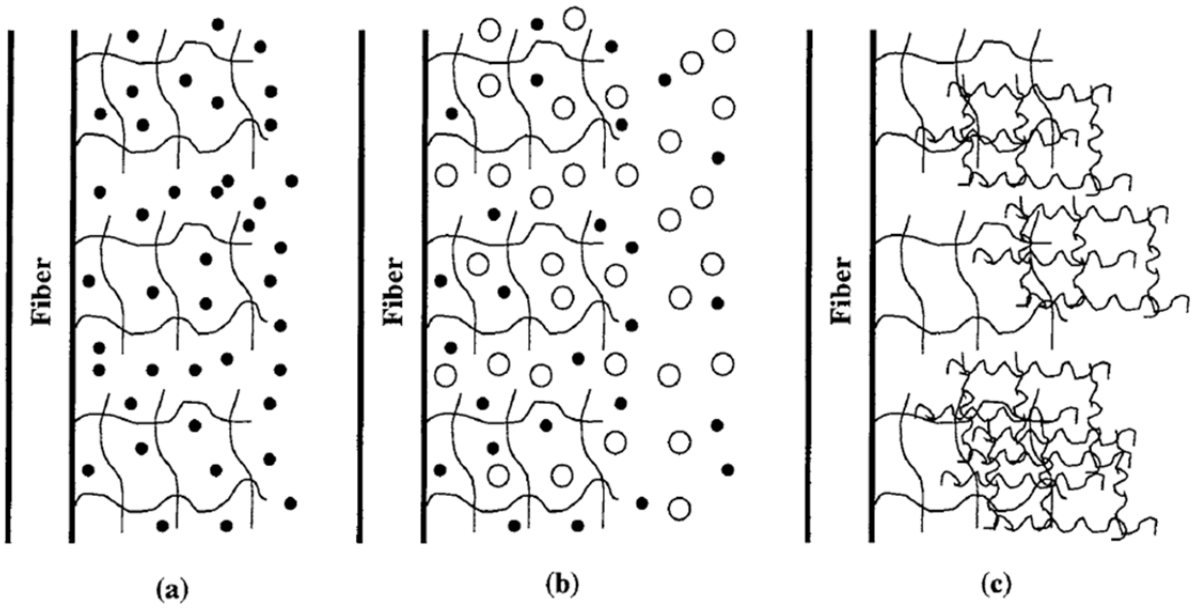

Figure 2. 7. Model IPN in glass fiber – thermoset composites a). Network represents bound sizing while filled circles depict unbound sizing; b). Interdiffusion of unbound sizing and resin (o) occurs and c). formation of an IPN between bound sizing & polymer matrix[36].

Of the most studies that employ e-glass fibers with silane coupling agents only, most do not relate to the extraordinary dynamics of the commercial sizing application. Pantano and Wittberg[37] showed that the thickness of the adsorbed layer of silane coupling agents was proportional to the length of organic tail in its structure. However, more complexity is introduced in commercial sizing applications and hence very few studies have focused on structure of sizing layer during industrial processing. Zinck et al.[38] demonstrated the synergistic effects of silane coupling agent and film former on the mechanical properties of the sized glass fibers as shown in **Figure 2.8.a**. The combination of both silane and film former produces fibers with maximum average tensile strength. Mader et al.[39] reported the

electrokinetic behavior of differently sized glass fibers consisting of silane and film formers. The aminosilane treatment changes the electrical charge of glass fiber surface from negative to positive and the addition of film dispersions does not significantly change the electrokinetic properties as shown in **Figure 2.8.b**.

Sizing	Average tensile strength (GPa)
Unsized	1.42
ɣ-aminopropyltriethoxysilane	1.78
Polyurethane film former	1.08
Polyvinyl acetate film former	1.01
Polypropylene film former	1.82
ɣ-aminopropyltriethoxysilane/ Polyurethane film former	1.82
ɣ-aminopropyltriethoxysilane/ Polypropylene film former	2.01

a).

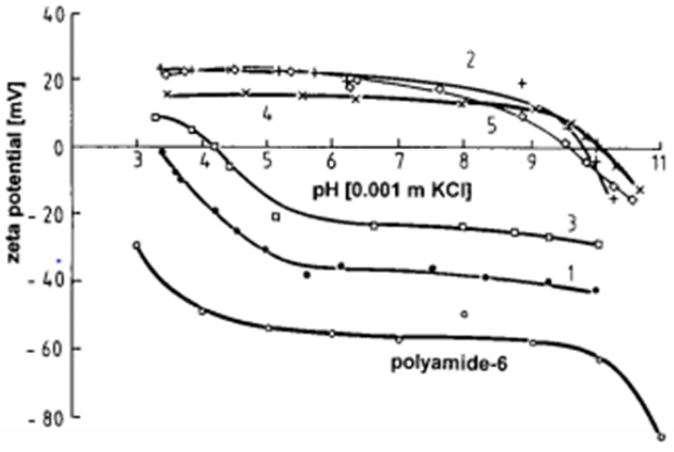

b).

Figure 2. 8. Effect of sizing components on interface properties a).Average tensile strength of differently sized glass fibers and b). Zeta potential vs pH variation for differently sized glass fibers – 1. Unsized glass fiber; 2. Aminosilane (A 1100); 3. Epoxy film dispersion; 4. A 1100/polyurethane film dispersion; 5. A 1100/epoxy film dispersion

The distribution of commercial sizings on glass fiber surface is non-uniform in nature and the formulation contains different auxiliaries or components other than silane coupling agents.

The optimization of these sizing layers on glass fibers is a complex art which involves a compromise between manufacturing, marketing, customer demands and other techno-economic parameters. For an improved fundamental approach of research and development in glass fiber composites, it is essential to develop small scale, short term methods and include other sizing components to analyze the sizing layers and their control their influence on overall composite properties.

Our overall objective is to study the surface interactions of different surface modification techniques on glass fibers and the glass-polymeric binder composite interface. We will accelerate our concept development with two parallel streams of research and development activity: 1) understanding the surface interactions at the interface, and 2) study the effects of tailoring interfacial adhesion on mechanical properties. The proposed activities of the project will provide a fundamental understanding of the thin film surface interactions in glass-polymer composites.

2.3. References

1. Loewenstein, K. L. The manufacturing technology of continuous glass fibers. **1973**.

2. Wallenberger, F. T.; Weston, N. E. In *In Glass fibers from high and low viscosity melts;* MRS Proceedings; Cambridge Univ Press: 2001; Vol. 702.

3. Dwight, D. W. In *1.08 - Glass Fiber Reinforcements;* Kelly, A., Zweben, C., Eds.; Comprehensive Composite Materials; Pergamon: Oxford, 2000; pp 231-261.

4. Musikant, S. *What every engineer should know about ceramics;* CRC Press: 1991; Vol. 28.

5. Karlsson, K. H.; Backman, R.; Hupa, L. In *In Models for liquidus temperatures;* Proc Sixth Eur Glass Soc Conf, Montpellier; 2002; .

6. Backman, R.; Karlsson, K.; Cable, M.; Pennington, N. Model for liquidus temperature of multi-component silicate glasses. *Physics and chemistry of glasses* **1997**, *38*, 103-109.

7. Lu, Z. P.; Liu, C. T. A new glass-forming ability criterion for bulk metallic glasses. *Acta Materialia* **2002**, *50*, 3501-3512.

8. Lu, Z.; Liu, C. Glass formation criterion for various glass-forming systems. *Phys. Rev. Lett.* **2003**, *91*, 115505.

9. Sakka, S.; Mackenzie, J. D. Relation between apparent glass transition temperature and liquids temperature for inorganic glasses. *J. Non Cryst. Solids* **1971**, *6*, 145-162.

10. Pahler, G.; Brückner, R. Structural and Mechanical Properties of Glass Fibers with Linear and Three Dimensional Network. *Glastechn.Ber* **1985**, *58*, 33-45.

11. Stockhorst, H.; Brückner, R. Structure sensitive measurements on e-glass fibers. *J. Non Cryst. Solids* **1982**, *49*, 471-484.

12. Sjögren, A.; Joffe, R.; Berglund, L.; Mäder, E. Effects of fibre coating (size) on properties of glass fibre/vinyl ester composites. *Composites Part A: Applied Science and Manufacturing* **1999**, *30*, 1009-1015.

13. Yang, L.; Thomason, J. L. Effect of silane coupling agent on mechanical performance of glass fibre. *J. Mater. Sci.* **2013**, *48*, 1947-1954.

14. Sims, G. D.; Broughton, W. R. In *2.05 - Glass Fiber Reinforced Plastics—Properties;* Kelly, A., Zweben, C., Eds.; Comprehensive Composite Materials; Pergamon: Oxford, 2000; pp 151-197.

15. Helwig, G. S.; Heseltine, R. W.; Pathmanathan, V. US 6,054,022, 2000.

16. Vaidya, N.; Pourdeyhimi, B.; Shiffler, D.; Acar, M. The manufacturing of wet-laid hydroentangled glass fiber composites: preliminary results. *INJ, pp55-59, Winter* **2003**.

17. Kim, J.; Sham, M.; Wu, J. Nanoscale characterisation of interphase in silane treated glass fibre composites. *Composites Part A: Applied Science and Manufacturing* **2001**, *32*, 607-618.

18. Andreevska, G. D.; Gorbatkina, Y. A. Adhesion of Polymeric Binders to Glass Fiber. *Product R&D* **1972**, *11*, 24-26.

19. Gutowski, W. S. Interface/interphase engineering of polymers for adhesion enhancement: Part I. Review of micromechanical aspects of polymer interface reinforcement through surface grafted molecular brushes. *The Journal of Adhesion* **2003**, *79*, 445-482.

20. Nishioka, G. M. Interaction of organosilanes with glass fibers. *J. Non Cryst. Solids* **1990**, *120*, 102-107.

21. DiBenedetto, A. T. Tailoring of interfaces in glass fiber reinforced polymer composites: a review. *Materials Science and Engineering: A* **2001**, *302*, 74-82.

22. Pape, P. G.; Plueddemann, E. P. Methods for improving the performance of silane coupling agents. *J. Adhes. Sci. Technol.* **1991**, *5*, 831-842.

23. Ishida, H.; Koenig, J. L. Effect of hydrolysis and drying on the siloxane bonds of a silane coupling agent deposited on E-glass fibers. *Journal of Polymer Science: Polymer Physics Edition* **1980**, *18*, 233-237.

24. Chiang, C.; Ishida, H.; Koenig, J. L. The structure of γ-aminopropyltriethoxysilane on glass surfaces. *J. Colloid Interface Sci.* **1980**, *74*, 396-404.

25. Naviroj, S.; Culler, S. R.; Koenig, J. L.; Ishida, H. Structure and adsorption characteristics of silane coupling agents on silica and E-glass fiber; dependence on pH. *J. Colloid Interface Sci.* **1984**, *97*, 308-317.

26. Ishida, H.; Chiang, C.; Koenig, J. L. The structure of aminofunctional silane coupling agents: 1. γ-Aminopropyltriethoxysilane and its analogues. *Polymer* **1982**, *23*, 251-257.

27. Laura, D. M.; Keskkula, H.; Barlow, J. W.; Paul, D. R. Effect of glass fiber surface chemistry on the mechanical properties of glass fiber reinforced, rubber-toughened nylon 6. *Polymer* **2002**, *43*, 4673-4687.

28. Park, S.; Jin, J.; Lee, J. Influence of silane coupling agents on the surface energetics of glass fibers and mechanical interfacial properties of glass fiber-reinforced composites. *Journal of Adhesion Science & Technology* **2000**, *14*, 1677-1689.

29. Shokoohi, S.; Arefazar, A.; Khosrokhavar, R. Silane coupling agents in polymer-based reinforced composites: a review. *J Reinf Plast Compos* **2008**, *27*, 473-485.

30. Drown, E. K.; Al Moussawi, H.; Drzal, L. T. Glass fiber 'sizings' and their role in fiber-matrix adhesion. *J. Adhes. Sci. Technol.* **1991**, *5*, 865-881.

31. Wu, H. F.; Dwight, D. W.; Huff, N. T. Effects of silane coupling agents on the interphase and performance of glass-fiber-reinforced polymer composites. *Composites Sci. Technol.* **1997**, *57*, 975-983.

32. Dibenedetto, A. T.; Connelly, S. M.; Lee, W. C.; Accorsi, M. L. The Properties of Organosiloxane/Polyester Interfaces at an E-Glass Fiber Surface. *The Journal of Adhesion* **1995**, *52*, 41-64.

33. Al-Moussawi, H.; Drown, E. K.; Drzal, L. T. The silane/sizing composite interphase. *Polymer Composites* **1993**, *14*, 195-200.

34. Thomason, J. L. The interface region in glass fibre-reinforced epoxy resin composites: 2. Water absorption, voids and the interface. *Composites* **1995**, *26*, 477-485.

35. Thomason, J. L. The interface region in glass fibre-reinforced epoxy resin composites: 3. Characterization of fibre surface coatings and the interphase. *Composites* **1995**, *26*, 487-498.

36. Tanoglu, M.; Ziaee, S.; Mcknight, S. H.; Palmese, G. R.; Gillespie, J. W., J. Investigation of properties of fiber/matrix interphase formed due to the glass fiber sizings. *J. Mater. Sci.* **2001**, *36*, 3041-3053.

37. Pantano, C. G.; Wittberg, T. N. XPS analysis of silane coupling agents and silane-treated E-glass fibers. *Surf. Interface Anal.* **1990**, *15*, 498-501.

38. Zinck, P.; MÃ¤der, E.; Gerard, J. F. Role of silane coupling agent and polymeric film former for tailoring glass fiber sizings from tensile strength measurements. *J. Mater. Sci.* **2001**, *36*, 5245-5252.

39. Mäder, E.; Grundke, K.; Jacobasch, H. -.; Wachinger, G. Surface, interphase and composite property relations in fibre-reinforced polymers. *Composites* **1994**, *25*, 739-744.

CHAPTER 3

Influence of sizing components on the interface properties in glass reinforced thermoset composites

Abstract

Sizing chemistry, which typically consists of silane coupling agents, imidazolines, film formers and other auxiliaries, has been used in the glass industry to promote adhesion between glass fibers and thermoset polymer coatings to form composites. These composites are subsequently coated with asphalt to form roofing shingles. The complex interactions at the glass-size interface are not well understood and little is known about its effects on composite properties. This work focuses on understanding the interactions of different sizing components on the glass fibers interfacial properties and corresponding composite properties. We found that the sizing chemistry has a strong influence on the mechanical performance of these composites. The isoelectric point is an important tool to gauge the dispersion properties of sized glass fibers in polyelectrolyte. The imidazoline component, though little is reported in the literature about its role in the sizing interface, is a key component contributing to the mechanical performance. TOF-SIMS imaging of the sizing interface on the glass fiber surface reveal that the silane and imidazoline components distribute in very different and distinct patterns.

3.1. Introduction

As most interactions between materials occur at the surface or interface between the materials, an understanding of this behavior at a molecular, microscopic, and macroscopic level is critical to controlling properties. Surface modification of materials allows the ability to tailor material interactions without changing the bulk properties[1]. In composite science, it is well known that the interfacial properties are governed by the chemical nature and physical compatibility between the fibers and the matrix[2]. There are different surface modification techniques applied to the glass fiber surfaces to appropriately tune the interface[3].

After the formation of glass fibers, they are passed through an applicator where a sizing is applied to the surface. The applicator rotates in the sizing bath to maintain a thin film formation of the size on the glass fiber surface. The sizing application improves the integrity and lubrication properties of the glass fibers as well as improves the binder compatibility and adhesion of glass fibers for the composite matrix. They also help protect the glass fibers from each other during processing and handling[4]. The sizing generally comprises a silane coupling agent, imidazolines, film formers, and lubricants[5]. These sized fibers are then reacted with stiff thermoset polymers to bind them together to form glass-polymer composite mats which are subsequently coated with asphalt, for instance, to form roofing shingles[6]. For tailoring the composite physical properties for a particular polymeric binder, the sizing formulation can be varied provided the interfacial interactions and surface chemistries are well understood[7].

Silane chemistry has found abundant use in glass fiber processing to form thin films on its surface[8] which has improved its bonding with the polymeric matrix material[9]. Organofunctional silanes are the most commonly used coupling agents in the glass composite

industry[10]. The film formers, such as polyvinyl alcohol, play a major role in maintaining the durability of the interface, improving impact resistance and promote the wetting of glass surfaces without affecting any other properties of the material[11]. Imidazoline chemistry has also been useful in sizing for improving the mechanical properties of the glass fibers. Hydroxyethyl-based imidazolines have found popularity in glass industry due to their unique structure of long unsaturated hydrocarbon tail with an imidazoline head group. All the sizing components in conjugation with each other govern the interphase structure as well as some properties of the glass-polymer composites[12]. The effect of chemistry and structure of only the silane-coupling agent during deposition on glass fiber surface is well known[8,13-15] while the combined effects of all these components are not well understood.

Prior research has shown that interphases formed by using pure silane, as compared to sizing, are different[16]. The silane component forms a multi-layered siloxane network when used alone[17] or in the sizing while the presence of other components helps in formation of a more rigid interphase with the polymer matrix[18]. There is a gap in the knowledge with respect to these surface interactions preventing precise tuning of their chemistries for enhanced product performance. For instance, if the structure of the sizing layers obtained and the synergistic effects of silane and imidazoline chemistries obtained from industrial processing are more fully elucidated, manufacturers would have a powerful tool for controlling composite performance.

The surface interactions between sizing and the glass fibers can be easily understood by studying the electrokinetic properties of the glass fiber surface[19,20]. The net charges on a glass fiber surface influence the distribution of the nearby ions in a polar medium[21]. When a glass

fiber surface is moving in a bulk liquid, for instance polyelectrolytes, a boundary layer attached to the surface moves with it causing the generation of a shearing surface. The electrical potential determined at the shearing surface is termed as zeta potential as shown in **Figure 3.1**. The electrokinetic behavior of glass fibers is of critical importance to its dispersability and electrostatic repulsion which further affects the composite properties. The zeta potential of a fiber surface is strongly affected by pH[22]. The variation in pH along with the isoelectric point, the pH at which zeta potential equals zero, also plays a crucial role in manipulating the processing parameters[23]. In order to achieve a good web formation during composite formation, the processing pH is operated near the isoelectric point of the sized glass fibers. Thus, matching the isoelectric point by controlling the sizing formulation and the pH during wet web formation is critical to achieving excellent fiber dispersion and subsequent optimal web structure. Also, depending on the product requirements, various sizing chemistries can be added to modify the electrokinetic properties of the glass fibers.

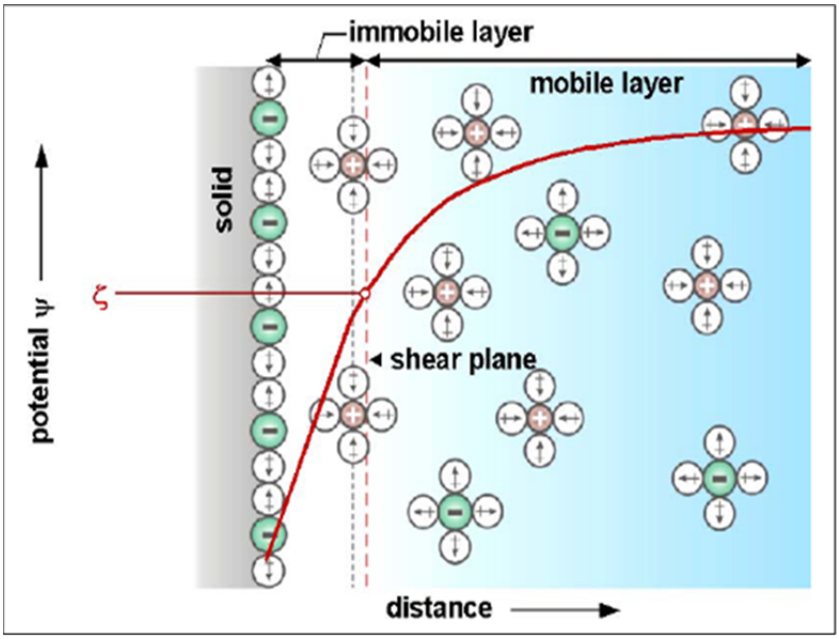

Figure 3. 1. Principle of zeta potential. Zeta potential represents the surface charge which occurs in the presence of an aqueous solution when functional groups dissociate or adsorb onto surfaces. Varying pH of the aqueous phase influences the equilibrium, giving insights into the chemical behavior of the surface.

The overall objective of this work is to study the surface interactions of different surface modification techniques on glass fibers and their effect on glass mat properties. This objective is accomplished by: 1). determining the role each sizing component has on glass surface properties through electrokinetic behavior; 2). understand the distribution of the individual sizing components within the glass-size interface on the glass fiber surface; and 3). relate these behaviors to determine the effect that the glass-size interface has on the mechanical performance of the glass-polymer composites.

3.2. Experimental Section

3.2.1. Sizing of glass fibers

The commercial glass fibers, Owens Corning (OC) glass fibers – OC 9501 which is boron free and Johns-Manville (JM) glass fibers – JM 137 which contains boron, each having different proprietary surface chemistries were obtained from GAF Materials Corporation. They were used for understanding the effect of different sizings on the glass fiber surface as compared to unsized glass fiber surface as a function of zeta potential. The sizing on the commercial sized fibers was burned off at 630 $\pm$ 2^{o}C for 10 mins to obtain unsized glass fibers.

Design of experiment (DOE) was used for understanding the interface effects of individual sizing components on the interface properties with four different silane levels and imidazoline levels to make different sizing formulations as shown in **Figure 3.2** with constant level of film former.

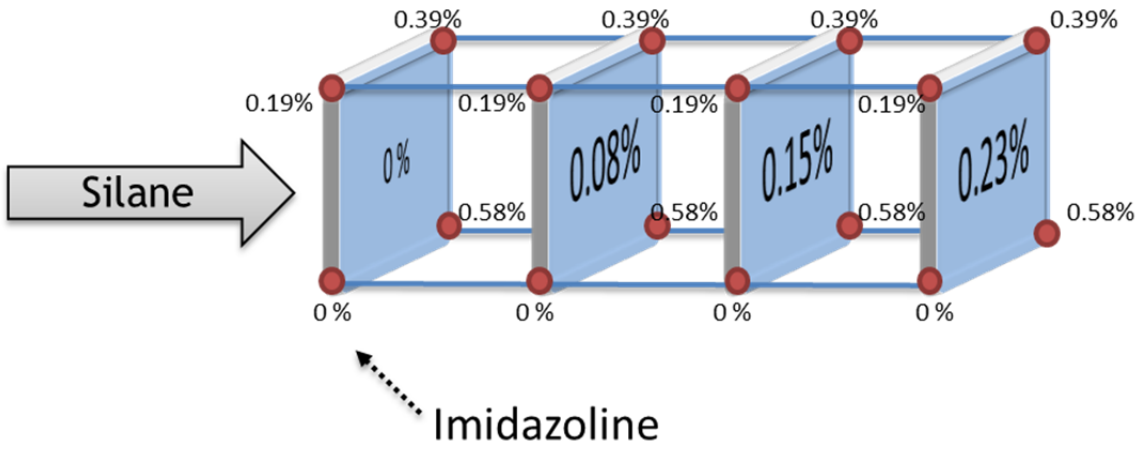

Figure 3. 2. DOE for silane and imidazoline levels. Four levels of silane were chosen – 0%, 0.08%, 0.15%, 0.23% and four levels of imidazoline were chosen – 0%, 0.19%, 0.39%, 0.58% to form an effective 4x4 full factorial design of experiment.

The sizing components used for this study were as follows: silane was ɣ-aminopropyltrimethoxysilane (Silquest A-1100), imidazoline was 1-Hydroxyethyl-2-cocoimidazoline (Cola Zoline C), as shown in **Figure 3.3** and the film former was mixture of polyvinyl alcohol (Selvol PVA 205) and hydroexy ethyl cellulose (Cellosize HEC). For coating each fiber with required sizing, the measured sizing components were pre-mixed and hydrolyzed in the sizing bath and applied onto the glass fibers via a rolling applicator rotating at about 20 to 25 feet per minute. The roller cycles through a well of size and is in contact with a group of glass fibers which are being pulled down from the extruder. The glass fibers are then fed into a chopper where the fibers are chopped to a specified length. From the DOE, 16 samples of fiber were produced with different combinations of silane and

imidazoline contents. Unsized e-glass fibers, commercial sized fibers and sizing components were all obtained by GAF Materials Corporation and the sizing application was conducted at their Nashville, TN facility.

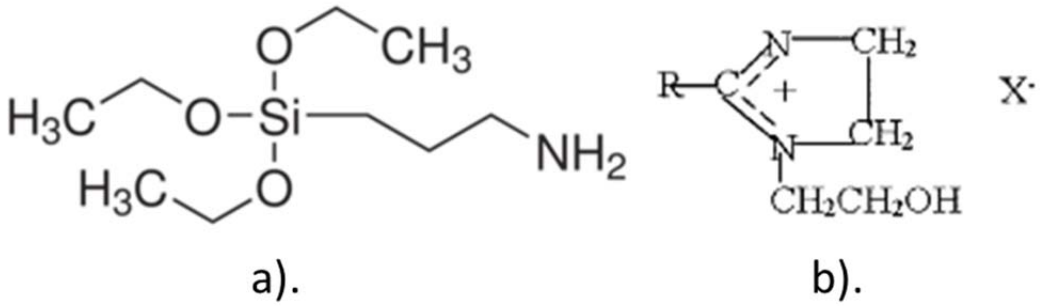

Figure 3. 3. (a). ɣ-aminopropyltriethoxysilane and (b). Hydroxyethyl imidazoline structures

3.2.2. Electrokinetic properties of glass fibers

The electrokinetic properties studied using an electrokinetic analyzer (Anton Paar SurPASS) is a useful surface analysis technique that can provide information about the acidic/basic nature of a given surface. The potential at the interface between the immobile and the diffuse layer is known as the electrokinetic or zeta potential. It determines the zeta potential by measuring the streaming current based on the Stern model.

A cylindrical cell was used for measurement of zeta potential of glass fibers. The fibers were stuffed in the cell such that adequate flow rate and pressure drop is maintained across the cell. A dilute electrolyte (0.001 M KCl; Fischer Scientific) is circulated through the cell containing the glass fibers, thus creating a pressure difference. A relative movement of the

charges in the electrochemical double layer on glass fiber surface occurs and gives rise to the streaming current which is detected by the electrodes placed at both sides of the sample. The standard HCl (0.1M, Fischer Scientific) and NaOH (0.1N, Fischer Scientific) were used in the automatic dispensing unit to understand the effect of pH on the zeta potential in the acidic and basic cycles respectively. The pH cycle were run only between pH 3 and 10, due to the amount of time required to obtain data for pH values beyond that range and the pH range outside that range would not be feasible for commercial processing.

3.2.3. Time-of-flight Secondary Ion Mass Spectrometry (TOF-SIMS) analysis of glass fibers

TOF-SIMS technique is a surface sensitive approach (~10-20Å) which provides semi-quantitative data about surface chemistries like surface composition, surface segregation of components. A typical spectrum is a plot of intensity counts versus mass by charge ratio (u). It was used as a technique to compare the presence and distribution of silane and imidazoline components on the different treated glass fiber surfaces.

TOF-SIMS analyses were conducted using a TOF-SIMS V (ION TOF, Inc. Chestnut Ridge, NY) instrument equipped with a Bi_n^{m+} (n = 1 - 5, m = 1, 2) liquid metal ion gun. The instrument vacuum system consists of a load lock for sample loading and an analysis chamber, separated by the gate valve. The analysis chamber pressure is maintained below 5.0×10^{-9} mbar to avoid contamination of the analyzed surfaces. For the high mass resolution spectra acquired in this study, a 128 by 128 pixel spectrum of a 100 µm by 100 µm area was acquired using a Bi^+ primary ion beam. For the mass spectral images, a 256 by 256 pixel image of a 200 µm by 200 µm area was acquired using a Bi_3^+ primary ion beam.

3.2.4. Glass Mat formation

The sized glass fibers from the DOE were used to make glass-polymer binder mats. The sized fibers were treated with the polyacrylamide solution (Nalclear 7768) with stirring for few minutes to help the fibers disperse well. The dispersed fibers are arranged on a perforated screen which is dipped in the binder solution. The co-binders used in this study were urea-formaldehyde resin (Casco Resin FG-413F) and acrylic polymer emulsion (Rhoplex GL-618). After the binder treatment, the excess binder is sucked off a vacuum pump and the fibers are cured in an oven at 213^{o}C for 2.5 min to form glass-polymer composite mats. All 16 fiber samples were used to create 16 different glass mats using the same binder treatment.

3.2.5. Mechanical properties of glass-polymer composite mat

The measurement of mechanical properties of the glass-polymer composite mats is one of the most important quality control processes in the roofing shingle industry. The attainment of maximum mechanical performance is the prime objective for most manufacturers. The testing parameters used for composite mats were mat tear, dry tensile strength and wet tensile strength.

The mat tear testing was performed on an Elmendorf-type tearing tester using ASTM D1922-09 for testing propagation tear resistance by pendulum method. The force required to propagate tearing across the mat is measured using a calibrated pendulum device which swings through an arc and tears the specimen from a precut slit. 16 samples of 2.5 x 3.5 inch each were tested and average reading was reported. The tensile strength testing was performed on a Thwing-Albert tensile tester using a load cell of about 1000 N. The load at

which the glass mat breaks is registered as the tensile strength. Since these mats are to be used in roofing shingles, the strength on wetting of these mats is also tested. The mats are dipped in boiling water for around 10 mins and the tensile testing is done after blotting out the water from mat's surface using a cotton tissue.

3.2.6. Statistical Analysis

The statistical analysis was performed and the prediction models were created using JMP 10 software and the data was considered significant for p values < 0.05.

3.3. Results and Discussion

3.3.1. Effect of sizing treatment on the electrokinetic properties of glass fibers

In this study, we obtained two different commercial sizing chemistries, Owens Corning (OC) glass fibers and Johns-Manville (JM) glass fibers, and burned off their sizings to create bare unsized glass surface. We studied the electrokinetic behavior of these sized and unsized glass fiber surfaces as a function of pH and the effect of two different commercial sizing chemistries on zeta potential. **Figure 3.4** shows the effect that sizing chemistry has on the glass fiber surface as a function of zeta potential for the two commercial sizing chemistries used in this study. When the zeta potential of the surface exhibits no net electrical potential, it is called the isoelectric point (IP). The IP for both OC and JM unsized fibers is lower than pH 3 while that for the sized fibers is between pH 6-7. This demonstrates the importance of the sizing as an IP of pH 6-7 will result in the best fiber dispersion during mat formation. The IP of unsized glass fibers is reported around pH 2 by Dong[24,25]. At pH above 3, the glass fibers

exhibit a negatively charged surface and the zeta potential is always negative with the magnitude of zeta potential increasing with increase in pH. The acidic silanol groups present on the glass fiber surface are responsible for the low IP of unsized glass fiber surface[26]. The high negativity of zeta potential between -80 to -90 mV at a pH of 9 for both unsized glass fibers demonstrates the hydrophobic character of the unsized glass fiber surface.

The proprietary sizing, which mainly consists of silanes, imidazolines and film former, when used for surface modification of glass fibers causes an increase in the IP of these glass surfaces. The IP shifts from around pH 2 to between pH 6-7 after sizing treatment for both fibers owing to the amino groups present in the sizing formulation. The JM sized fiber surface demonstrates higher IP (pH~7) than the OC sized fiber surface (pH 6) indicating the presence of higher number of amino groups in the sizing formulation or a greater treated area. The low negative zeta potential between -20 to -30 mV at pH 9 for both sized fibers indicates reduction in the hydrophobic character of the glass fiber surface and can be attributed to the presence of water soluble silane groups in the sizing formulation. Both commercial sizings demonstrate an IP in the pH range 6-7 which helps in good fiber dispersion properties.

It is observed that the fiber-fiber interactions need to be minimized in order to form a uniform glass web. In order to achieve good web formation, the glass fibers need to come closer and the operating pH should ideally be near the IP of sized glass fibers (neutral pH). Also, there are many different parameters like mechanical agitation, auxiliary chemistry which play a role in influencing dispersion properties, however, the electrokinetic properties

of glass fibers is very important[24]. Thus, zeta potential provides a unique tool to understand the glass fiber surfaces and its effect on formation of composites.

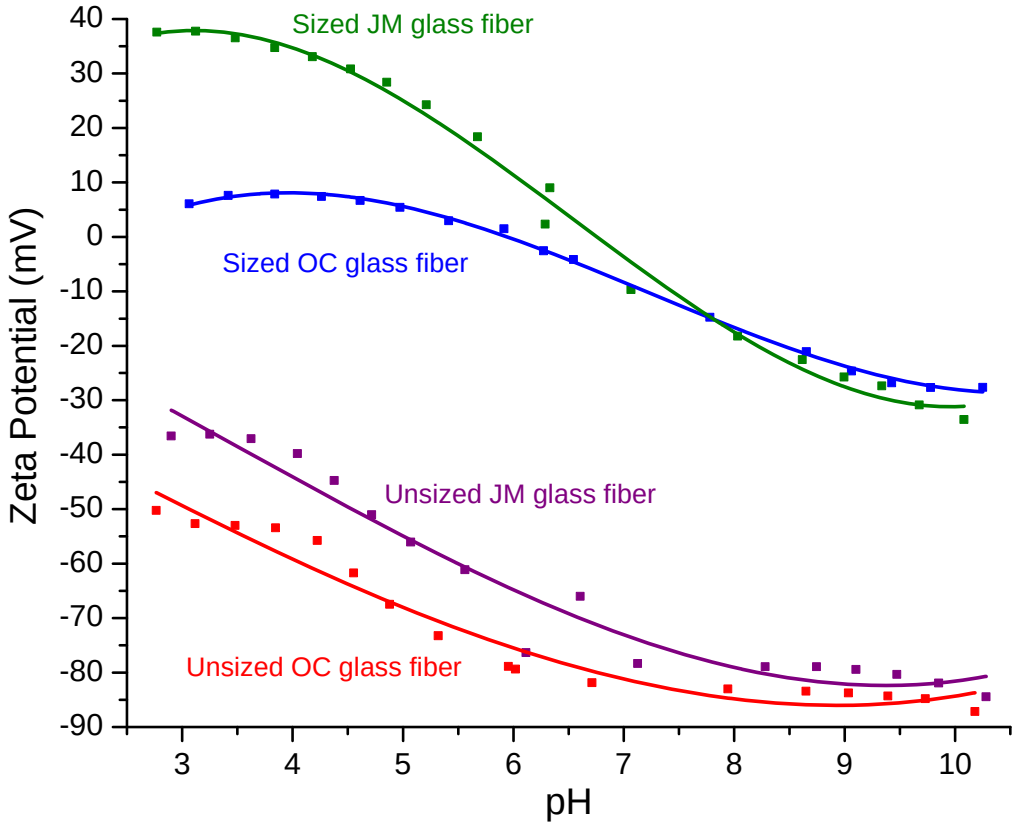

Figure 3. 4. Zeta potential as a function of pH for different proprietary sizing chemistries and comparison of unsized and sized glass fibers for those chemistries to demonstrate the electrokinetic behavior of glass fibers on sizing treatment.

3.3.2. Role of each sizing component on the surface properties

The formation of electrochemical double layer is influenced by the character of the surface (hydrophobic/hydrophilic) and the adsorption of dissolved ions in the medium. Sizing

treatment of glass fibers completely changes the original surface properties of the glass fibers. To understand the effect of individual components of sizing on the electrokinetic behavior of glass fibers, we prepared our design of experiments using a model silane, A 1100 or ɣ-aminopropyltrimethoxysilane (APTES), and varied the concentration (w/w) in sizing bath as 0%, 0.08%, 0.15% and 0.23% and the imidazoline as 0%, 0.19%, 0.39%, 0.58% keeping other auxiliaries constant. We analyzed all sixteen glass fiber surfaces generated from our design of experiments for their electrokinetic behavior.

Figure 3.5.a. shows the effect of only silane concentration (no imidazoline present in the sizing) as a function of zeta potential. The untreated glass fiber surface does not exhibit a clear IP and lies at pH < 3. We can assume the IP lies near the reported value by Dong of pH 2. On treating the glass surface with silane, the IP drastically shifts to pH 9.5. The zeta potential of the glass fiber surface changes from negative to positive value after sizing indicating the unsized surface is negatively charged and the APTES imparts positive charge to the surface. Silane condensation reaction takes place on the glass fiber surface leading to formation of a siloxane layer on the glass surface via hydrogen bonding[27]. The free amino groups present in the silane impart positive charges to the silane treated glass surface. As the concentration of silane increases from 0.08% to 0.23%, the IP shows a slight increase to pH 10 due to the presence of higher amount of free amino groups present on the surface. The 0.08% and 0.15% silane both show similar positive zeta potential at pH 9 indicating the reduced hydrophobic nature of the surface as compared to the unsized surface. At 0.23% silane, the zeta potential value is higher indicating increase in the hydrophilic character of the surface. The higher silane concentrations contain increased amino groups which causes

increase in the hydrophilic nature of the surface. However, a high positive zeta potential is observed for 0.08% silane as compared to the 0.15% and 0.23% silane at pH 4. Thus, the IP increases and the hydrophobic character of the surface decreases with an increase in the concentration of APTES present in the sizing without any imidazoline. Also, this suggests that sizing with only silane component would not result in the optimal mat structure.

Figure 3.5.b. shows the effect of only imidazoline concentration (no silane present in the sizing) as a function of zeta potential. On treating the unsized glass surface with 0.19% imidazoline, the IP shifts to pH 5. The positive charge on the imidazoline ring structure has high affinity towards the highly negatively charged untreated glass fiber surface. This strong electrostatic interaction may result in exposing the free nitrogen groups to the surface imparting positive charge to the glass surface. At 0.39% imidazoline, the IP shifts to around pH 7 while at 0.58% imidazoline the IP increases further to pH 7.5 due to the increasing number of free nitrogen groups available on the glass surface. At pH 9, the presence of imidazoline increases the negative zeta potential indicating reduction in the hydrophobic character of the surface as compared to unsized glass fiber surface. However, the imidazoline treatment concentrations of 0.19%, 0.39% and 0.58% exhibit similar hydrophobic nature of the glass fiber surface. The IP increases while the hydrophobic character of the surface remains constant with an increase in the concentration of imidazoline in the sizing without any silane. Also, this suggests that the imidazoline component should be critical in increasing fiber dispersion during glass mat formation and assist with achieving optimal mat structure.

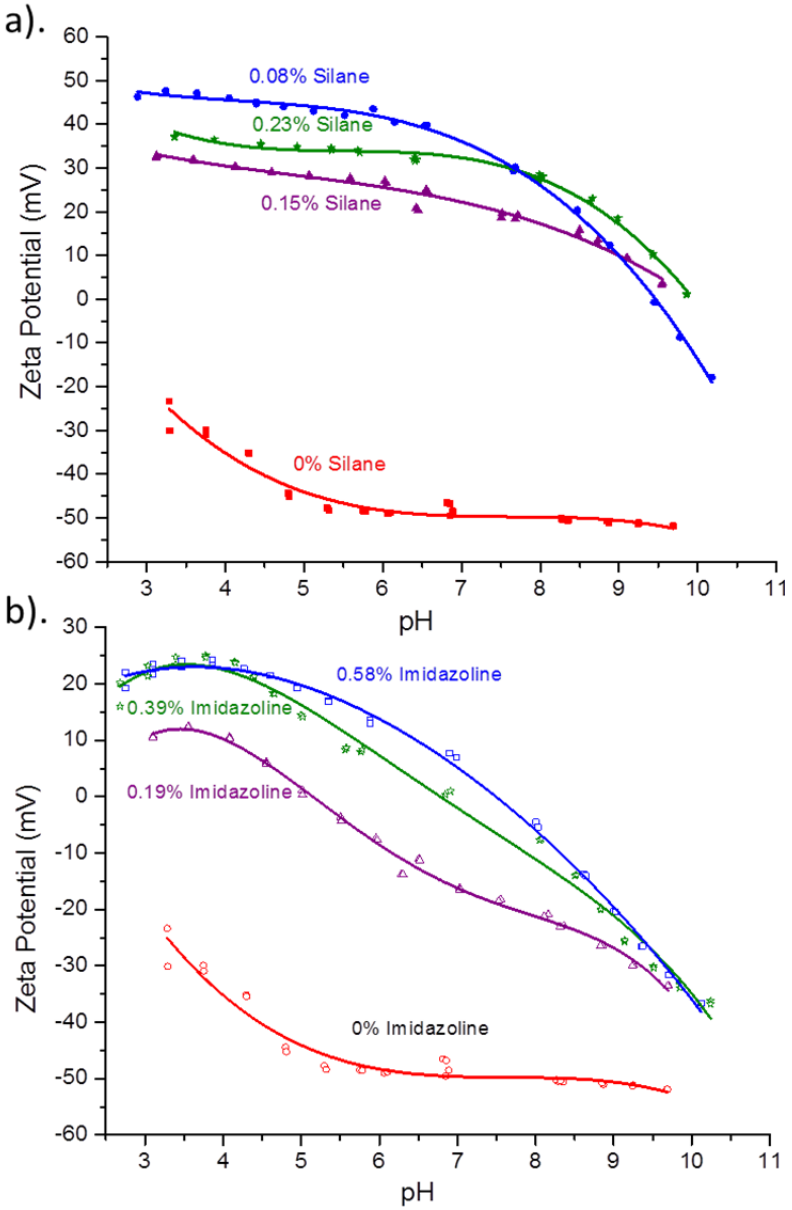

Figure 3. 5. Zeta potential as a function of pH to elucidate the change in electrokinetic behavior of glass fibers as function of a). change in silane concentration at 0%, 0.08%, 0.15%, 0.23% in sizing without imidazoline; and b). change in imidazoline concentration at 0%, 0.19%, 0.39%, 0.58% in sizing without silane.

Comparing **Figure 3.5 a. and b.**, the observed positive charges of the free nitrogen group in imidazoline (IP~ pH 5-7.5) are lower in comparison to that on the free amino groups present in APTES (IP~ pH 9.5-10). The imidazoline treatment shows negative zeta potential between -20 to -30 mV at pH 9 while the silane treatment shows positive zeta potential between +10 to +20 mV at the same pH. This indicates that the silane treatment causes more reduction in the hydrophobic character as compared to the imidazoline treatment. Also, the high positive zeta potential at pH 4 between 30 to 40 mV for silane treatment as compared to 10 to 20 mV at the same pH for imidazoline treatment indicates the protonation of free nitrogen groups present in imidazoline is weaker as compared to the protonation of the amino groups present in silane. The individual effect of silane and imidazoline components show different trends and the presence of silane and imidazoline together in the same sizing system lead to interesting results as shown in **Figure 3.6**.

When 0.08% silane and 0.19% imidazoline is used in the formulation, the IP changes from that of the individual components suggesting possible interactions between the silane and imidazoline. The IP of pH 7.2 for this formulation lies between the IP of pH 9.4 for 0.08% silane and 0% imidazoline and the IP of pH 5.2 for 0% silane and 0.19% imidazoline. This indicates that addition of imidazoline to the pure silane formulation leads to pH ideal for good fiber dispersion in polyelectrolytes. At 0.08% silane, with increase in the imidazoline content, the IP reduces initially and then increases at 0.58% imidazoline. One of the possible explanations for this observation is that at lower imidazoline concentrations, the silane chemistry has stronger interactions with glass fiber surface than the imidazoline. However, as the imidazoline content increases, there is transition in reactivity changing the silane

condensation kinetics. At very high imidazoline concentrations (0.58%), there are possible strong electrostatic interactions between imidazoline and glass fiber surface resulting in excess silane present on the fiber surface which causes increase in IP (nears IP of pH 9.4 for only silane). Similar trends were also observed for variation of imidazoline at 0.15% silane. At 0.23% silane, no conclusive trends were visible with increase in the imidazoline concentrations. At very high silane and imidazoline concentrations, the competing reactions and excess components may contribute towards loss of clear conclusions.

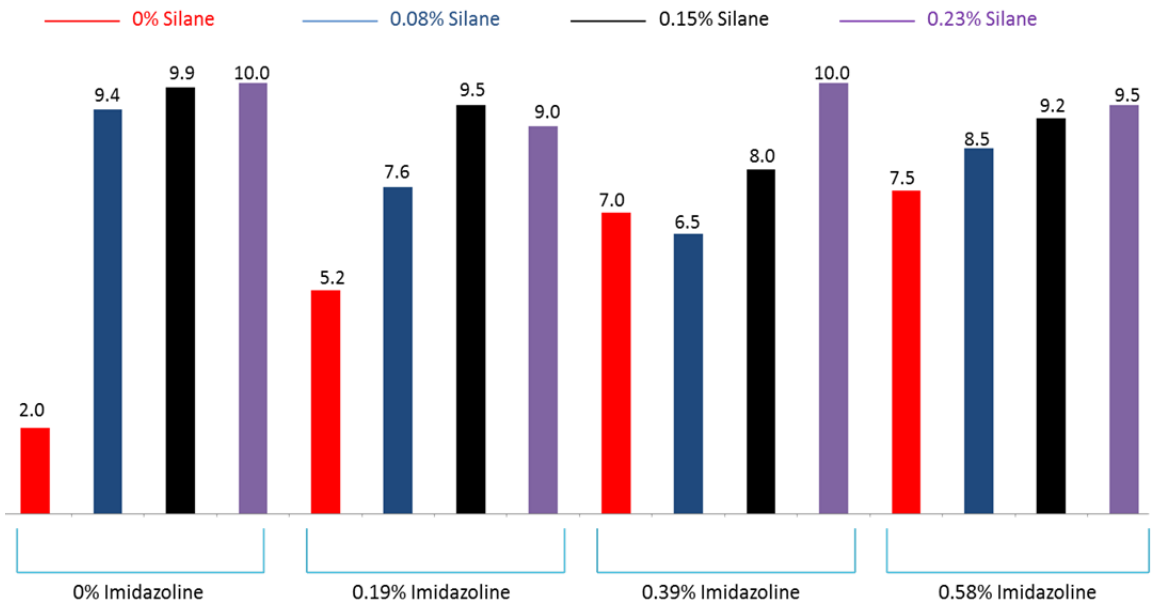

Figure 3. 6. Effect of change in combined silane (0%, 0.08%, 0.15%, 0.23%) and imidazoline concentrations (0%, 0.19%, 0.39%, 0.58%) within a sizing formulation on the isoelectric point of sized glass fibers.

The response of electrokinetic properties caused by silane and imidazoline concentrations within sizing formulation was statistically measured. The isoelectric probability is calculated from the IP values shown in **Figure 3.6** and significance of the component is determined if the probability is less than 5% of the population. The silane component is the only significant contributing factor ($p = 0.0006$) while the imidazoline (0.3831) and the interactions between silane and imidazoline components (0.0561) are not significant in determining the isoelectric point for this study. It is important to understand that the model assumes that higher is the IP value, more significant is the particular component. The silane chemistry significantly changes the glass fiber surface chemistry as shown in **Figure 3.5.a**. The amount of silane present in the sizing formulation will determine the isoelectric point as per the statistical model. However, we know that the IP of pH 6-7 is significant for good fiber dispersion properties of sized glass fibers in polyelectrolyte which indicates the significance of imidazoline component.

The prediction model profile estimates that the increase in silane concentration causes a linear increase in the isoelectric point in the sizing system. The increase in silane concentration causes an increase in the basic pH which results in poor fiber dispersion properties. The increase in the imidazoline causes slight increase in isoelectric point but minimal as compared to the effect of silane as per this prediction model. The imidazoline keeps the isoelectric point near pH 7 which helps in achieving good fiber dispersion properties. The interactions between silane and imidazoline are not significant in influencing electrokinetic properties. This analysis has been useful in establishing the important role of

both silane and imidazoline in influencing the electrokinetic properties at the glass fiber-size interface.

3.3.3. Distribution of the individual sizing components within the glass-size interface

The composition of selective sized glass fibers from this study was analyzed by TOF-SIMS spectroscopy. Only negative ion spectra were used for peak comparisons because of the low intensity observed for characteristic peaks in the positive mode. TOF-SIMS imaging was employed to assess the distribution of sizing components at the glass-size interface[28,29]. Both positive and negative ion images were useful for understanding this distribution.

The negative ion TOF SIMS spectra of the three samples show ions with varied ion intensities (**Figure 3.7**) suggesting different surface chemistries. The silane and imidazoline treatment have different effects on the surface chemistry of the glass fibers which can be seen by looking at certain specific peaks from the TOF-SIMS. The peak at 27 amu is assigned to BO^- which is originated from the nascent glass fiber surface. After treating with silane and imidazoline, the peak intensity at 27 amu is reduced indicating coverage of the fiber surface with the treatment. The peak at 43 amu is assigned to $SiCH_3^-$ which can be originated from both the glass surface as well as the silane. Highly reduced ion intensity of this ion from the imidazoline sample indicates that the surface of glass fibers is covered by imidazoline.

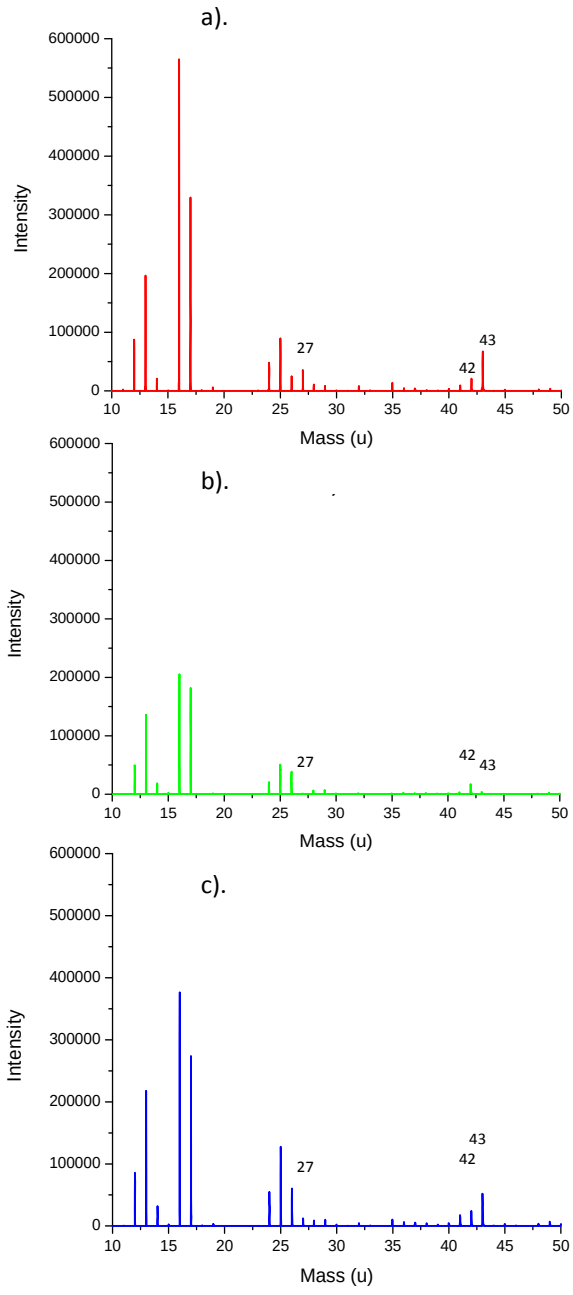

Figure 3. 7. TOF-SIMS negative ion spectra of surface of glass fibers with a). 0% silane and 0% imidazoline, b). 0% silane and 0.58% imidazoline, and c). 0.23% silane and 0% imidazoline to understand the effect of each component on the surface composition of glass fibers and identify characteristic peaks to differentiate the surface chemistries.

The distribution of the combined imidazoline and silane on glass fibers surface was also investigated. The TOF-SIMS technique can generate high lateral resolution images of ions of interest[30]. The TOF-SIMS software allows for overlay of these spectral images that have been encoded with colors for understanding such two- or three-way interactions.

Figure 3.8 shows the interaction of silane and imidazoline components on the surface of the sized glass fibers obtained from negative ion TOF SIMS mass spectra. The characteristic negative secondary ion for silane is $SiCH_3^-$ at 43 amu and for imidazoline as CNO^- at 42 amu. The green color in the image indicates the presence of silane while the red color indicates the presence of imidazoline. The silane appears to be uniformly distributed all over the glass fiber surfaces. The imidazoline shows non-uniform distribution and some extent of agglomerations on the individual glass fiber surface in the presence of silane. Similar effects were observed in positive ion mass spectral images and in different samples. This suggests that silane chemistry dominates imidazoline chemistry for reacting on the glass fiber surface. Also, the imidazoline shows a tendency to agglomerate on the surface and is not present uniformly throughout the glass fiber surface. These possible aggregated structures of imidazoline orient themselves in a different way than the silane structure when used together in a sizing system.

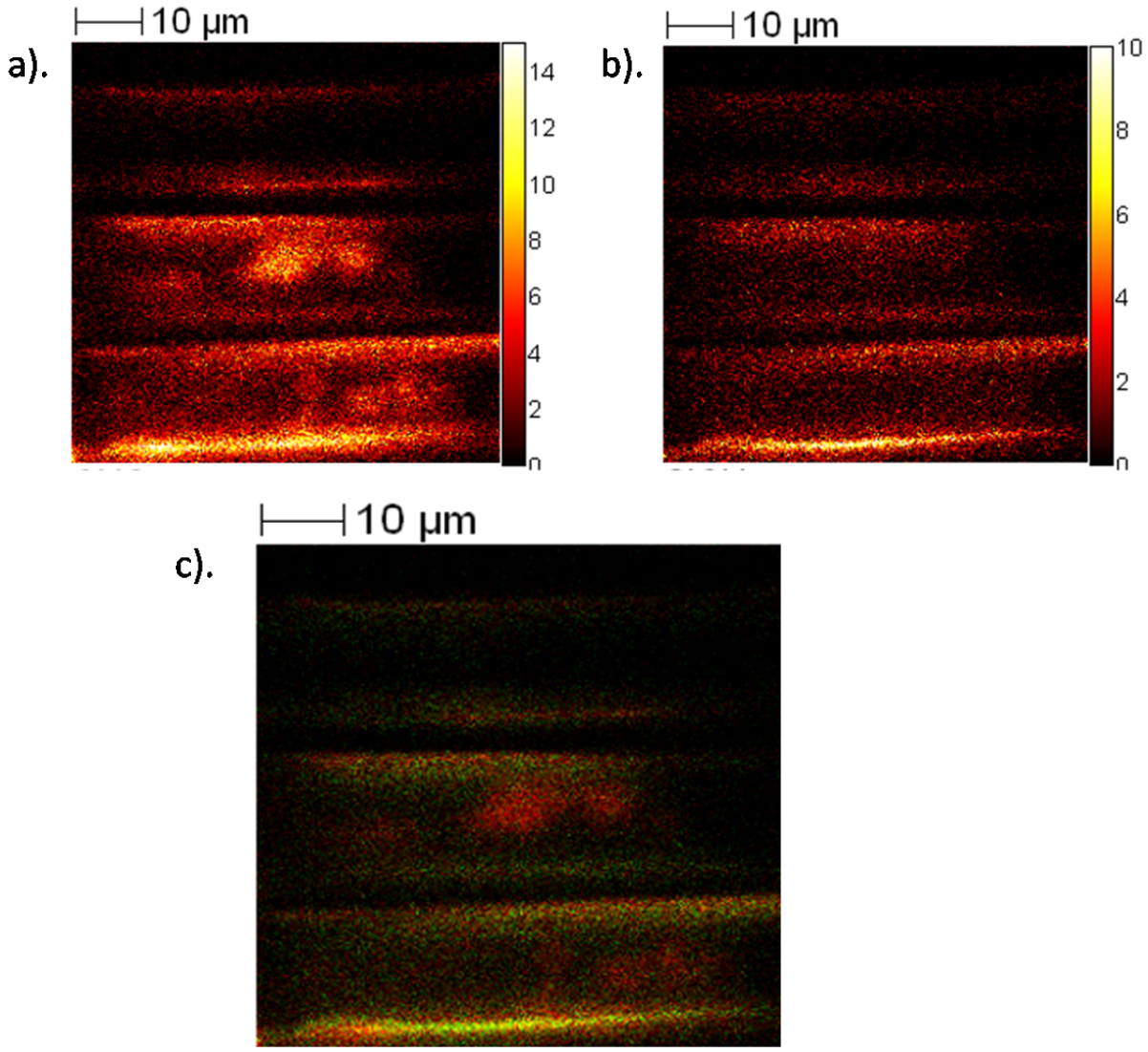

Figure 3. 8. Negative ion TOF SIMS mass spectral images demonstrating the distribution of silane and imidazoline components on size-glass interface; a). CNO^- at 42 amu is identified as the characteristic ion for imidazoline showing non-uniform distribution with agglomeration in center; b). $SiCH_3^-$ at 43 amu is identified as the characteristic ion for silane showing comparatively uniform distribution; c). superimposed images of CNO^- and $SiCH_3^-$ showing distribution of silane (green) and imidazoline (red) in a sizing formulation.

Figure 3.9 shows the interaction of silane and imidazoline on the surface of glass fibers obtained from positive ion TOF SIMS mass spectral images. The silane dominant species, $C_2H_5O^+$, seems to be distributed all over the fiber surface. The peak at 98amu assigned to $C_6H_{12}N^+$ is characteristic ion for imidazoline deposition. The imidazoline shows large amount of deposition in form of agglomerates/aggregates on the glass fiber surface in presence of silane. Overlaid image (**Figure 3.9.c**) of these two ions clearly shows the distribution of these components in a sizing system. The silane seems evenly distributed while the imidazoline shows large depositions in specific areas. This may suggest formation of some micelle structure due to the nature of long chain alkanes present in the fatty imidazoline structure. These results improve our current understanding of deposition of imidazoline and silane components in sizing on the surface of glass fibers. TOF-SIMS imaging helps us in understanding the distribution characteristics of the two sizing components used in this study on the glass fiber surface.

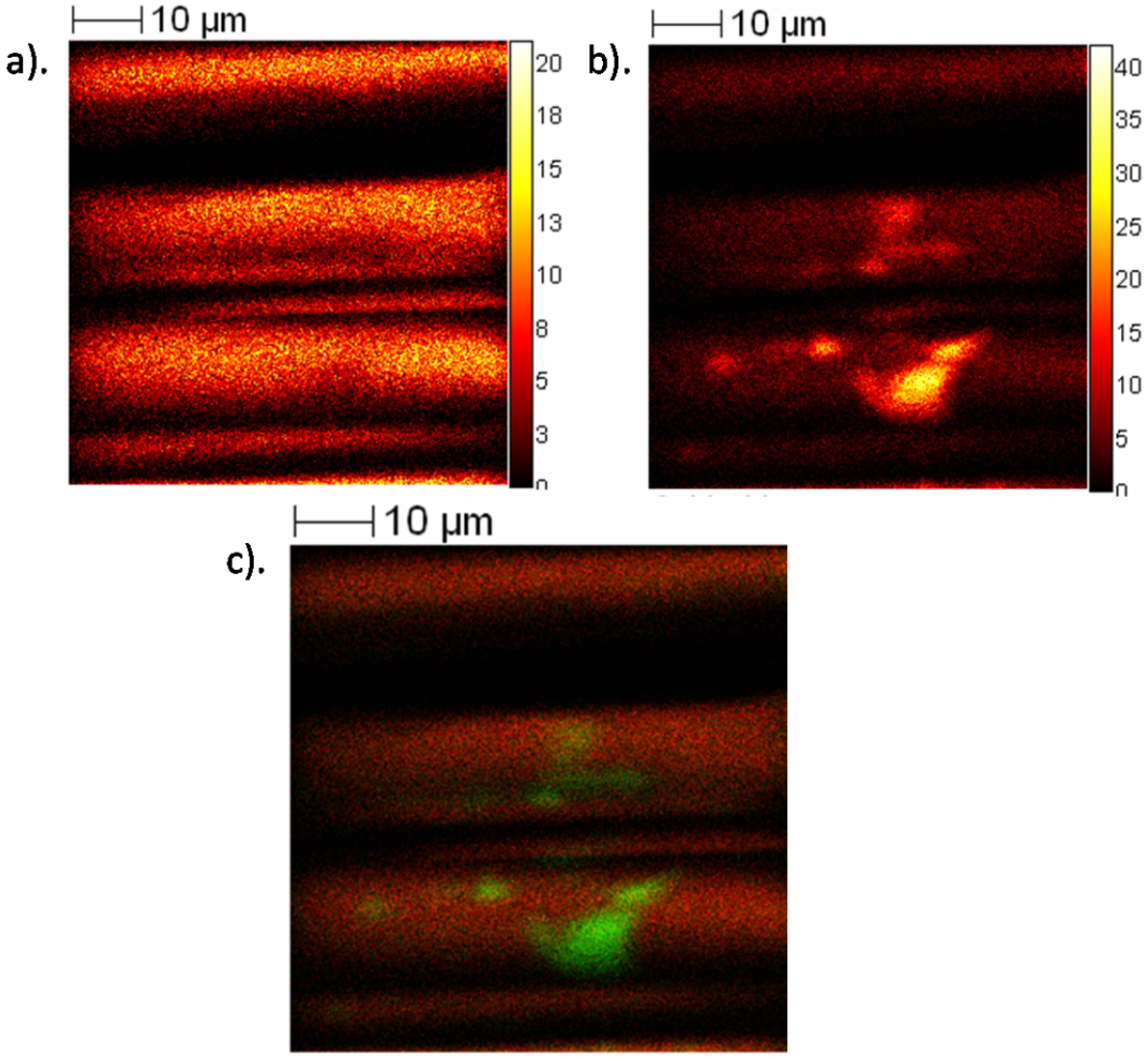

Figure 3. 9. Positive ion TOF SIMS mass spectral images showing the distribution of silane and imidazoline components on size-glass interface; a). $C_2H_5O^+$ at 45 amu is identified as the characteristic ion for silane which shows its uniform distribution; while b). $C_6H_{12}N^+$ at 98 amu is identified as the characteristic ion for imidazoline which shows peculiar agglomeration at center of fibers; and c). superimposed images of $C_2H_5O^+$ and $C_6H_{12}N^+$ showing distribution of silane (red) and imidazoline (green) in a sizing formulation.

3.3.4. Effect of the glass-size interface on the mechanical performance of the glass-polymer composites

Having characterized the surface properties of glass fibers at the glass-size interface, the next step was to determine the impact of the interface on the mechanical performance of their composites. The sixteen variedly sized glass fibers developed in this study were used to generate glass-polymer binder composites by the same method and their mechanical properties were measured.

Figure 3.10 shows the variation of mechanical properties of glass-polymer binder composite, namely dry tensile strength, mat tear strength and wet tensile strength, as a function of the silane and imidazoline concentrations in the sized glass fibers. These trends provide important information regarding the effect of each of these sizing components on the composite properties. The higher is the value of each property, better is its mechanical performance.

The dry tensile strength shows an increase with increase in the imidazoline concentration for most of the silane concentrations. The increase in the silane concentration on the other hand shows a reduction in the dry tensile strength for most of the imidazoline concentrations. Almost similar trends for the increase in imidazoline concentration are observed for the mat tear strength and wet tensile strength with a few exceptions. The increase in silane causes the shift of isoelectric point to high basic pH which leads to poor dispersion properties of these sized glass fibers while the increase in imidazoline controls the isoelectric point to be near the pH range of 6-7 which is important for good dispersion. Improved fiber dispersion in polyelectrolytes is essential for formation of good wet web structure which in turn is

important for good glass composite structure resulting in enhanced mechanical performance. Thus, increase in imidazoline concentration leads to increase in the mechanical performance of the composite. However, when no silane is used in the sizing formulation, the addition of 0.19% imidazoline leads to a decrease in the mat tear strength and wet tensile strength. At high imidazoline concentrations, though the mat tear recovers, the wet tensile strength does not change. The silane provides bonding site for the polymer binder and its presence is important for achieving good mechanical performance. An excess amount of silane not only increases the isoelectric point of the sized glass fibers but may also interfere with imidazoline distribution on the fiber surface leading to a decrease in the mechanical performance. So, an ideal system would have minimum silane and maximum imidazoline present in its sizing formulation. The highest dry and wet tensile strength values of the composite are obtained for 0.08% silane and 0.58% imidazoline sized glass fibers while the highest mat tear strength is obtained for 0.15% silane and 0.58% imidazoline sized glass fibers.

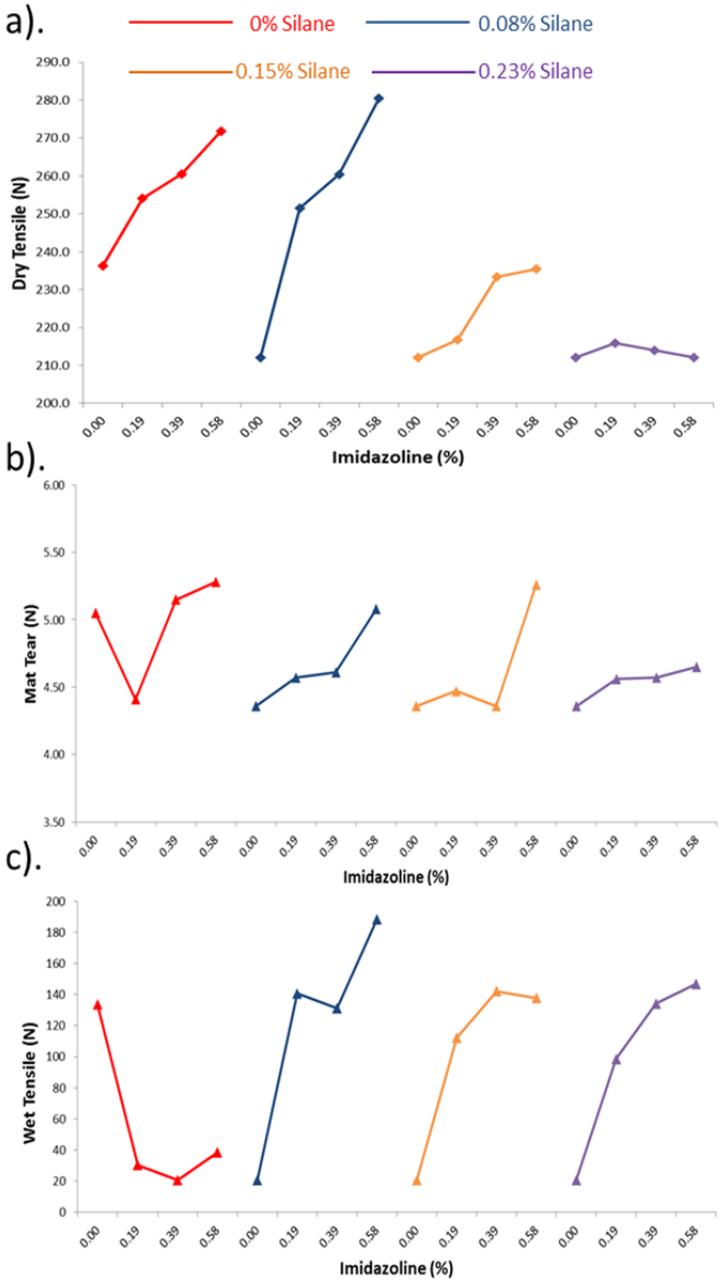

Figure 3. 10. Trends in a). dry tensile strength, b). mat tear strength and c). wet tensile strength as a function of imidazoline concentration (0%, 0.19%, 0.39%,0.58%) for each of the different silane concentrations (0%, 0.08%,0.15%, 0.23%) used in the sizing formulation.

Table 3.1 shows the statistical response of silane and imidazoline concentrations on the tear strength, dry tensile strength and wet tensile strength of the glass-polymer composite mats formed. The individual silane and imidazoline levels are significant and have a large effect on the mat tear. However, the higher order interactions between these two factors do not contribute towards the mat tear ($P < 0.05$). The dry tensile strength is affected by the individual silane and imidazoline levels as well as the higher order interactions between the two are significant ($P < 0.05$). This suggests that the interface plays a major role in dictating dry tensile strength in the glass mats. In case of wet tensile strength, the only significant factor is imidazoline level. The silane level and the higher order interactions between the two factors do not contribute towards the wet tensile strength ($P < 0.05$) and elucidates the importance of imidazoline at the interface. When the glass mat is wet with water, the imidazoline level at the interface dictates the tensile strength. The silane and the imidazoline components have interactions within the interface which affects the mechanical performance of the glass mats.

Table 3. 1. Significance on sizing parameters for increasing or decreasing the glass mat physical properties as predicted by the probability factor (significant if $p < 0.05$)

Sizing Formulation Component	Probability of Glass Mat Property		
	Tear Strength	Dry Tensile Strength	Wet Tensile Strength
Silane	**0.0350**	**<0.0001**	0.2925
Imidazoline	**0.0090**	**0.0006**	**0.0356**
Interaction between silane and imidazoline	0.8091	**0.0366**	0.0531

3.5. Conclusions

The sizing treatment of glass fibers is an important step during the glass-polymer composite formation and causes changes in its surface chemistry. The imidazoline component keeps the isoelectric point near neutral pH which is important for improved fiber dispersion properties. As silane concentration increases, the tear strength and dry tensile strength decreases with little effect on wet tensile strength. As imidazoline concentration increases, the tear strength as well as dry and wet tensile strength increases. The interaction between the two components is significant in influencing the tear strength. Thus, the glass-size interface dictates the mechanical performance of the composites. Also, the silane and imidazoline components distribute themselves in different ways in the glass-size interface. The silane seems to distribute itself uniformly while the imidazoline tends to agglomerate on the glass fiber surface.

3.6. References

1. Tanoglu, M.; McKnight, S. H.; Palmese, G. R.; Gillespie Jr, J. W. The effects of glass-fiber sizings on the strength and energy absorption of the fiber/matrix interphase under high loading rates. *Composites Sci. Technol.* **2001**, *61*, 205-220.

2. Gao, S. L.; Mäder, E.; Plonka, R. Coatings for glass fibers in a cementitious matrix. *Acta Materialia* **2004**, *52*, 4745-4755.

3. Wu, H. F.; Dwight, D. W.; Huff, N. T. Effects of silane coupling agents on the interphase and performance of glass-fiber-reinforced polymer composites. *Composites Sci. Technol.* **1997**, *57*, 975-983.

4. Sjögren, A.; Joffe, R.; Berglund, L.; Mäder, E. Effects of fibre coating (size) on properties of glass fibre/vinyl ester composites. *Composites Part A: Applied Science and Manufacturing* **1999**, *30*, 1009-1015.

5. Yang, L.; Thomason, J. L. Effect of silane coupling agent on mechanical performance of glass fibre. *J. Mater. Sci.* **2013**, *48*, 1947-1954.

6. Olmos, D.; González-Benito, J. Visualization of the morphology at the interphase of glass fibre reinforced epoxy-thermoplastic polymer composites. *European Polymer Journal* **2007**, *43*, 1487-1500.

7. Nishioka, G. M. Interaction of organosilanes with glass fibers. *J. Non Cryst. Solids* **1990**, *120*, 102-107.

8. Tesoro, G.; Wu, Y. Silane coupling agents: the role of the organofunctional group. *J. Adhes. Sci. Technol.* **1991**, *5*, 771-784.

9. Thomason, J. L.; Adzima, L. J. Sizing up the interphase: an insider's guide to the science of sizing. *Composites Part A: Applied Science and Manufacturing* **2001**, *32*, 313-321.

10. Plueddemann, E. P. *Silane coupling agents;* Plenum Press: New York, 1982; .

11. Zinck, P.; Mader, E.; Gerard, J. F. Role of silane coupling agent and polymeric film former for tailoring glass fiber sizings from tensile strength measurements. *J. Mater. Sci.* **2001**, *36*, 5245-5252.

12. DiBenedetto, A. T. Tailoring of interfaces in glass fiber reinforced polymer composites: a review. *Materials Science and Engineering: A* **2001**, *302*, 74-82.

13. Allen, K. W. Silanes as the interphase in adhesive bonds. *J. Adhes. Sci. Technol.* **1992**, *6*, 23-32.

14. DiBenedetto, A. T.; Lex, P. J. Evaluation of surface treatments for glass fibers in composite materials. *Polymer Engineering & Science* **1989**, *29*, 543-555.

15. Osterholtz, F. D.; Pohl, E. R. Kinetics of the hydrolysis and condensation of organofunctional alkoxysilanes: a review. *J. Adhes. Sci. Technol.* **1992**, *6*, 127-149.

16. Cech, V.; Prikryl, R.; Balkova, R.; Vanek, J.; Grycova, A. The influence of surface modifications of glass on glass fiber/polyester interphase properties. *Journal of Adhesion Science & Technology* **2003**, *17*, 1299.

17. Plueddemann, E. P. In *Performance of Silane Coupling Agents;* Springer US: 1991; pp 153-181.

18. Thomason, J. L. In *Interfaces and interfacial effects in glass reinforced thermoplastics;* Sørensen, B. F., Mikkelsen, L. P., Lilholt, H., Goutianos, S. and Abdul-Mahadi, F. S., Eds.; Proceedings of the 28th Risø International Symposium on Materials Science: Interface

Design of Polymer Matrix Composites – Mechanics, Chemistry, Modelling and Manufacturing ; 2007; pp 75-92.

19. Saraç, A. S.; Bismarck, A.; Kumru, M. E.; Springer, J. Electrografting of poly(carbazole-co-acrylamide) onto several carbon fibers: Electrokinetic and surface properties. *Synth. Met.* **2001**, *123*, 411-423.

20. Chiu, H.; Wang, J. The relationship between zeta-potential and pull-out shear strength on modified UHMWPE fiber reinforced epoxy composites. *Polymer Composites* **1998**, *19*, 347-351.

21. Schramm, L. L.; Mannhardt, K.; Novosad, J. J. Electrokinetic properties of reservoir rock particles. *Colloids and Surfaces* **1991**, *55*, 309-331.

22. Bismarck, A.; Kumru, M. E.; Song, B.; Springer, J.; Moos, E.; Karger-Kocsis, J. Study on surface and mechanical fiber characteristics and their effect on the adhesion properties to a polycarbonate matrix tuned by anodic carbon fiber oxidation. *Composites Part A: Applied Science and Manufacturing* **1999**, *30*, 1351-1366.

23. Nardin, M.; Papirer, E.; Schultz, J. An electrokinetic study of the interactions between glass fibers and aqueous solutions of calcium. *J. Colloid Interface Sci.* **1982**, *88*, 204-213.

24. Dong, D. In *Fiberglass surface and its electrokinetic properties;* Technical Association of the Pulp and Paper Industry, Ed.; 1998 TAPPI Proceedings - Nonwovens Conference And Trade Fair; Tappi Press: Atlanta, Ga., 1998; pp 305-315.

25. Zhuang, R. C.; Burghardt, T.; Plonka, R.; Liu, J. W.; Mäder, E. Affecting glass fibre surfaces and composite properties by two stage sizing application. *eXPRESS Polymer Letters* **2010**, *4*.

26. Rosenholm, J. M.; Linden, M. Wet-Chemical Analysis of Surface Concentration of Accessible Groups on Different Amino-Functionalized Mesoporous SBA-15 Silicas. *Chem. Mater.* **2007**, *19*, 5023-5034.

27. Pape, P. G.; Plueddemann, E. P. Methods for improving the performance of silane coupling agents. *J. Adhes. Sci. Technol.* **1991**, *5*, 831-842.

28. Fardim, P.; Durán, N. Modification of fibre surfaces during pulping and refining as analysed by SEM, XPS and ToF-SIMS. *Colloids Surf. Physicochem. Eng. Aspects* **2003**, *223*, 263-276.

29. Fardim, P.; Gustafsson, J.; von Schoultz, S.; Peltonen, J.; Holmbom, B. Extractives on fiber surfaces investigated by XPS, ToF-SIMS and AFM. *Colloids Surf. Physicochem. Eng. Aspects* **2005**, *255*, 91-103.

30. Biesinger, M. C.; Miller, D. J.; Harbottle, R. R.; Possmayer, F.; McIntyre, N. S.; Petersen, N. O. Imaging lipid distributions in model monolayers by ToF-SIMS with selectively deuterated components and principal components analysis. *Appl. Surf. Sci.* **2006**, *252*, 6957-6965.

CHAPTER 4

Influence of Surface Treatments on Glass Fibers and their wetting behavior

Abstract

Surface modification of glass fibers has helped to tailor its material interactions without changing the bulk properties. The glass fibers and binder have shown improved interactions due to various surface treatments on glass fibers like sizing and the use of polyelectrolyte treatments. The effects of these surface treatments on the surface properties of glass fibers and their synergistic interactions have not been extensively explored. In this work, we identify and distinguish between the sizing, polyelectrolyte and binder treatments on glass fibers. We discuss the effects of sizing and polyelectrolyte treatments on the surface chemistry of glass fibers and study the interactions between sized glass fibers and polyelectrolyte solution. The wetting properties indicate that polyelectrolyte treatment and sized glass fibers demonstrate hydrophilic synergistic interactions. The polyelectrolyte treatment on sized glass fibers covers the surface uniformly with non-specific adsorption after repeated cycles. The binder treatment on glass fibers improves the hydrophilic nature of the glass fiber surface.

4.1. Introduction

As it is well known that interfacial properties are governed by the chemical nature and physical compatibility between the fibers and the matrix, there are different surface modification techniques applied to the glass fiber surfaces to appropriately tune the interface[1]. The interface between glass fibers and the polymeric matrix is the most critical area in the glass composites[2]. If the composite is too rigid, the interface may lose its impact strength while poor adhesion at the interface may cause a reduction in tensile strength. Silane chemistry has popularly been used for surface modification of the glass fiber surfaces to improve the adhesion between glass fibers and polymer resin[3]. It serves the critical purpose of providing the chemical covalent linkage between the glass fibers and the polymeric binder. The silane coupling agent is first hydrolyzed and then the hydrolyzed silane condenses and reacts with the silanol groups on the glass fiber surface to form an interpenetrating siloxane network.

In the wet laid processing of glass mats, these sized glass fibers are chopped and then are dispersed in polyelectrolyte solutions[4]. The polyelectrolyte solution, also known in the industry as white water, consists of auxiliaries like surfactants, defoaming agents, and viscosity modifiers[5]. The non-ionic surfactants help in steric stabilization while the defoaming agents and viscosity modifiers are useful in maintaining the viscosity and foam properties during the mechanical agitation in dispersion process[6]. The most commonly used polyelectrolytes in glass fiber industry are polyacrylic acid, fatty amine alkoxylates and amine oxides. Uniform and dense mats are one of the key objectives in glass mat manufacturing. These properties are influenced greatly by the polyelectrolyte chemistry

along with other mechanical parameters like temperature, agitation energy, and raw material additions[7]. However, the dispersion of glass fibers in polyelectrolytes and the formation of glass web have shown to desire different properties. A greater repulsion between glass fibers has shown to achieve good fiber dispersion while the formation of a uniform glass web has required minimization of the fiber-fiber interactions. Generally, the solution to ensure good fiber dispersion and uniform glass web formation is a compromise between the two fiber interactions[8]. Thus, the interactions between sizing and polyelectrolyte are very important. There is a need to understand the interactions between glass fibers and these chemistries. The effect of these treatments on surface chemistry of glass fibers has not been explored. In this study, we consider only the polyelectrolyte chemistry contributions without any mechanical parameters. We discuss the effects of sizing and polyelectrolyte treatments on the surface chemistry of glass fibers as well as the interactions between sized glass fibers and polyelectrolyte solution.

The surface interactions are studied by understanding the wetting properties of these individual glass fibers. The wettability of fiber surfaces towards a liquid is a critical parameter in determining their interaction during processing[9]. The size and geometry of glass fibers makes it difficult and unreliable to measure the static contact angle with a goniometer[10]. In this study, dynamic contact angles of glass fibers are measured using the Wilhelmy balance technique[11]. The Wilhelmy method, where a microbalance is used to measure the wetting force, has often been employed for measuring the dynamic properties of thin fibers[12]. A single fiber is suspended on a microbalance and the beaker of the testing liquid sits below on a stage. For measurement, the liquid first advances towards the fiber at a

constant set velocity until the fiber surface contacts the liquid surface[13]. The liquid then continues to move in similar direction for a specified length of fiber. This is known as the advancing mode of dynamic contact angle which gives the advancing contact angle. After moving the specified length, the liquid moves away in the opposite direction until the liquid is no longer in contact with the fiber surface. This is known as the receding mode of dynamic contact angle which gives the receding contact angle. The difference between advancing and receding contact angle is known as hysteresis[14]. The force exerted on the fiber surface can be determined by the following equations[15]:

$$\text{Total force of fiber} = \text{Wetting force} + \text{Weight of fiber} - \text{Buoyancy force}$$

$$F = \gamma P \cos\theta + W - \rho g h A$$

Where;

F = Measured force

γ = Surface tension of wetting liquid

P = Wetted perimeter of glass fiber at liquid-air interface

θ = Contact angle of fiber surface

W = Weight of fiber

ρ = Density of wetting liquid

g = Gravitational acceleration

h = Immersion depth of fiber in wetting liquid

A = Cross-sectional area of fiber

The weight of the fiber is tared prior to every measurement and the buoyancy force is included in the measured force. With these assumptions, the force equation changes to the following:

$$F = \gamma P \cos\theta$$

The overall objective of this work is to understand the effects of sizing and polyelectrolyte treatments on the surface properties of glass fibers during formation of glass fiber – polymer composites. The individual objectives that we want to accomplish to attain the overall objective are as follows:

1. Determine the effects of sizing, polyelectrolyte and polymeric binder treatments on the surface composition of glass fibers
2. Determine the effects of sizing, polyelectrolyte and polymeric binder treatments on dynamic contact angle
3. Understanding synergistic interactions between size and polyelectrolyte as a function of dynamic contact angle

4.2. Materials and Methods

4.2.1. Glass fiber surface treatments

The commercial sized glass fibers from Owens Corning (OC) have proprietary surface chemistry and were obtained by GAF Materials Corporation. These glass fibers have proprietary sizings on their surface. The sized fibers were treated with the polyacrylamide Nalclear 7768, a commonly used polyelectrolyte for this application, in a beaker with

continuous stirring for few minutes until the fibers are dispersed well. The polyacrylamide treated fibers were taken out from the beaker and stored in petri dishes. The polyacrylamide treated fibers are then dipped in the binder solution. The co-binders used in this study were urea-formaldehyde resin (Casco Resin FG-413F) and acrylic polymer emulsion (Rhoplex GL-618). After the binder treatment, the fibers are cured in an oven at 213^{o}C for 2.5 min to form glass-polymer composites. The curing leads to formation of a fused fiber structure at lab scale and the individual binder treated glass fibers were carefully removed for further testing.

The following corollary has been used for describing the samples and various treatments in this paper:

Table 4. 1. Description of sample labeling used for surface treatments on glass fibers

Surface treatment	Method
Sized glass fibers	Sizing applied glass fibers as obtained
Polyelectrolyte treated glass fibers	Sized glass fibers treated with polyelectrolyte
Binder treated glass fibers	Polyelectrolyte treated sized glass fibers are immersed in binder solution and then cured

4.2.2. Time-of-flight Secondary Ion Mass Spectrometry (TOF-SIMS) analysis of glass fibers

TOF-SIMS is a surface sensitive technique which provides semi-quantitative data on surface chemistries such as elemental and molecular compositions, segregation of chemical components from top 10-20 Å of the surface. A typical spectrum is a plot of secondary ion

intensity counts versus mass to charge ratio (amu). In this paper, it has been used as a technique to compare the presence and distribution of silane and imidazoline components on the differently treated glass fiber surfaces.

TOF-SIMS analyses were conducted using a TOF-SIMS V (ION TOF, Inc. Chestnut Ridge, NY) instrument equipped with a Bi_n^{m+} (n = 1 - 5, m = 1, 2) liquid metal ion gun. The instrument vacuum system consists of a load lock for sample loading and an analysis chamber, separated by the gate valve. The analysis chamber pressure is maintained below 5.0 x 10^{-9} mbar to avoid contamination of the surfaces to be analyzed. For the high mass resolution spectra acquired in this study, a 128 by 128 pixel spectrum of a 100 μm by 100 μm area was acquired using a Bi_3^+ primary ion beam under High Current Bunching Mode. For the mass spectral images, a 256 by 256 pixel image of a 200 μm by 200 μm area was acquired using a Bi_3^+ primary ion beam under Burst Alignment Mode.

4.2.3. Dynamic contact angle

The contact angle measurements were performed using a Data Physics DCAT 11 Model dynamic contact angle measuring system and tensiometer system with SCAT 11 software. The single glass fiber interactions were studied using the dynamic contact angle. The single glass fibers were attached on the special single fiber assembly on the DCAT with the help of special glue. For each sample, single individual fibers were carefully hung on the assembly at 1mm distance apart and ensured that the fibers were not touching or overlapping. The fibers were hung such that they are perpendicular to the wetting liquid surface and the length of each of the fibers was kept similar by using small scissors. Once the assembly was prepared, it was loaded on the DCAT and the wetting liquid was poured in the beaker below. It was

ensured that the fibers and the liquid surface was absolutely still before any measurement. A special case Wilhelmy balance method was used for measuring the dynamic contact angle. The average diameter of glass fiber (r) was measured under confocal microscope and used for each treatment for calculating the wetting parameters. The wetting parameters were calculated for each fiber via the following equation and multiplied by number of fibers used on the assembly to determine the total wetted parameters:

Wetted length = $2\pi r$

Wetted area = πr^2

Even though the fibers were cut for equal lengths, there is a possibility that the wetting liquid first had contact with individual fibers at different times. This results in fluctuations in wetting forces during initial immersion. The data for calculating contact angle was fitted after 1mm immersion depth to ensure all single fiber interactions were recorded for calculation of the dynamic contact angle. Also, it was ensured that none of the results were considered in case one or more of the fibers came off, buckled, fell into the wetting liquid or did not stay perpendicular to the surface while entering[16]. The SCAT software plots the contact angle data from 1mm to the chosen immersion depth and fits a linear regression line to the data. This regression line is extrapolated to zero depth of immersion and is reported as the dynamic contact angle.

The DCAT was also used for the measurement of static surface tension of wetting liquids as a function of time. The measurement employs Wilhelmy plate method by means of a platinum plate PT 11 according to standard DIN 53914 for surface tension of unknown liquids with assumption of complete wetting of the plate.

4.3. Results and Discussion

4.3.1. Effects of treatments on surface composition of glass fibers

To determine the effects of different surface treatments of sizing, polyelectrolytes and binder on the surface composition of glass fibers, we used Time-of-flight secondary ion mass spectrometry (TOF-SIMS). We also used it to determine the specific ions belonging to each treatment and see how each of them covers the glass fiber surface.

4.3.1.1. Negative ion spectrum

The negative ions generate poor mass resolution spectrum causing difficulty in distinguishing between different surface treatments. However, it still provides a good tool to understand the effects of each surface treatment on the glass fiber surface.

Figure 4.1 shows the effect of polyelectrolyte treatment on the sized glass fiber surface. The comparison of peaks is helpful to identify particular ions belonging both to size and polyelectrolyte treatments. The sized glass fibers show strong peaks for O^- (16 amu) and Si^- (28 amu) which show a reduction in intensity in the polyelectrolyte treated glass fibers. Also, the peaks of CN^-(26 amu), C_2HO^- (41 amu) and CNO^- (42 amu) show a great increase in the polyelectrolyte treated glass fibers. The changes of the intensities of these ions are due to the presence of polyacrylamide in the white water. It is very difficult to unambiguously differentiate these samples due to the presence of amide groups in all the different surface treatments of interest - sizing, polyelectrolyte and the binder treatments. However, the intensity variations for certain ions can help to confirm the surface modification. These peaks are plotted for comparing the change in peak intensity separately in **Figure 4.2**.

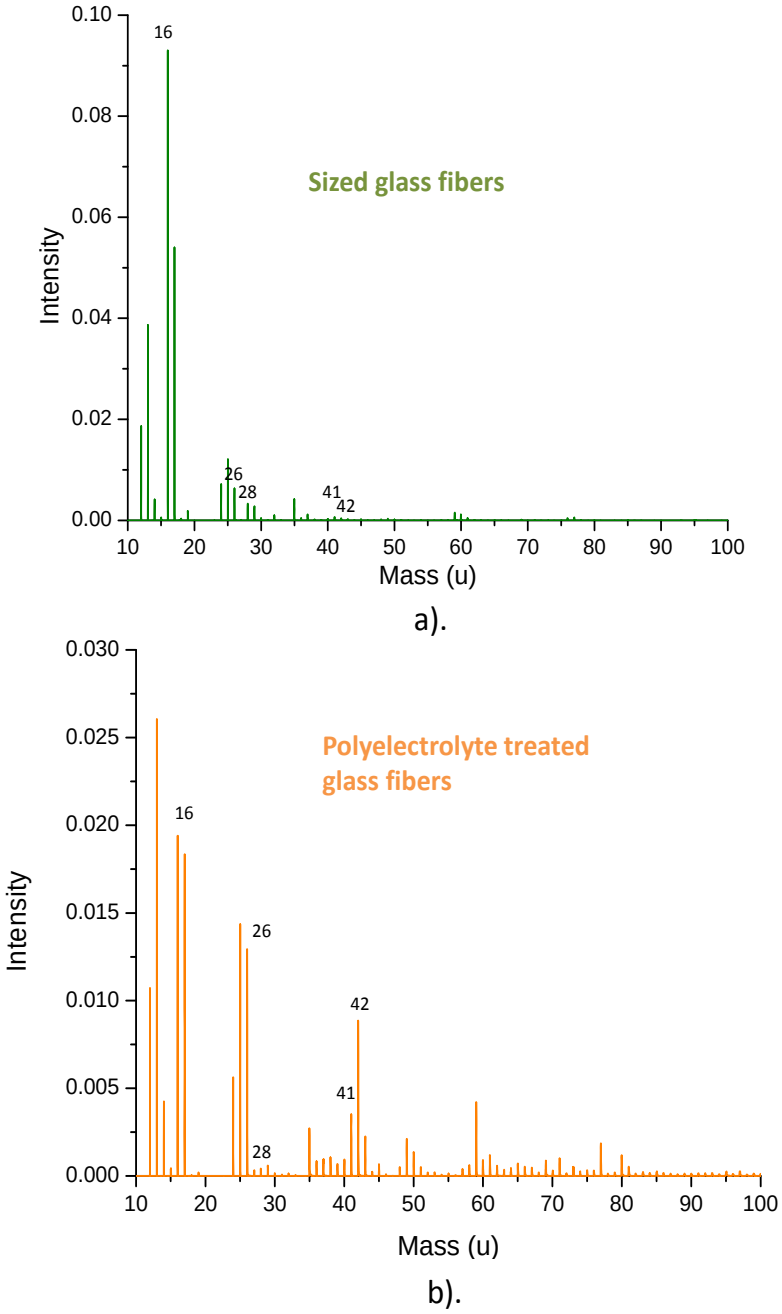

Figure 4. 1. TOF-SIMS negative ion spectra of surface of glass fibers which are a). sized and b). polyelectrolyte treated for identification of particular ions belonging to each treatment.

Figure 4.2 shows the comparison of peak intensities for the ions identified in Figure 1 to distinguish between sized glass fibers and polyelectrolyte treated glass fibers. The Si and O linkages form the core surface of glass fibers. The sizing, which mainly comprises of alkoxysilanes, also has Si and O elements in abundance. Once the sized glass fibers are treated with polyelectrolyte, the polyelectrolyte covers the surface of these sized glass fibers. This causes a reduction in the ion intensities of O^- (16 amu) and Si^- (28 amu) after polyelectrolyte surface treatment. The polyelectrolytes main constituent is polyacrylamide which has amide species in abundance. This leads to an increase in the ion intensities of CN^- (26 amu), C_2HO^- (41 amu) and CNO^- (42 amu) after polyelectrolyte treatment.

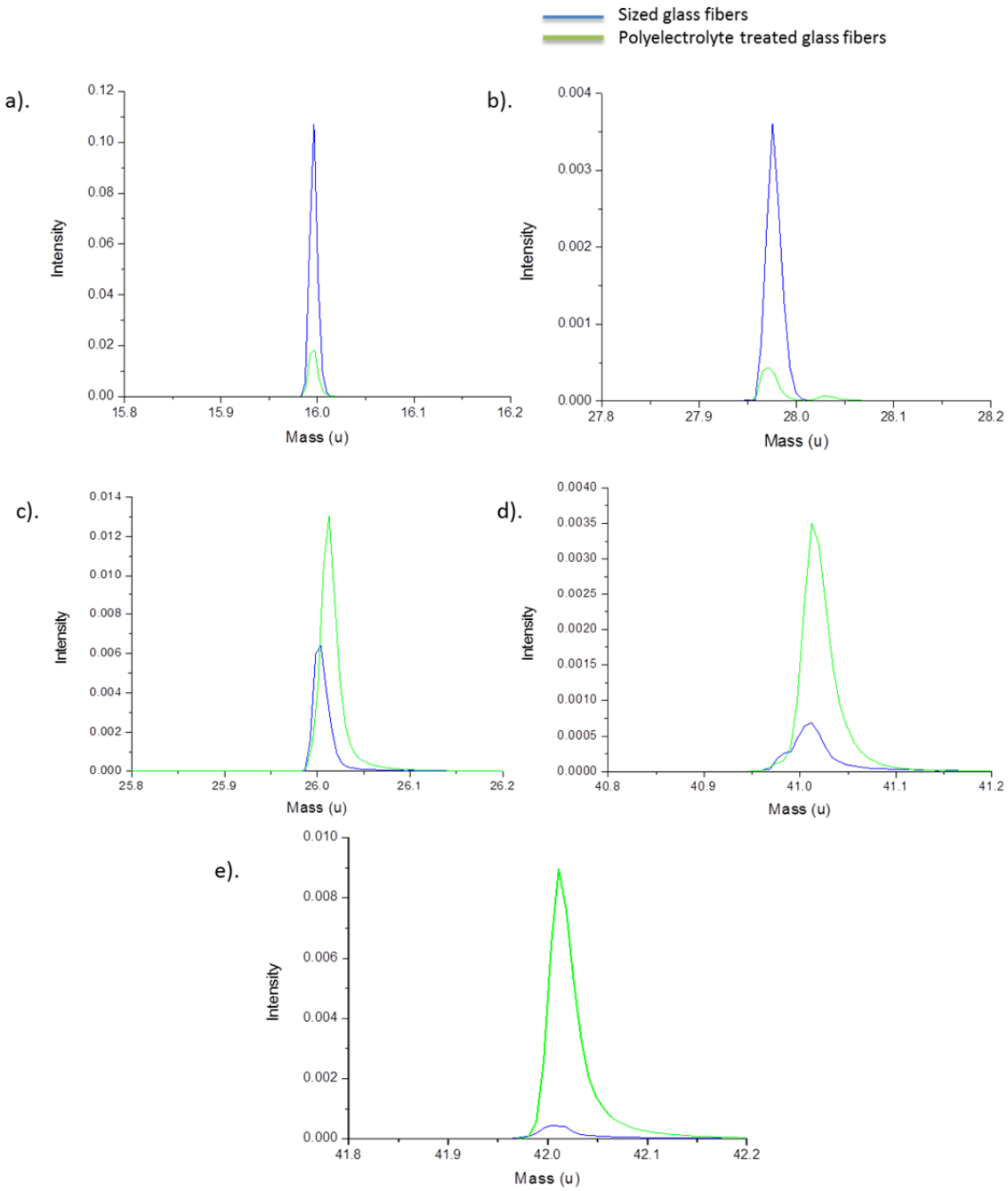

Figure 4. 2. Peak intensity comparison of TOF-SIMS negative ion spectra to distinguish sized glass fibers and polyelectrolyte treated glass fibers for each of the following ions: a). O^- (16 amu), b). Si^- (28 amu), c). CN^-(26 amu), d). C_2HO^- (41 amu), and e). CNO^- (42 amu).

The O^- and Si^- ions are specific to sizing which show a drastic decrease in intensity after polyelectrolyte treatment while the CN^-, C_2HO^-, CNO^- ions which are specific to polyelectrolyte show a drastic increase in intensity indicating coverage of sizing treatment by polyelectrolyte

Figure 4.3 shows the comparison of TOF-SIMS negative ion spectra polyelectrolyte treated and binder treated glass fibers. Although it is very difficult to associate and define peaks belonging to the polyelectrolyte treatment, the binder treated glass fibers show some unique peaks belonging to the binder which can be useful to differentiate between the two treatments. The peaks of $C_2HN_2^-$ (53 amu), $CH_3N_2O^-$ (59 amu), $C_2N_3^-$ (66 amu), $C_2HN_2O^-$ (69 amu) can be prominently seen in the binder treated glass fibers having high ion intensities but are present in the white water treated glass fiber as well. Other less prominent peaks present in the binder treated glass fibers can be identified as belonging to surfactant in the binder and are completely absent or present at very low intensity in the polyelectrolyte treated glass fibers. These peaks are identified as SO_3^- (80 amu), SO_4^- (96 amu) and HSO_4^- (97 amu). These results confirm the presence of binder on the glass fiber surface. The peak intensities of these peaks are further discussed in Figure 4. Also, some characteristic ions of sized glass fiber including Si^- (28 amu), SiO_2^- (60 amu) and SiO_3^- (76 amu) show higher ion intensities in the binder treated glass fibers but very low intensities in the polyelectrolyte treated glass fibers. This may suggest that during binder treatment process, polyacrylamide was washed off from surface.

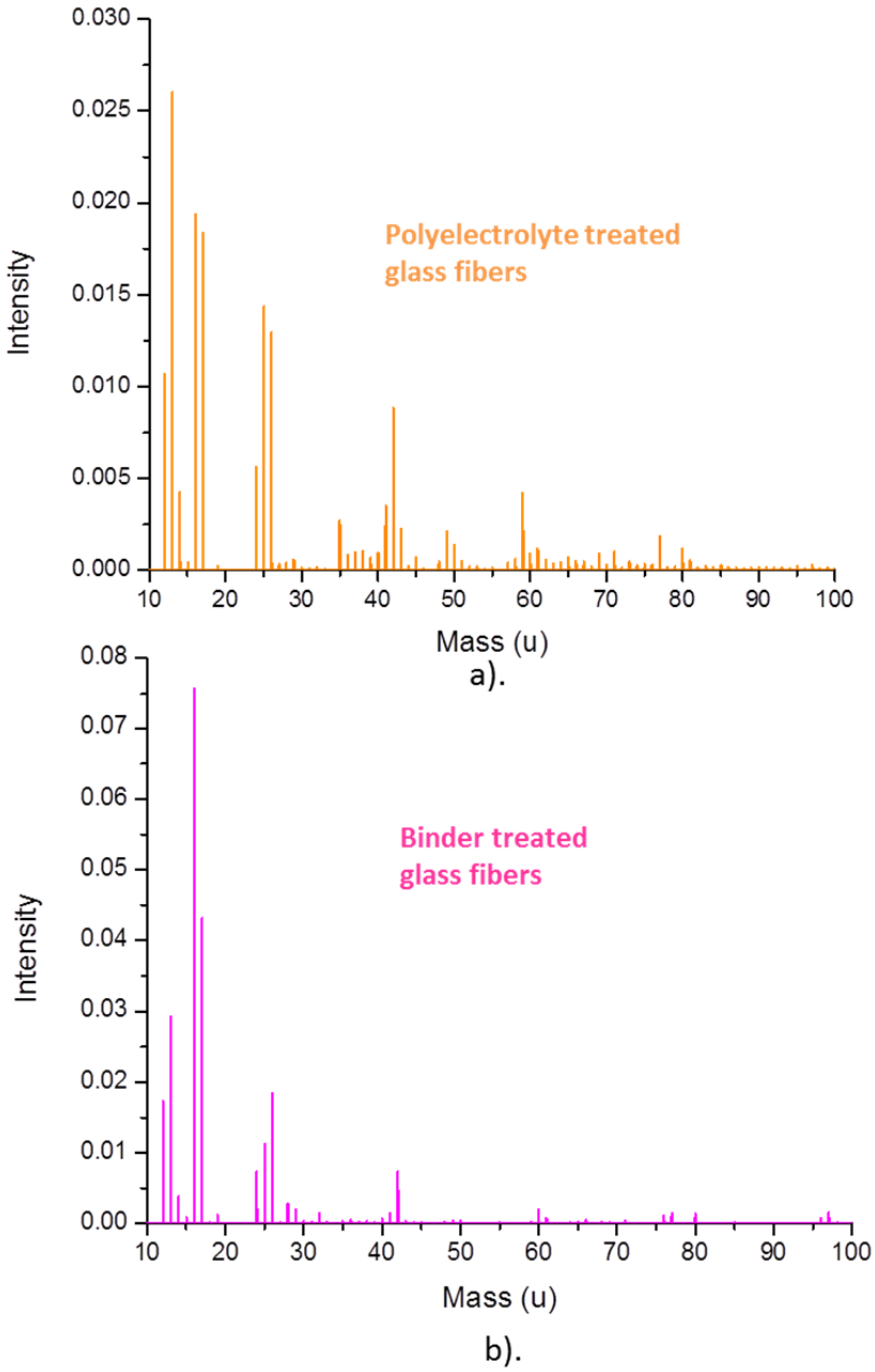

Figure 4. 3. TOF-SIMS negative ion spectra of surface of glass fibers which are a). polyelectrolyte treated and b). binder treated

Figure 4.4 shows the comparison of peak intensities for the ions identified in Figure 3 to distinguish between polyelectrolyte treated and binder treated glass fibers. The presence of amide, in both polyelectrolyte and binder, makes it difficult to identify the N based specific ions for each treatment. However, the surfactant molecules, which are an integral moiety in the binder formulation, are useful in distinguishing binder treatment from polyelectrolyte treatment. The SO_4^- (96 amu) and HSO_4^- (97 amu) ions are present in minimum quantities in the polyelectrolyte while show strong presence in the binder. As seen earlier from Figure 3, the polyelectrolyte comes off during the binder treatment while the binder specific surfactant ions cover the surface of glass fibers and hence show high higher intensities.

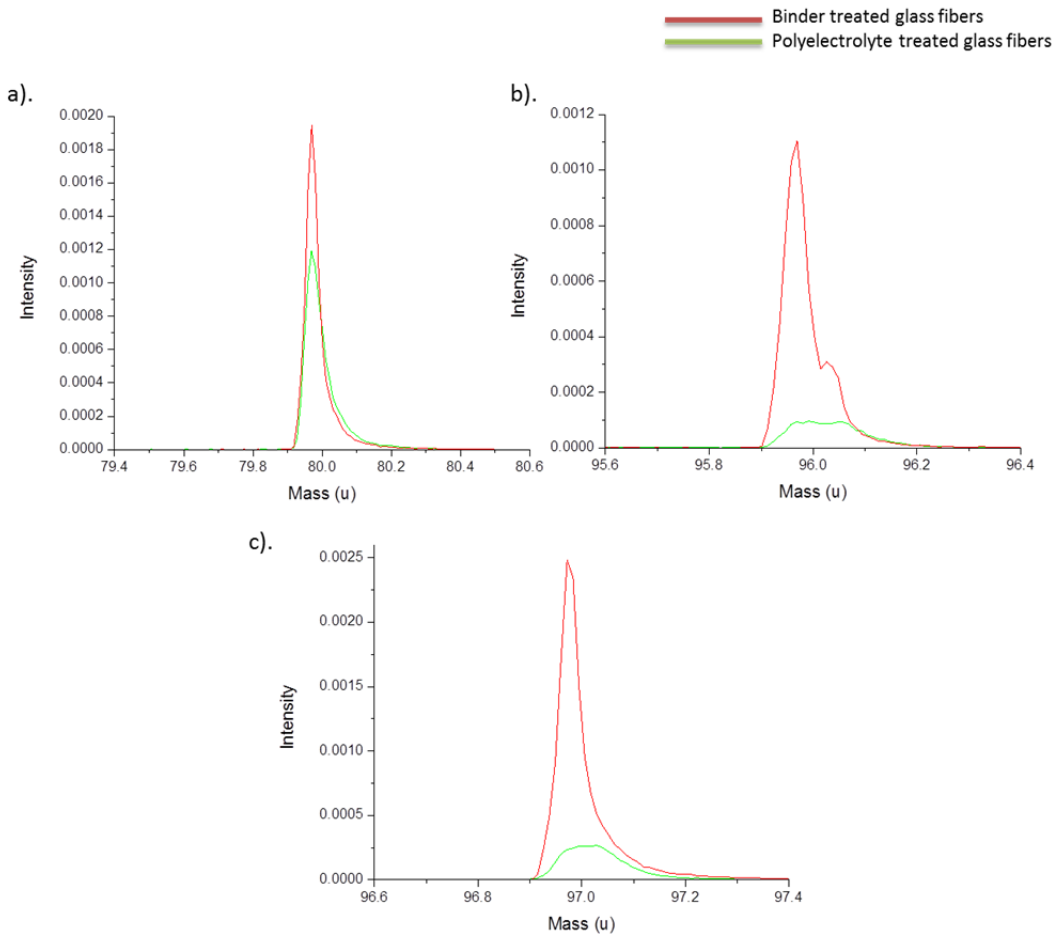

Figure 4. 4. Peak intensity comparison of TOF-SIMS negative ion spectra to distinguish between polyelectrolyte treated glass fibers and binder treated glass fibers for each of the following ions: a). SO_3^- (80 amu), b). SO_4^- (96 amu) and c). HSO_4^- (97 amu). Due to the similarity in amide chemistry in both polyelectrolyte and binder, the surfactant part of the binder is very useful to understand the presence and coverage of binder. The binder appears the similarity in amide chemistry in both polyelectrolyte and binder, the surfactant part of the binder is very useful to understand the presence and coverage of binder. The binder appears to cover the polyelectrolyte treatment.

The spectrum of binder treated glass fibers were compared to that with glass mats with binder to ensure the treatment simulation was correct. The spectra looked identical for both negative and positive ions (Appendix B) for both the samples. The negative ion spectrum for both fibers and mat showed poor mass resolution while the positive ion spectrum showed reduced intensity for the glass fibers due to the fiber structure and waviness which presents a challenge in collecting high mass resolution spectrum. Also, the fibers are not completely flat lying at some places and there are multiple fibers adjacent to each other which results in poor mass resolution.

4.3.1.2. Positive ion spectrum

The positive ions generated high resolution mass spectrum which helped in easily distinguishing between all the surface treatments on glass fibers.

The effect of polyelectrolyte treatment on sized glass fiber surfaces can be studied from **Figure 4.5**. The prominent peak of Si^+ (28 amu) in the sized glass fiber sample is considerably reduced in the polyelectrolyte treated fiber. However, in this case, most of the other peaks are difficult to differentiate due to the presence of amide in both treatments. Some other peaks like $C_3H_5^+$ (41 amu), $C_2H_3O^+$ (43 amu) can be identified belonging to sized glass fibers. These peaks show reduced intensity in the polyelectrolyte treated glass fibers as shown in **Figure 4.6**. Some peaks not shown in this image belong to long chain fatty amide like $C_{20}H_{40}NO^+$ (310 amu) are very high in the sized glass fibers. These probably belong to the long alkyl chain imidazoline present in the sizing formulation. This peak is not observed with strong intensity on the polyelectrolyte treated fibers showing this treatment may be covering the sized glass fiber surface.

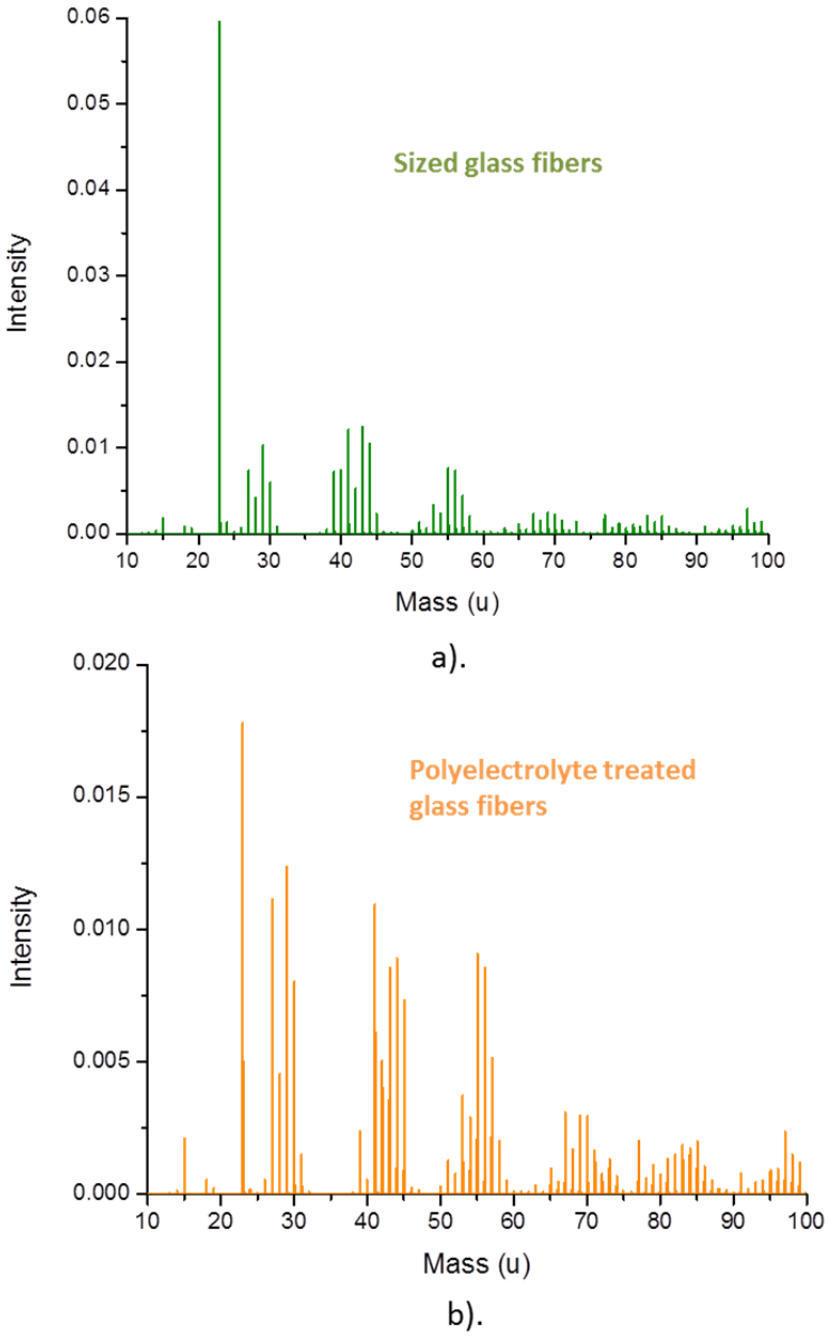

Figure 4. 5. TOF-SIMS positive ion spectra of surface of glass fibers which are a). sized and b). polyelectrolyte treated

The $C_3H_5^+$ (41 amu), $C_2H_3O^+$ (43 amu) ions belong to the alkoxy part of the alkoxysilanes present in the sizing. The $C_3H_5^+$ (41 amu) peak has good presence in polyelectrolyte but is lower than that present in sizing while $C_2H_3O^+$ (43 amu) shows very little presence in polyelectrolytes as shown in **Figure 4.6**. The 43 amu when plotted exclusively shows two distinct peaks separated by a very small mass unit (~ 0.04 amu) which makes it difficult to define them. The 43.02 amu peak is for the $C_2H_3O^+$ ion, which is of importance to differentiate sizing and polyelectrolyte treatment.

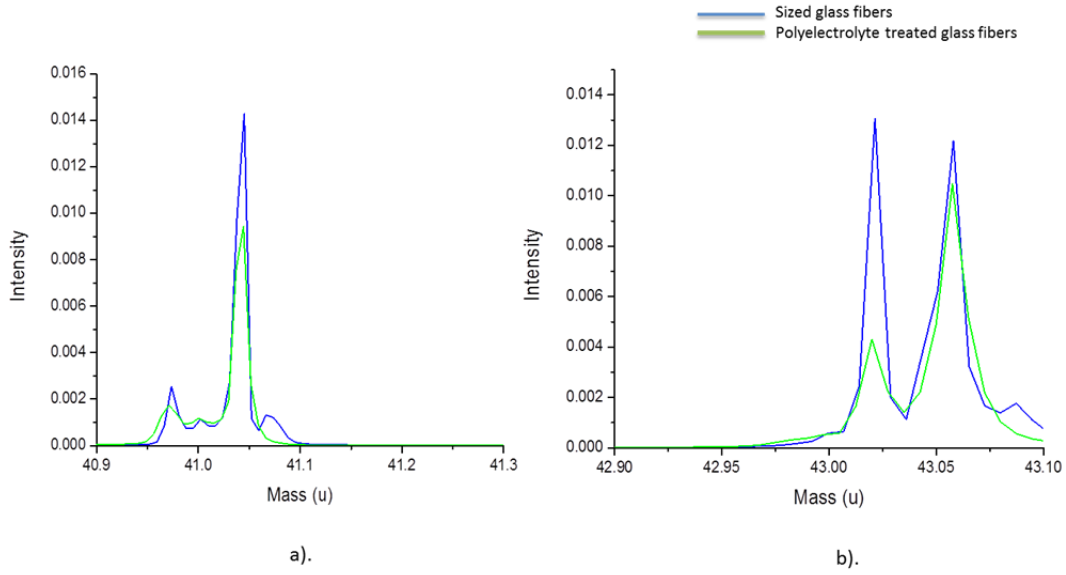

Figure 4. 6. Peak intensity comparison of TOF-SIMS positive ion spectra to distinguish sized and polyelectrolyte treated glass fibers for a). $C_3H_5^+$ (41 amu), and b). $C_2H_3O^+$ (43 amu) ions. The reductions in intensities of these sizing specific ions indicate coverage with polyelectrolytes.

Figure **4.7** shows the comparison of polyelectrolyte treated and binder treated glass fibers. The unique peaks belonging to the binder can be easily identified in the binder treated glass fiber as CH_4N^+ (30 amu), $C_2H_4N^+$ (42 amu), $C_2H_3N_2O^+$ (71 amu), and $C_3H_5N_2O^+$ (85 amu). The binder peaks are very sharp and peculiar and are prominently visible in the binder treated glass fibers and show very low intensity or are absent in the polyelectrolyte treated fiber.

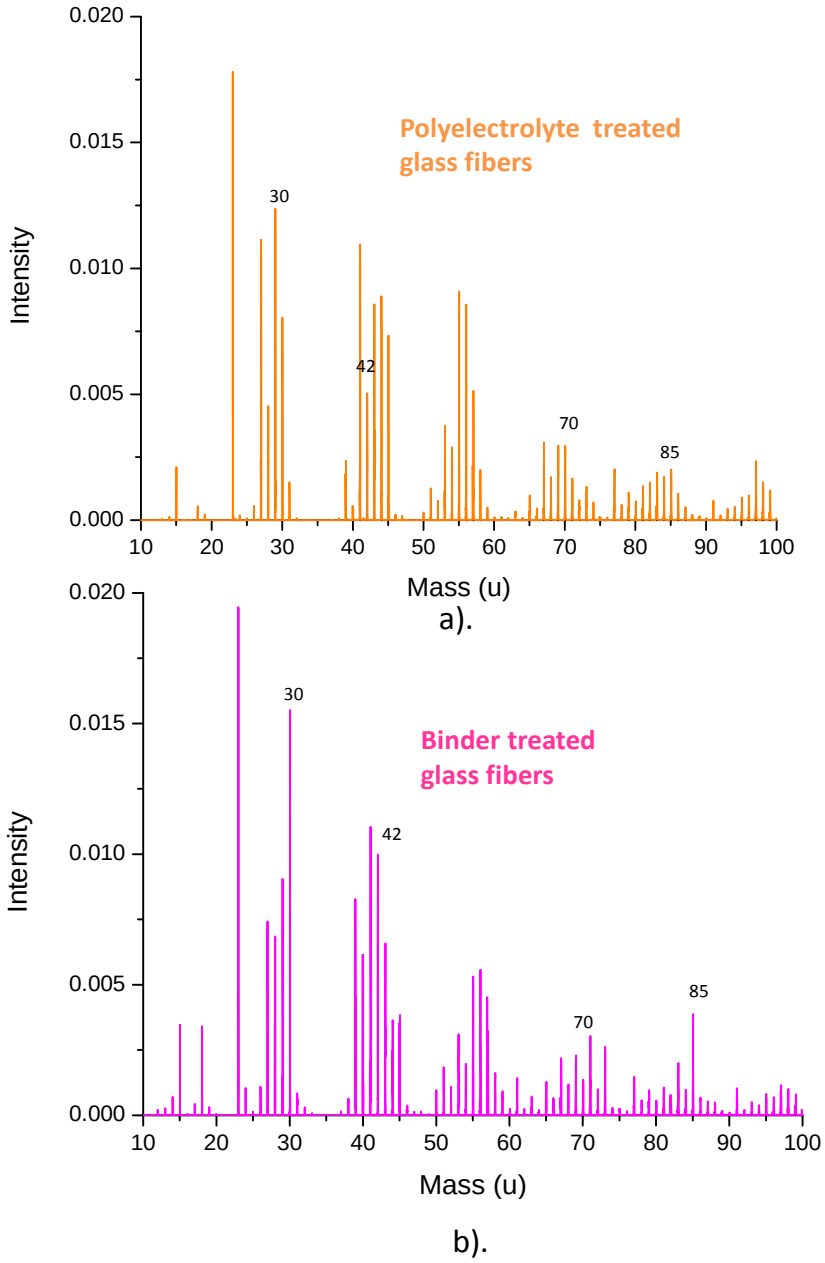

Figure 4. 7. TOF-SIMS positive ion spectra of surface of glass fibers which are a). polyelectrolyte treated and b). binder treated

The CH_4N^+ (30 amu), $C_2H_4N^+$ (42 amu), $C_2H_3N_2O^+$ (71 amu), and $C_3H_5N_2O^+$ (85 amu) ions belong to the urea-formaldehyde (U-F) resin modified with acrylic polymer binder. The nitrogen containing ions belonging mainly to the highly cross-linked three dimensional network structure of U-F resin peak show distinctly in the binder treated glass fibers. They are completely absent in the polyelectrolyte treated glass fibers and all the four ions show presence of a different species adjacent to the respective fragment (the difference in mass of peak heights is about 0.1 amu) as shown in **Figure 4.8**. This confirms the presence of binder on the glass fiber surface and helps differentiate it from the polyelectrolyte treatment.

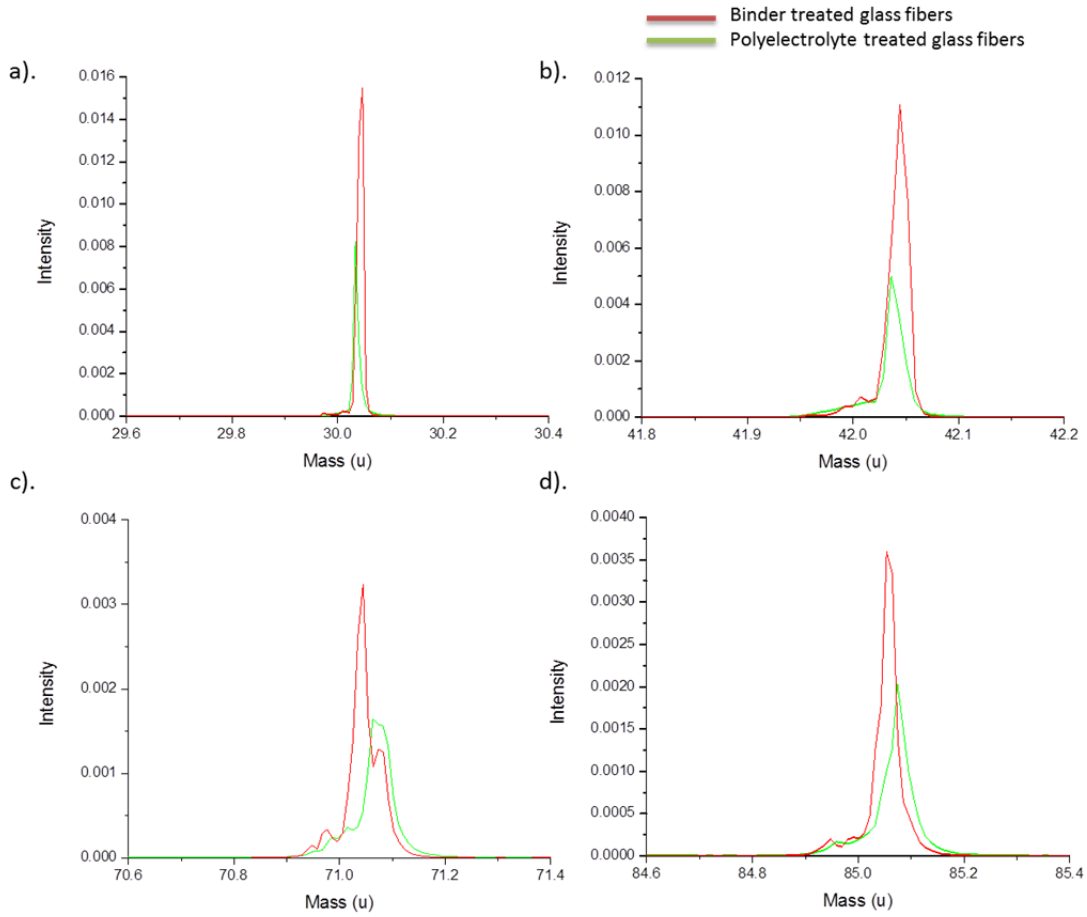

Figure 4. 8. Peak intensity comparison of TOF-SIMS positive ion spectra to distinguish polyelectrolyte treated and binder treated glass fibers for each of the following ions: a). CH_4N^+ (30 amu), b). $C_2H_4N^+$ (42 amu), c). $C_2H_3N_2O^+$ (71 amu), and d). $C_3H_5N_2O^+$ (85 amu). The high intensity of each of the unique ions belonging to the binder in comparison to polyelectrolyte indicates the coverage of binder on the glass fiber surface.

4.3.2. Effect of surface treatments on dynamic contact angles

We studied the effect of treatments like sizing, polyelectrolyte and binder on the surface properties of the glass fibers using dynamic contact angle measurements. It can specifically

help us understand the effect of different surface treatments on the wetting properties of the glass fibers. There are mainly two different significant directional effects that are observed in dynamic contact angle measurements using this modified Wilhelmy plate method. There is a contrast in forces measured in the advancing as well as in the receding directions. The difference between the advancing and the receding contact angle is known as the hysteresis and the force plot for the two directions is known as the hysteresis loop. The advancing forces give information on the hydrophobic forces acting on the fiber surface as the fiber tries to advance through the wetting liquid while the receding forces give information on the hydrophilic forces acting on the fiber surface as the fiber tries to leave the liquid surface.

The typical force plot obtained during dynamic contact angle measurements is shown in **Figure 4.9** for the interactions of sized glass fibers with deionized water. At the initial contact of sized glass fiber with water, the forces show a very small positive value indicating downward force acting on fiber which would indicate it is slightly hydrophilic in nature. The hysteresis is evident as the wetting force in the advancing direction is much lower than the wetting force in the receding direction. As the fiber comes out of water and the contact is broken, there is no wetting force recorded further. Since this test was conducted by hanging about five fibers, the force curves tend to be extremely wavy and they enter the water in the first 1 mm immersion depth at different times. However, it gives true information regarding the wetting behavior after 1 mm immersion depth. The sized glass fibers appear to be slightly hydrophilic with an advancing contact angle of around 85 degrees and receding contact angle of around 57degrees as shown in **Table 4.2**. The sizing contains alkoxysilanes which have affinity for water and impart hydrophilic properties while the imidazoline component imparts

the hydrophobic component. This results in a slightly hydrophilic surface for sized glass fibers. Uniform distribution of sizing on glass fiber surface is important for achieving improved glass mat properties.

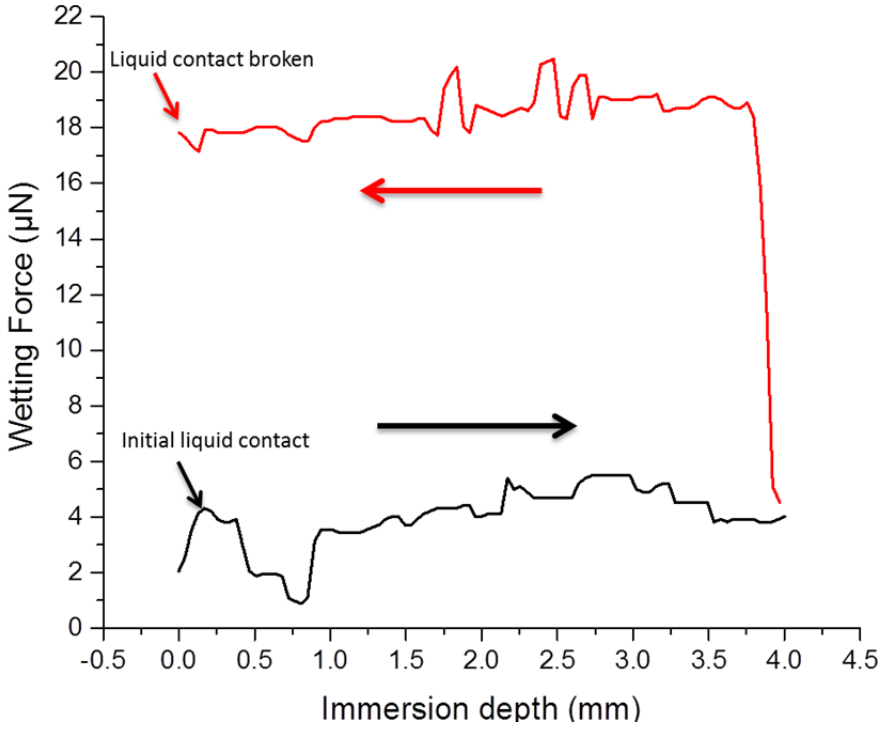

Figure 4. 9. Force plots obtained for sized glass fibers interaction with water for advancing (black) and receding modes (red) of dynamic contact angle. The small hydrophilic force at the initial contact between the sized glass fibers and water suggest slightly hydrophilic nature of the sizing treatment.

Figure 4.10 compares the dynamic contact angle loops for sized glass fibers, polyelectrolyte treated glass fibers and binder treated glass fibers. The sized glass fiber surface shows

moderately uniform contact angle in both advancing and receding cycles over its immersion depth indicating uniform sizing coverage over the glass fibers. The polyelectrolyte treated glass fibers show an advancing contact angle of about 90 degrees and a receding contact angle of around 61 degrees as shown in **Table 4.2**. The amide groups present in the polyelectrolyte tend to impart the hydrophobic nature to the glass fiber surface. The polyelectrolyte does not chemically react with the sizing on the glass fiber surface but does adsorb on the sized glass fiber surface. The coverage of polyelectrolyte on the sized glass fiber surface is non-uniform as there is considerable variation in the contact angle along the fiber length. The polyelectrolyte treated glass fibers appear more hydrophobic as compared to the sized glass fibers.

Table 4. 2. Effect of surface treatments on dynamic contact angles

Surface treatment	**Advancing contact angle (degrees)**	**Receding contact angle (degrees)**
Sized glass fibers	84.8 $\pm$ 0.8	57.2 $\pm$ 0.7
Polyelectrolyte treated glass fibers	89.8 $\pm$ 1.9	61.5 $\pm$ 16
Binder treated glass fibers	86.1 $\pm$ 1.5	54.5 $\pm$ 2

The washing of polyelectrolyte treated glass fibers removes most of the polyelectrolyte that has covered sized glass fibers and renders it back to slightly hydrophilic with an advancing contact angle of 75 degrees with no statistical difference from sized glass fibers. The washing

of polyelectrolyte treated glass fibers with water not only removes the polyelectrolyte but also leaves the surface wet which leads to retention of water as the fiber pulls out of water during receding direction.

The binder treated glass fibers shows highly non-uniform coverage of binder on the glass fiber surface. The advancing contact angle is around 86 degrees while the receding contact angle is about 55 degrees. The Urea-Formaldehyde modified acrylic binder has certain hydrophilic moieties which imparts slightly hydrophilic nature to the binder treated glass fibers. Also, the binder treatment covers the previous sizing and polyelectrolyte treatments but the coverage is non-uniform. The receding cycle is dictated by the hydrophilic character of the fiber surface and the binder treated glass fibers have non-uniformly coated hydrophilic moieties present on their surface which causes the large variations in receding contact angle.

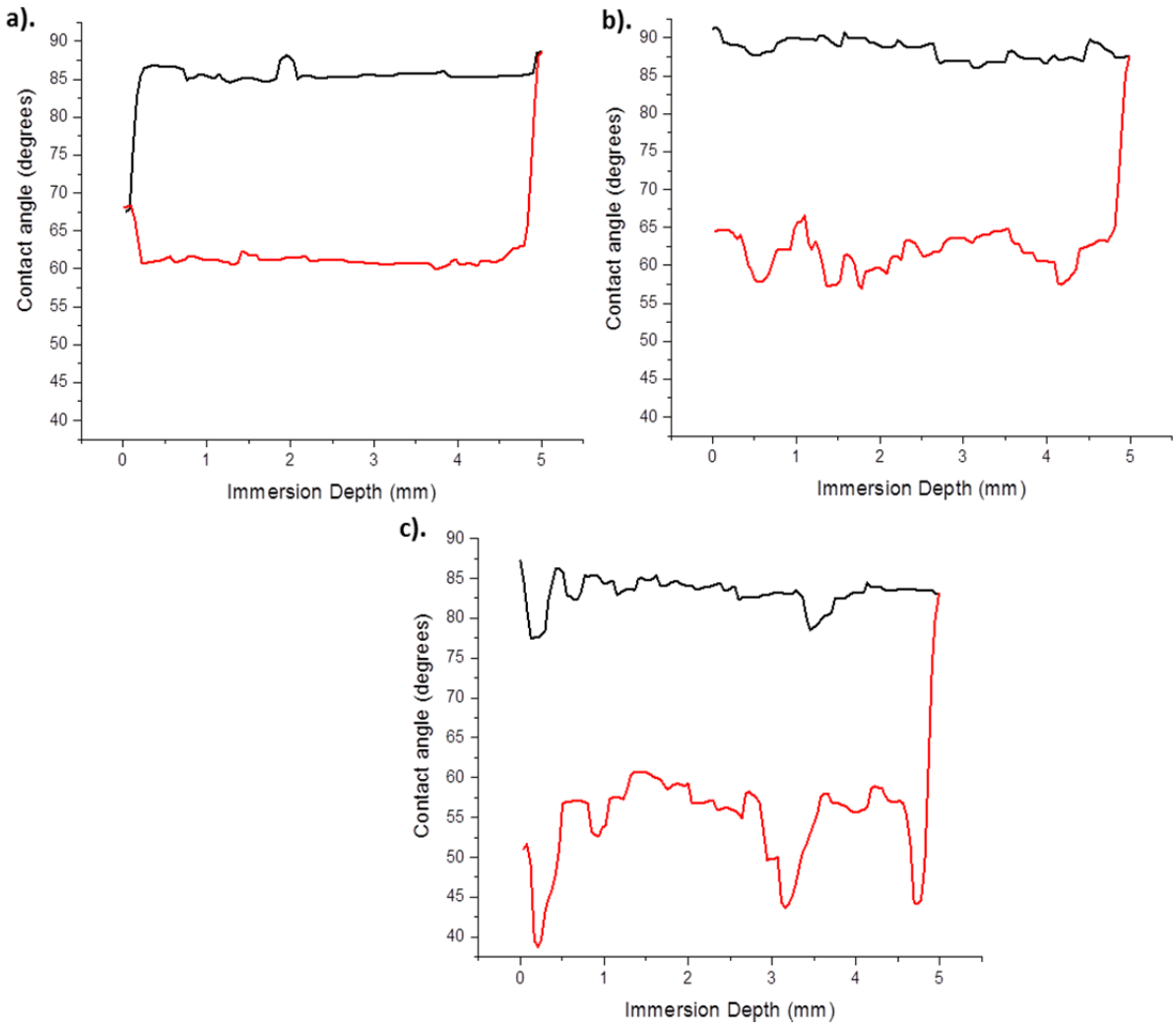

Figure 4. 10. Dynamic contact angle loops showing advancing (black) and receding (red) contact angles for a). sized glass fibers, b). polyelectrolyte treated glass fibers and c). binder treated glass fiber surfaces interaction with water. The polyelectrolyte treatment shows hydrophobic nature while the sized surface and binder treated surface shows slightly hydrophilic nature. The receding contact angle for binder is very wavy due to non-uniform retention of water by the binder treated glass fibers.

4.3.3. Wetting behavior of sized glass fibers with polyelectrolyte

Apart from understanding the wetting properties of glass fibers after different surface treatments, we also wanted to understand the interactions between sized glass fibers and the polyelectrolyte. This can provide valuable information about the interactions during dispersion of glass fibers during the glass mat formation process.

We used polyacrylamide as our testing liquid and sized glass fibers as the testing body. The surface tension of polyacrylamide was measured using DCAT by Wilhelmy plate method[17]. The surface tension as a function of time obtained is plotted in **Figure 4.11**. When a flat plate is partially immersed in the liquid with a horizontal upper force, the total force needed to keep the plate immobile is related to the weight of the plate, surface tension of liquid and buoyancy forces. As the weight and buoyancy is dealt by the instrument and software, the surface tension can directly be measured. As the plate touches the polyelectrolyte solution, the initial wetting forces recorded are very high at the liquid/air interface which results in a higher value. The surface tension will decrease as a function of time as less force is needed to keep the plate immobile once it has touched the liquid at the interface. The decrease continues till an equilibrium is obtained and the average surface tension for the polyelectrolyte solution is recorded as 28 mN/m. This value is useful for understanding the interactions of polyelectrolyte with sized glass fibers.

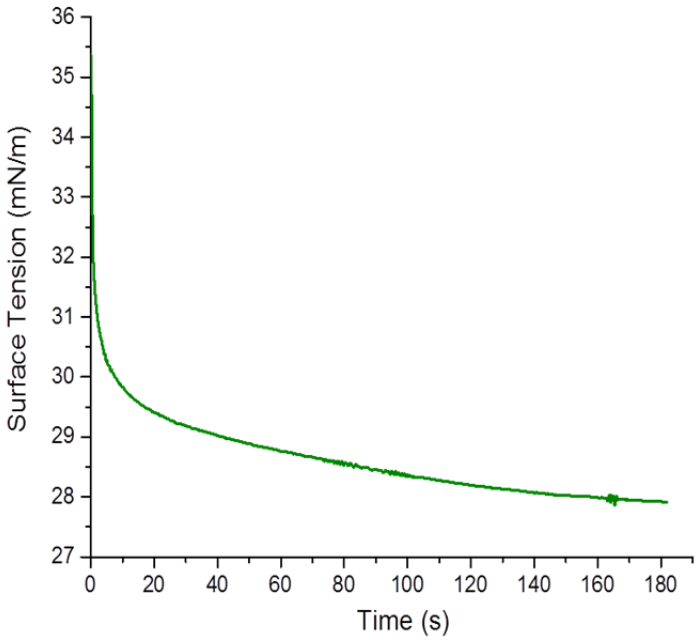

Figure 4. 11. Surface tension variation with time for polyelectrolyte solution for Wilhelmy plate

The polyelectrolytes are mainly used for the purpose of dispersion of glass fibers. During the dispersion process, the sized glass fibers interact multiple times with a glass fiber surface. We study the process by studying the wetting properties of sized glass fibers in the polyelectrolyte by dipping it for multiple cycles. The interactions of polyelectrolyte with sized glass fibers for five continuous wetting cycles are shown in **Figure 4.12** and the dynamic contact angle data is shown in **Table 4.3**. In the first cycle, the sized glass fibers are dry and have had no previous contact with the polyelectrolyte. An advancing contact angle of 77 degrees suggests moderately hydrophilic interactions between sized glass fibers and polyelectrolyte. There is significant hysteresis observed for the first cycle with an advancing contact angle of about 77 degrees and a receding contact angle of about 57 degrees. The

possible causes of contact angle hysteresis mentioned in literature include but are not limited to surface roughness, surface chemical heterogeneity, surface reorientation of functional groups and other time dependent interactions between liquid and solid surface[18]. In this case, the chemical surface heterogeneity, observed in TOF-SIMS analysis and dynamic contact angle measurements, seems responsible for the large hysteresis. The sizing on the glass fiber surface is non-uniform which results in non-specific physical adsorption of polyelectrolyte on its surface. A wettability gradient may be created between the upper and lower length of the fibers as different parts of the sizing interact with polyelectrolyte for different periods of time. After the first cycle, there is some polyelectrolyte already physically adsorbed on the sized glass fibers before interacting with the polyelectrolyte in subsequent cycles. In all the other cycles, the hysteresis decreases significantly as compared to the first cycle. The improved wetting properties in these cycles cause the reduction in the hysteresis to about 4 degrees. When the sized glass fibers are dispersed in the polyelectrolyte solutions, there are hydrophilic interactions between the liquid and fiber surface and the polyelectrolyte covers the sized glass surface by non-specific physical adsorption after repeated cycles. Thus, the polyelectrolyte wets the surface of sized glass fibers during the dispersion process and doesnot come off in subsequent cycles which is important for obtaining improved dispersion properties for formation of web structure.

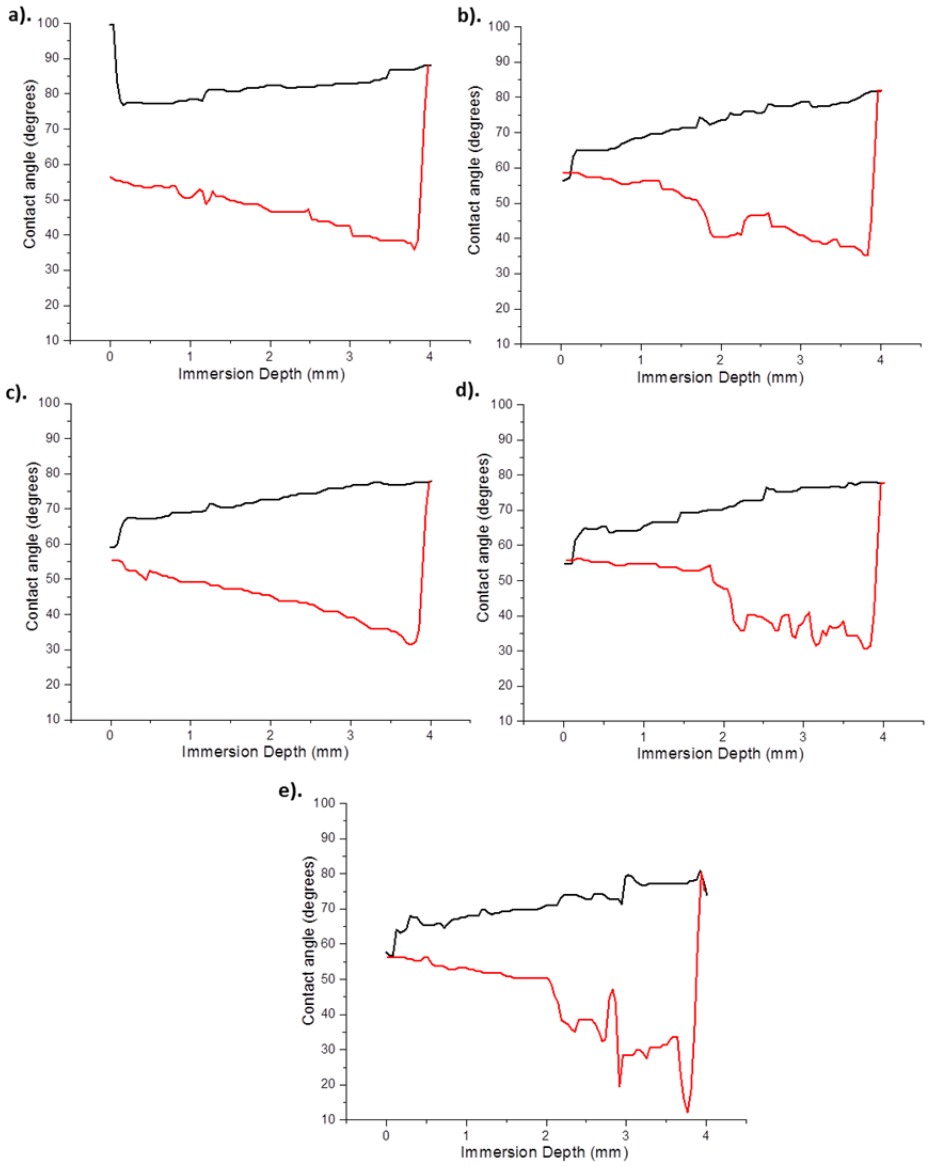

Figure 4. 12. Dynamic contact angle loops for interaction of polyelectrolyte with sized glass fibers in advancing (black) and receding (red) directions for a). 1st cycle b). 2nd cycle c). 3rd cycle d). 4th cycle e). 5th cycle. After the first cycle, polyelectrolyte appears to be adsorbed on glass fiber surface which leads to improved hydrophilic properties and the improved wetting leads to decrease in hysteresis.

Table 4.3. Advancing and Receding contact angles for sized glass fibers with polyelectrolyte for five continuous wetting cycles

Cycle	Advancing contact angle (degrees)	Receding contact angle (degrees)	Hysteresis (degrees)
1	76.7	52.5	24.2
2	65.5	53.8	11.7
3	66.2	51.3	14.9
4	62.2	57.5	4.7
5	63.9	59.7	4.2

4.4. Conclusions

The treatments on glass fibers during glass mat formation have significant effects on the surface properties of the glass fibers and the surface homogeneity/heterogeneity of each of these surface treatments can dictate the glass mat properties. The control over these surface properties is important for achieving improved glass mat properties. From the TOF-SIMS data obtained on glass fibers, the positive ions generated high resolution spectrum which helped us to identify and distinguish the sizing, polyelectrolyte and binder treatments on glass fibers. The dynamic contact angle provided important information on the wetting behavior of glass fibers. The sizing present on glass fibers showed surface heterogeneity and the polyelectrolyte treatment completely covered the surface of sized glass fibers after repeated cycles with hydrophilic interactions between sized glass fibers and the

polyelectrolyte. However, the polyelectrolyte appears to easily wash off the surface. The binder treatment also non-uniformly covered the previous polyelectrolyte and sizing treatments on glass fiber surface.

4.5. References

1. Tanoglu, M.; McKnight, S. H.; Palmese, G. R.; Gillespie Jr, J. W. The effects of glass-fiber sizings on the strength and energy absorption of the fiber/matrix interphase under high loading rates. *Composites Sci. Technol.* **2001**, *61*, 205-220.

2. Wu, H. F.; Dwight, D. W.; Huff, N. T. Effects of silane coupling agents on the interphase and performance of glass-fiber-reinforced polymer composites. *Composites Sci. Technol.* **1997**, *57*, 975-983.

3. Cech, V.; Prikryl, R.; Balkova, R.; Vanek, J.; Grycova, A. The influence of surface modifications of glass on glass fiber/polyester interphase properties. *Journal of Adhesion Science & Technology* **2003**, *17*, 1299.

4. Jaffee, A. M.; Kajander, R. E. US 6187697 B1, 2001.

5. Helwig, G. S.; Heseltine, R. W.; Pathmanathan, V. US 6,054,022, 2000.

6. Jaffee, A. In *In Fiber-white water interaction and control;* TAPPI Proceedings ; 1991; , pp 181-188.

7. Dong, D. Effects of white water chemistry and forming wire structures. *International Nonwovens Journal* **June 2001**, *10(2)*, 14-20.

8. Dong, D. In *Fiberglass surface and its electrokinetic properties;* Technical Association of the Pulp and Paper Industry, Ed.; 1998 TAPPI Proceedings - Nonwovens Conference And Trade Fair; Tappi Press: Atlanta, Ga., 1998; pp 305-315.

9. Deng, Y.; Abazeri, M. Contact angle measurement of wood fibers in surfactant and polymer solutions. *Wood Fiber Sci.* **1998**, *30*, 155-164.

10. Sauer, B. B.; Carney, T. E. Dynamic contact angle measurements on glass fibers: Influence of fiber diameter on hysteresis and contact line pinning. *Langmuir* **1990**, *6*, 1002-1007.

11. Yuan, Y.; Lee, T. R. In *Contact angle and wetting properties;* Surface Science Techniques; Springer: 2013; pp 3-34.

12. Krueger, J. J.; Hodgson, K. T. Single-fiber wettability of highly sized pulp fibers. *Tappi J.* **1994**, *77*.

13. Kamath, Y. K.; Dansizer, C. J.; Weigmann, H. -. Wetting behavior of human hair fibers. *J Appl Polym Sci* **1978**, *22*, 2295-2306.

14. Fuentes, C.; Tran, L. Q. N.; Dupont-Gillain, C.; Vanderlinden, W.; De Feyter, S.; Van Vuure, A.; Verpoest, I. Wetting behaviour and surface properties of technical bamboo fibres. *Colloids Surf. Physicochem. Eng. Aspects* **2011**, *380*, 89-99.

15. Tran, L. Q. N.; Fuentes, C.; Dupont-Gillain, C.; Van Vuure, A.; Verpoest, I. Wetting analysis and surface characterisation of coir fibres used as reinforcement for composites. *Colloids Surf. Physicochem. Eng. Aspects* **2011**, *377*, 251-260.

16. Lodge, R. A.; Bhushan, B. Wetting properties of human hair by means of dynamic contact angle measurement. *J Appl Polym Sci* **2006**, *102*, 5255-5265.

17. Princen, H. M. Capillary phenomena in assemblies of parallel cylinders: II. Capillary rise in systems with more than two cylinders. *J. Colloid Interface Sci.* **1969**, *30*, 359-371.

18. Lam, C.; Wu, R.; Li, D.; Hair, M.; Neumann, A. Study of the advancing and receding contact angles: liquid sorption as a cause of contact angle hysteresis. *Adv. Colloid Interface Sci.* **2002**, *96*, 169-191.

CHAPTER 5

Binder distribution on surface of glass fiber composites

Abstract

Urea-formaldehyde modified acrylic polymeric binders have been used in the glass composite industry for the past decade. The glass mats formed with these binders have resulted in improved strength and stability of the resulting asphalt roofing shingles. However, the distribution of the binder on glass mat surfaces is not well understood and roofing industry has little control over the binder distribution. We found out that the binder deposits at the cross points between the glass fibers as well as non-uniformly coats on the single glass fiber surface. The binder deposition is non-uniform throughout the mat surface with no control on the distribution. The glass mat with binder demonstrates an unstable and dynamic surface which changes from hydrophobic to hydrophilic interactions with time. The binder coating covers the underlying sizing and polyelectrolyte chemistry on the glass fiber surface. The selective cross-point binder deposition might enable a reduction in the total amount of binder used without compromising the mechanical performance of the glass mats.

5.1. Introduction

Surface modification of materials allows the ability to tailor material interactions without changing the bulk properties[1]. In the case of glass fibers, the surface of fibers is modified by coating with sizing to improve compatibility[2] and enhance adhesion with polymeric binders[3]. These sized glass fibers are held together by binder to form the glass fiber composite mats[4]. Glass fiber mats have found increasing application in the building materials industry for making asphalt roofing shingles[5].

One of the popular methods of making these glass mats is by wet-laid processing. The sized glass fibers are chopped into required fiber length and are introduced into the polyelectrolyte slurry with agitation to disperse the fibers finely. The fibers along with the slurry are deposited along a moving screen to remove the excess water and form a web-like structure. Excellent fiber dispersion results in a more uniformly isotropic web structure. The resin or binder is then spray applied onto this web and the resulting mat is then passed through drying and curing cycles to remove water and cure the binder respectively. The resulting glass mats exhibit uniform fiber distribution and consistent mat weight distribution[6].

Thermoset resins have found great popularity as a binder in glass composite application mainly due to the low costs and high strengths[7]. They are low molecular weight monomers which have functional groups for cross-linking reactions[8]. They are cured to form a highly cross-linked three dimensional network structure which is infusible and insoluble in most solvents[9]. Some of the typical binders which are used in industry are formaldehyde based resins, phenolic resins, acrylic resins, polyamide resins[10]. Epoxy resins and epoxy vinyl resins with rubber modifications have shown to be a useful binder choice for glass mats[11].

Various attempts have been made to reduce the undesirable emissions from formaldehyde based resins such as addition of scavengers such as urea[12,13]. Urea-formaldehyde (U-F) based thermoset resins have been the most popular for past decade in the glass composite industry[14]. However, some U-F resin binders create hydrophilic, rigid and brittle composite structures which can crack and break easily and are deemed unfit for use in roofing shingles[15]. Hence, the U-F resins are chemically modified with hydrophobic latex type polymers or thermoset resins which results in higher tear strength resilient glass mats. These modifiers promote hydrolysis resistance and polymer flexibility[16]. Glass mat flexibility is important for achieving high speeds on the production lines as well as for maximum roofing product performance. The choice of resin binder and modifier provides the manufacturer with greater control over the composite properties[17]. The U-F resins have commonly been modified by fortifying the resin with large amounts of latex/emulsion polymers such as polyvinyl acetate, vinyl acrylic, styrene-butadiene[18,19]. Also, styrene-maleic anhydride (SMA) modifiers have been found useful in the glass mat industry for U-F resins[20]. Binders generally used for glass mats are required to be of low viscosity in the uncured state and yet possess characteristics so as to form rigid thermoset polymeric binder for the glass fibers on curing. Viscous binders have shown to be tacky and lead to accumulation of binder on fibers causing dense glass mats and other product problems[21].

The roofing industry has given little emphasis on the binder distribution on the glass fibrous mat surface. The industry has focused on improving the mechanical performance of roofing shingles at lower costs. The binder is the component which holds these glass fibers together and understanding the distribution of binder on the mat surface can play a key role in

improving control over processing and performance while potentially cutting material costs by reducing the amount of binder used. Tamura et al. have successfully demonstrated control over binder distribution, as shown in **Figure 5.1**, by utilizing the electrical characteristics of the material[22]. The application of this technology to glass fiber mats has resulted in a tremendous decrease (about 70-80%) in the material costs. The technique made it possible to selectively bind the glass fibers at the cross-points. The technique is based upon the principle that the glass fibers are electronegative, water is neutral and the developed binder with special surfactant is electropositive. At cross-points, due to the high density of negative glass fibers, the electrical pulling power is higher as compared to other points. When the binder solution is sprayed, the cross points exhibit an increased electrical pulling power which attracts the positive binder resulting in cross-point binder deposition.

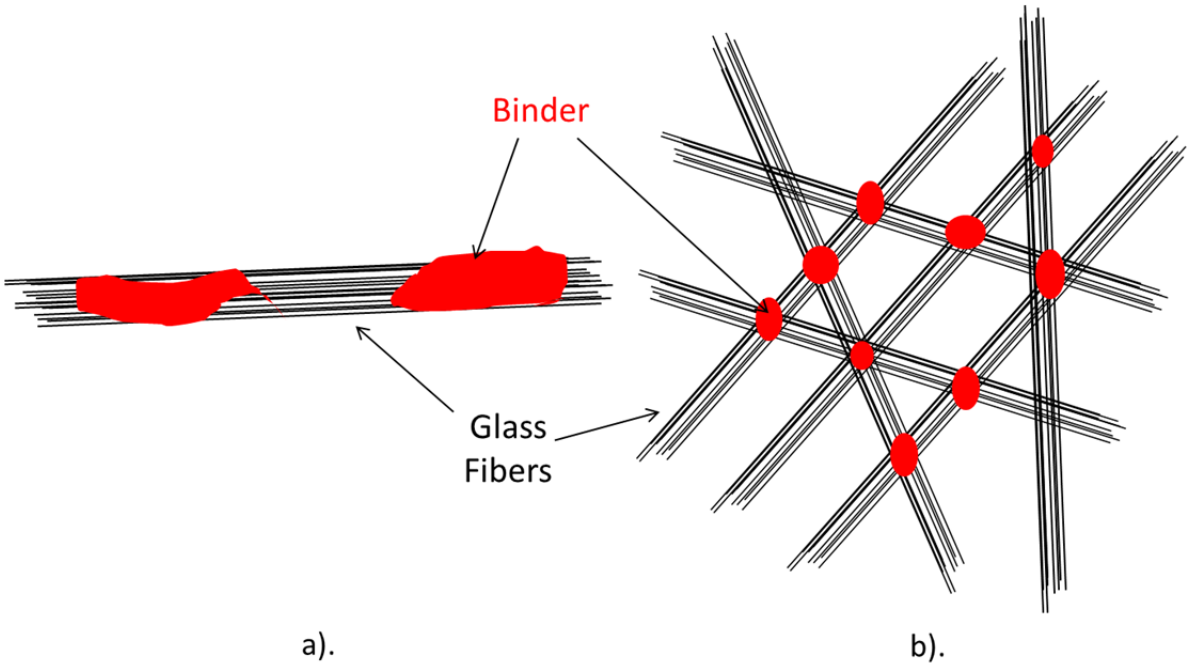

Figure 5. 1. Hypothetical models for the distribution of the binder on glass fiber surfaces with different processing techniques. a). Traditional binding treatment with little or no control over binder deposition. b). Surface binding treatment of glass fibers developed by Tamura et al.[22] to bind selectively only at the cross-points of filaments giving good control over binder deposition.

The distribution of binder on glass mat surfaces from industrial processing is not well-known and is poorly documented. Very little emphasis has been directed by manufacturers towards understanding how binder distributes during the glass mat processing. However, the distribution of binder on the surface of glass mats is an important factor in maintaining uniform mat properties during production as well as the subsequent mechanical properties of

the glass mats. From our discussions with GAF Material Corporation, it is understood that the control over binder deposition on the mat still invokes much debate within the industry.

The overall objective of this work is to improve the understanding of the adhesion between glass fibers and binder in glass fiber mats. The individual objectives that we want to accomplish to attain the overall objective are as follows:

1. Understand the topographical differences between glass mats with and without binder
2. Determine the surface sensitivity of glass fibers in glass mats
3. Identify distribution of binder on the glass mat surface

5.2. Experimental Methods

5.2.1. Glass Mat Formation

The commercial sized glass fibers from Owens Corning (OC) and Johns Manville (JM) having proprietary surface chemistry were obtained by GAF Materials Corporation. These sized glass fibers were used to make glass composite mats. The sized fibers were treated with the polyacrylamide (Nalclear 7768), a commonly used polyelectrolyte for this application, with stirring for few minutes to help the fibers disperse well. The dispersed fibers are arranged on a perforated screen which is dipped in the binder solution. The co-binders used in this study were urea-formaldehyde resin (Casco Resin FG-413F) and acrylic polymer emulsion (Rhoplex GL-618). After the binder treatment, the excess binder is removed by a vacuum pump and the fibers are cured in an oven at 213^{o}C for 2.5 min to form glass-polymer composite mats. The glass mats without binder were formed by the same procedure without

use of any binder solution. The mat was taken from the perforated screen and heat treated in an oven at 213^{o}C for 2.5 min. The delicate structure of the glass mats without binder required storage in envelopes to prevent them from falling apart.

5.2.2. Binder coated glass slide

The same co-binder formulation of urea-formaldehyde resin (Casco Resin FG-413F) and acrylic polymer emulsion (Rhoplex GL-618) was used to coat on a glass slide to understand the effect of binder. The glass slide was cleaned with hot water and dried. The binder formulation was added on the glass slide drop-wise until the surface was completely covered and then cured in an oven at 213^{o}C for 2.5 min to simulate the binder curing during glass mat formation.

5.2.3. Chemical tagging of binder

The dye used for chemical tagging of binder in this study was a basic dye, Basic Violet 16. The dye dissolves in water and not in the binder itself. The dye was pre-dissolved in water and mixed with the pre-dissolved co-binder formulation of urea-formaldehyde resin (Casco Resin FG-413F) and acrylic polymer emulsion (Rhoplex GL-618). The glass mats were then prepared using the same procedure described previously.

5.2.4. Surface characterization

5.2.4.1. Confocal microscopy on glass mats

The glass mats with and without binder were observed under a confocal microscope for mapping the differences in surface topography and for understanding the binder distribution

on glass mat surfaces. An Olympus LEXT OLS4000 3D Laser Microscope was used. The laser section light source is a 405nm semiconductor laser while the color section has a white LED light source. The glass mat of size 10mm x 10mm was placed on a motorized stage and observed with objective lens at different magnifications (5x, 10x, 20x, 50x, 100x).

5.2.4.2. Contact angle measurement

The contact angle measurements were performed using an OCA 20 Model DataPhysics video-based optical contact angle measuring system with SCA 20 software. The glass mat was cut into 10mm x 10mm samples and the contact angle was measured with six such different samples for each mat. For both mats with and without binder, two mats each were used for contact angle measurement. For the glass slide with binder, each slide was measured at 12 different locations and three such slides were used for measurement. The total average of the means of contact angle obtained is reported along with the standard deviation.

5.2.4.3. Time-of-flight Secondary Ion Mass Spectrometry (TOF-SIMS) analysis

TOF-SIMS is a surface sensitive technique which provides semi-quantitative data on surface chemistries such as elemental and molecular compositions, segregation of chemical components from top 10-20 Å of the surface. A typical spectrum is a plot of secondary ion intensity counts versus mass to charge ratio (amu). In this paper, it has been used as a technique to compare the presence and distribution of silane and imidazoline components on the differently treated glass fiber surfaces.

TOF-SIMS analyses were conducted using a TOF-SIMS V (ION TOF, Inc. Chestnut Ridge, NY) instrument equipped with a Bi_n^{m+} (n = 1 - 5, m = 1, 2) liquid metal ion gun. The

instrument vacuum system consists of a load lock for sample loading and an analysis chamber, separated by the gate valve. The analysis chamber pressure is maintained below 5.0 x 10^{-9} mbar to avoid contamination of the surfaces to be analyzed. For the high mass resolution spectra acquired in this study, a 128 by 128 pixel spectrum of a 100 μm by 100 μm area was acquired using a Bi_3^+ primary ion beam under High Current Bunching Mode. For the mass spectral images, a 256 by 256 pixel image of a 200 μm by 200 μm area was acquired using a Bi_3^+ primary ion beam under Burst Alignment Mode.

5.2.4.4. Optical Microscopy

A Nikon optical microscope was used to image dye-binder glass mats with NIS software.

5.3. Results and Discussion

5.3.1. Topographic binder distribution

In this study, we compared the topography of glass mats formed with and without binder to understand the effect of the presence of binder and how does the binder distribute under confocal microscopy. **Figure 5.2** shows the topographical differences between glass mats formed with and without binder as seen under a confocal microscope. The glass mat with binder appears dense as it shows large chunks of material deposition all over the area. It is also well consolidated and fibers are fused within the matrix. The deposition appears parallel to the glass fibers as well as between them. The glass mat without binder appears less dense with no deposition and is very porous and the structure has minimum integration due to the lack of binder. The glass fibers do not show any deposits on their surface or between them

even at higher magnifications. The glass fibers appear smooth with little processing debris visible on the fibers. The depositions appearing in the glass mats with binder can be confirmed as the binder. The binder doesn't seem to be present throughout the mat area but is seen in some specific regions. Also, the amount of binder deposited in between the fibers is very high. Similar results were obtained for JM glass mats with and without binder which were formed by similar process. Also, the side of the glass mat where vacuum suction was applied for removing excess binder did not dictate the surface chemistry. Both sides showed similar binder distribution under confocal microscope and contact angle data showed similar surface sensitivity (Appendix C).

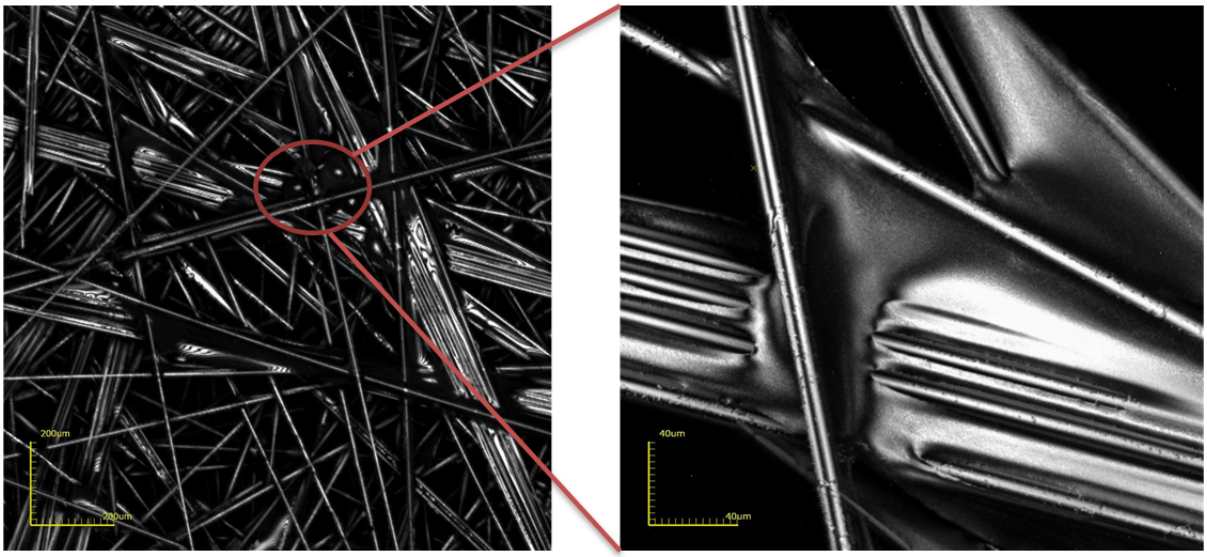

a). OC mat with binder

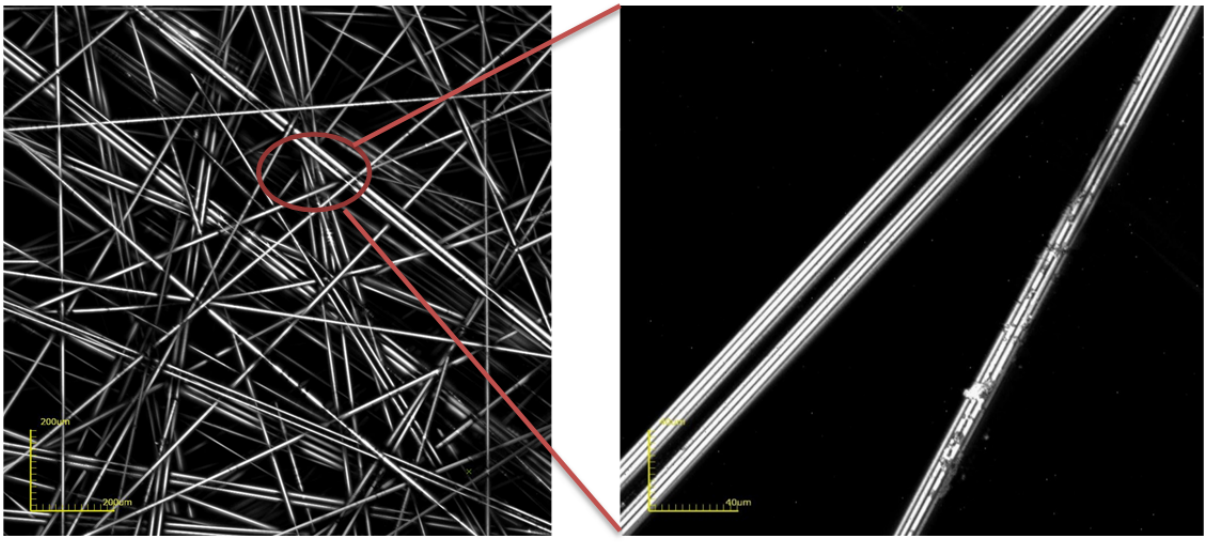

b). OC mat without binder

Figure 5. 2. Confocal microscopy of a). glass mats with and b). without binder demonstrating the topographical differences between them. The left side demonstrates images of particular area of interest in the mat and the right side shows the magnified images at a particular junction of glass fibers indicated by the red circle.

Figure 5.3 shows binder deposition behavior at different locations within the glass mat with binder as observed under the confocal microscope. In most of the areas, the binder deposition is very similar to observed in Figure 2. The binder seems to be present between parallel running glass fibers at different locations. The binder also seems to deposit at the cross-points between single fibers or even at cross-points of bundles of glass fibers. The higher magnification images show that the binder deposits at the cross-points and does not appear to coat on the surface of these glass fibers. The binder also deposits in large amounts at some places while it is absent in some areas across the mat surface. The binder also appears to prominently wet the surface of the glass fibers. During the binder coating process, the binder is attracted to the sized glass fibers, where it reacts with the silane present in the sizing. The capillary action between glass fibers causes the movement of the liquid binder and the binder wets the fiber surface. Thus, the coating process also plays a major role in dictating the deposition mechanism apart from the silane component.

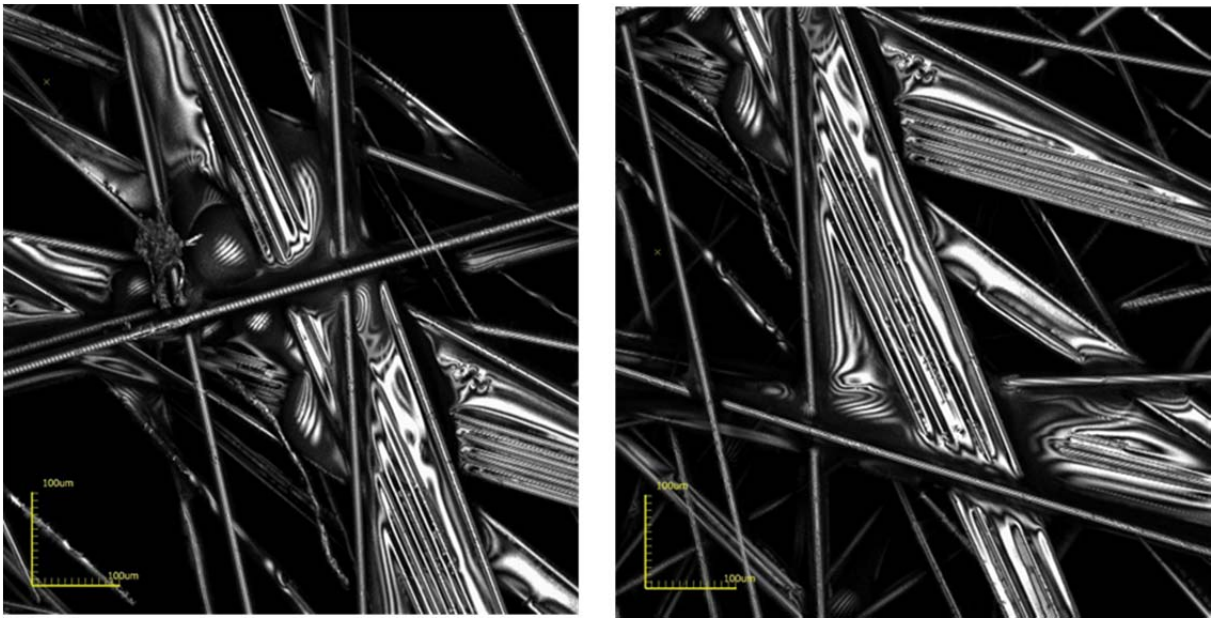

Figure 5. 3. Binder deposition at different positions across the glass mat with binder as observed under confocal microscopy. The binder seems to non-uniformly deposit at the cross-point between glass fibers as well as between individual glass fibers across the glass mat.

5.3.2. Binder labeling for glass mats

To enhance our understanding on the binder distribution, we labeled the binder with a basic dye, Basic Violet 16 and observed the dye-binder using different microscopy tools. **Figure 5.4** shows the dye labeled glass mats with binder under an optical microscope at different locations and magnifications. The dye attached to the binder is a useful tool to observe the binder deposition behavior. The dye can be seen in similar places where the binder is deposited. Similar to Figures 5.2 and 5.3, the dye is observed in large chunks at the cross-points between single fibers or even at cross-points of bundles of glass fibers. Other than the

cross-points, the dye also seems to be present on the glass fiber surfaces as seen by the red color throughout the glass mat surface. There is a possibility of minimum dye uptake by the glass fiber surfaces or the presence of unbound dye on these glass fiber surfaces. Another explanation for this observation is the presence of binder in form of a thin layer on glass fiber surfaces. The thin binder layer does not appear to be uniform across the glass mat with certain fibers showing dark red color while some demonstrating light red color.

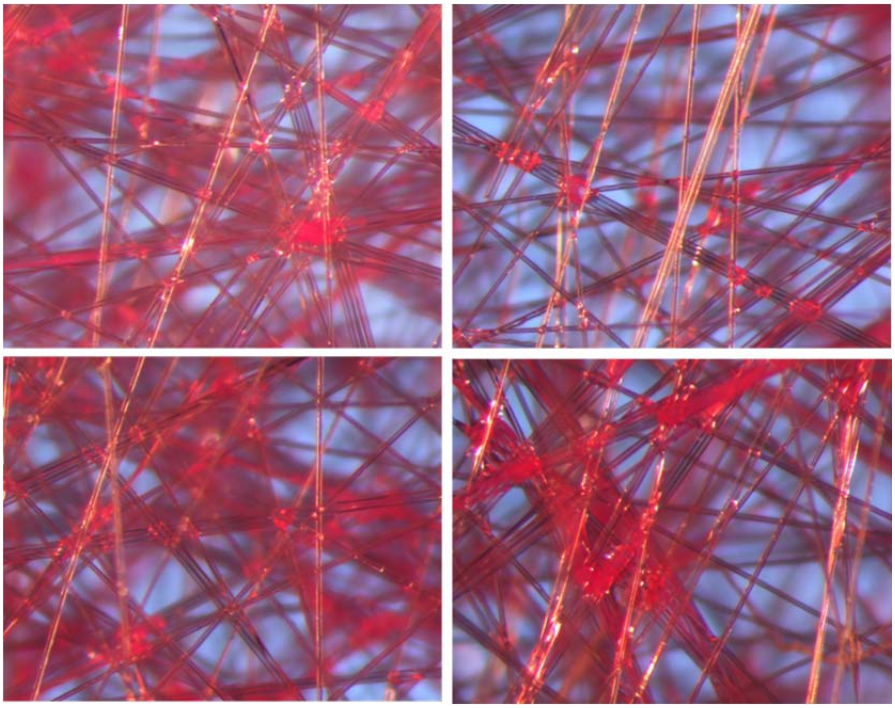

Figure 5. 4. Chemical tagging of binder with dye in glass mat with binder as observed under an optical microscope across random different locations of the glass mats elucidating the binder deposition. The dye can be observed on cross-points between glass fibers as well as on surface of some of the glass fibers.

Figure 5.5 shows the differences between color and laser modes of confocal microscope for observation of the chemical tagging of binder with dye in glass mats. The color mode shows the red color attached to binder all over the viewing mat area while the laser mode shows only chunks of binder deposited on the surface. This color mode shows the red color all over the fiber surfaces which was not very clear in the images obtained from optical microscope. The chemical tagging confirms the presence of binder at the cross-points but also indicates the presence of thin layer of binder on the glass fibers along the glass mat.

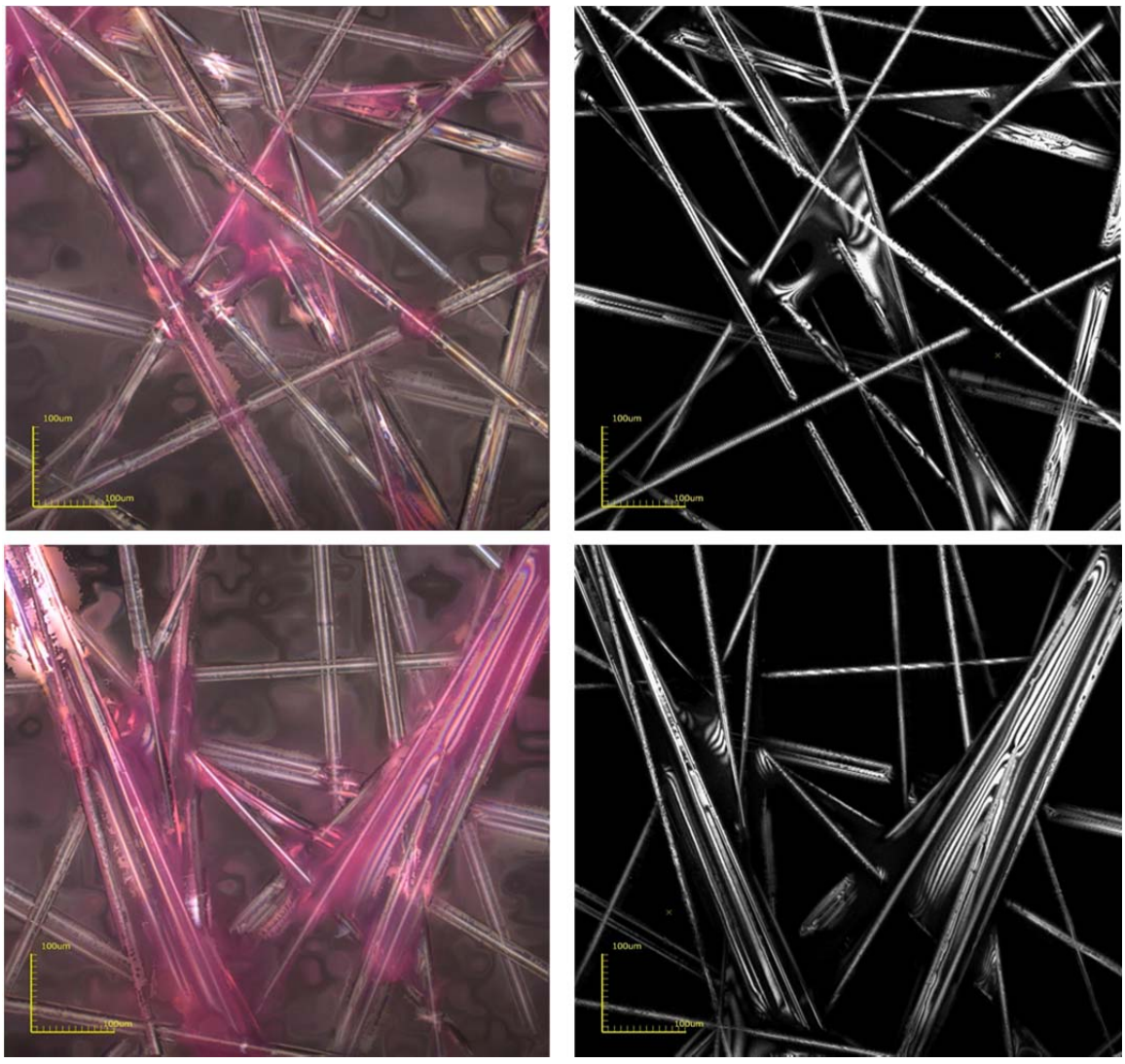

Figure 5. 5. Chemical tagging of binder with dye in glass mat with binder as observed under a confocal microscope comparing the color (left) and laser (right) modes on the microscope. The dye seems to be present on surface of glass fibers under the color mode which is not visible in the laser mode.

5.3.3. Surface sensitivity of glass fibers

We also tried to study the wetting properties of these glass mats and the effect of presence of binder on them during processing. We studied the wetting characteristics of only the binder by depositing it on a clean glass slide and compared those values with the glass mats with and without binder obtained from the processing plant. **Table 5.1** shows the mean average contact angle measurements for glass mats with and without binder and also a binder coated glass slide. The surface of the glass mat without binder as compared to that with binder does not show a statistically significant difference in contact angle as shown in **Figure 5.6**. For both mats, the contact angle is very stable and does not show any change as a function of time. The glass mat without binder shows greater standard deviations with contact angle values possibly due to the presence of uneven sizing on the glass fibers. In comparison, the binder on the glass slide has a lower contact angle and is slightly hydrophilic in nature. The binder on the glass slide exhibits wetting behavior with the water droplet as the contact angle changes as a function of time. The deposition of binder on the glass mat surface should exhibit slightly hydrophilic nature similar to the binder coated glass slide.

Table 5. 1. Contact angle data for glass mat with & without binder and binder on glass slide

Sample description	Contact angle (degrees)
Glass mat with binder	116.42 $\pm$ 6.32
Glass mat without binder	112.49 $\pm$ 8.38
Binder on glass slide	68.5 $\pm$ 2.39

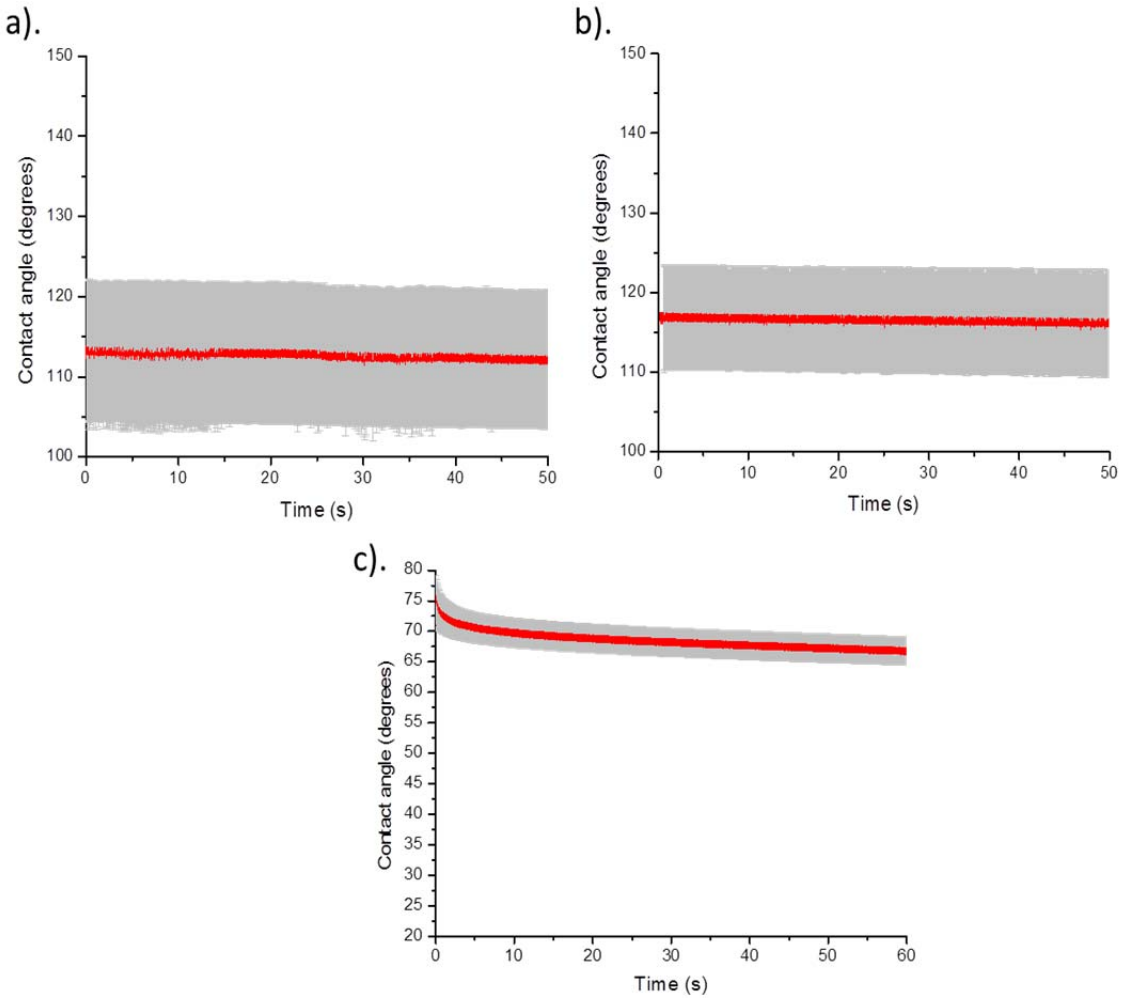

Figure 5. 6. Contact angle variation with time for a). glass mat without binder; b). glass mat with binder and; c). binder on glass slide. The binder is moderately hydrophilic and exhibits wetting behavior with time when on the glass slide but doesnot significantly change the hydrophobic character on depositing on glass fiber surface during glass mat formation.

However, there is no such difference observed in contact angle. The binder deposits in between as well as parallel to glass fibers within the matrix, but there is little evidence of its presence on the surface of glass fibers which possibly prevents any interaction with the water droplet. Hence, we wanted to look the microstructure during this interaction. When the droplet interaction is viewed under confocal microscope, as shown in **Figure 5.7**, the droplet shows wetting on the glass mat with binder after a few minutes. The surface is dynamically unstable and the interactions with binder take longer time than stable hydrophilic surfaces. The interactions observed in **Figure 5.6** are limited to one minute. The glass mat structure may be responsible for the minimal interaction of water droplet with the binder. The air pockets in the glass mat interact with the droplet rather than glass mat surface itself causing hydrophobic interactions. However, the water droplet shows significant reduction in its size indicating good wetting characteristics by the fourth minute. The droplet completely disappears within 10 minutes as it wets the glass fiber surface due to combination of hydrophilic interactions between the binder and glass fiber surface and water evaporation. The interactions between the water droplet and binder are very slow and change from partial wetting to complete wetting. Most stable hydrophilic surfaces show wetting quickly (around one minute) while stable hydrophobic surfaces exhibit non-wetting behavior consistently with time. This wetting mechanism indicates the possible additional presence of binder as non-uniform thin coating on the glass fiber surfaces which cannot be determined using the contact angle and confocal microscopy techniques. Thus, the surfaces of glass mat with the binder are dynamically unstable exhibiting slow hydrophilic interactions between the binder and glass fiber surface.

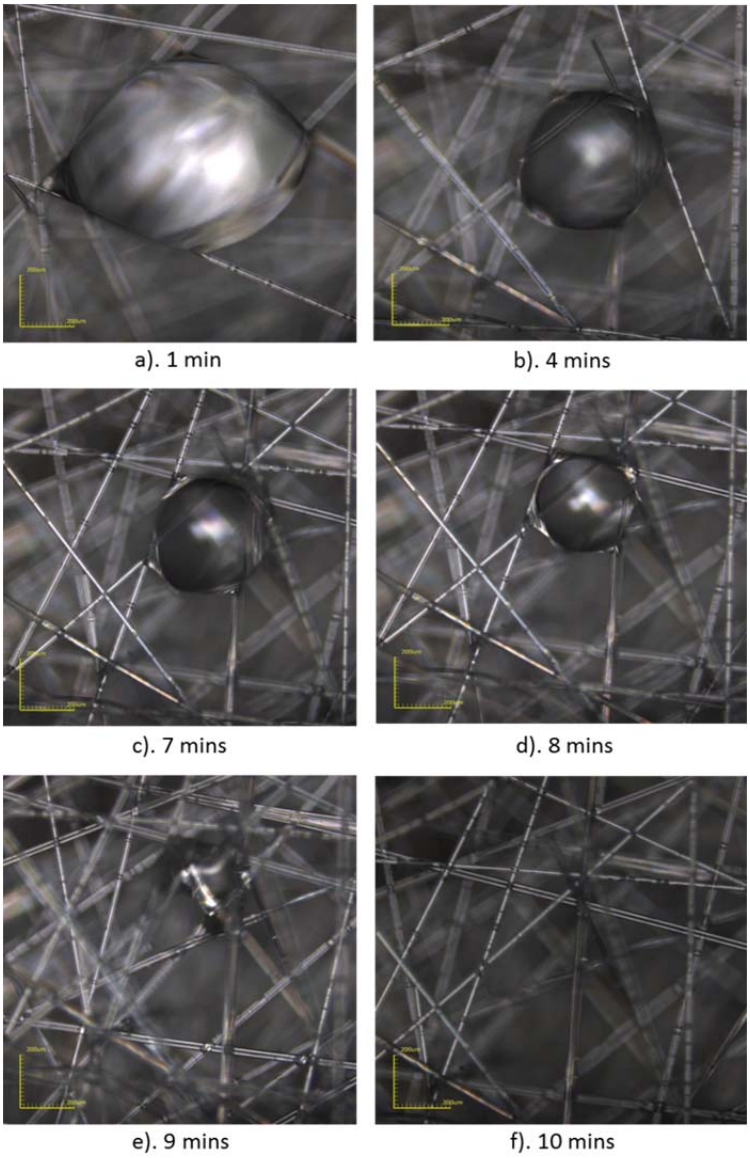

Figure 5. 7. Wetting mechanism of glass mat with binder as observed under the confocal microscope for studying the surface sensitivity of the glass fibers for 10 minutes. There is not much change in the droplet in the first minute, however with time the droplet size slowly decreases. The water droplet disappears along the cross-points of the glass fibers and is not visible after 10 minutes.

The interaction of water droplet with binder present in glass mats revealed the initiation of wetting after a few minutes and complete wetting after 10 minutes. It is important to understand the water droplet wetting behavior and confirm if there are any effects of water droplet evaporation on wetting. The wetting of water droplet on glass mats was compared with a hydrophobic proprietary fluorocarbon coating on PET film for 10 minutes. The hydrophobic coating was chosen such that it ensured there was no wetting with the surface.

Figure 5.8 shows the change in volume of water droplet sitting on the surface of glass mat and the hydrophobic coating. The change in droplet volume for glass mat shows resemblance with the confocal microscopy images observed for the glass mat. The droplet size shows a decrease after four minutes and the wetting behavior was also measurable till four minutes. After that, the droplet starts to wet along the glass mat surface and the contact angle software does not measure any further changes in the contact angle or the droplet volume. On the other hand, the droplet on the hydrophobic coating shows the expected slow and gradual change in water droplet volume. At four minutes, there is a significant difference between the changes in water droplet volume for the two samples. Even after 10 minutes, the water droplet does not completely disappear and the change in water droplet volume due to evaporation is also very small. This indicates that the water droplet interactions observed under confocal microscopy are due to wetting behavior between the water droplet and binder on glass mats.

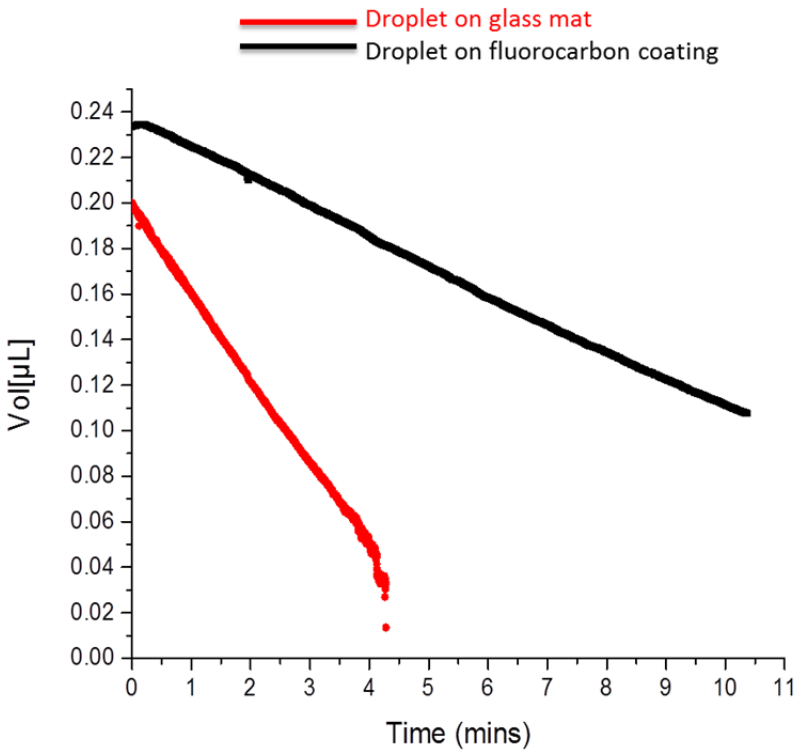

Figure 5. 8. Comparison of change in water droplet volume as a function of time for the droplet on glass mat and droplet on hydrophobic coating suggests that the change in droplet on glass mat with time was due wetting of binder present in the glass mats.

5.3.4. Binder identification and distribution on glass mat surface using TOF-SIMS

The binder can be confirmed to be present on the cross-points of the glass fibers within the glass mat. However, there is a possibility of the binder being present elsewhere in the glass mat. The confocal microscopy and contact angle are insufficient for this purpose. Hence, we use TOF-SIMS surface analysis of the glass mats to confirm where is the binder present. We

identify the specific ions belonging to the binder, glass fibers and use the imaging tool in TOF-SIMS to define the location of binder within the glass mat.

5.3.4.1. Negative Spectrum

Figure 5.9 shows the comparison of negative ion mass spectra for glass mat with and without binder as well as glass slide coated with binder. The peculiar peaks which can be seen in the binder on glass slide are $CH_3N_2O^-$ (59 amu), $C_2N_3^-$ (66 amu), $C_2HN_2O^-$ (69 amu). Some other peaks which define the binder characteristics belonging to auxiliaries like surfactants, emulsion agents are as follows: C_3N^- (50 amu), $C_2H_3N_2O^-$ (71 amu), SO_3^- (80 amu), $C_2H_3SO_2^-$ (91 amu), SO_4^- (96 amu), HSO_4^- (97 amu). All these peaks can be useful to distinguish between glass mat with and without binder Most of these peaks are seen in the glass mat with binder and are absent or present as very weak signals in the glass mat without binder. The glass mat without binder shows distinct peaks for SiO_2^- (60 amu), SiO_2H^- (61 amu), SiO_3^- (76 amu), SiO_3H^- (77 amu) which belong to the sizing as well as glass fiber surface without any binder deposition. The glass mat with the binder has a rough surface which caused the intensity to be low for some of the defined peaks. The absolute intensity should not be used to compare the peaks with each other because they are affected by a number of aspects including sample roughness, matrixes and analysis conditions. However the relative intensities of different peaks can be used to determine surface modification. Since the information depth of TOF SIMS is only 1-2 nm, ions attributed from substrate will show much decreased intensities if the surface is successfully modified and covered. Note that ions specific to glass mat without binder including SiO_2^- (60 amu), SiO_2H^- (61 amu), SiO_3^- (76 amu), SiO_3H^- (77 amu) show much lower intensities in the binder mat spectrum. In

contrast, CN^- (26 amu) and CNO^- (42 amu) ion intensities appear to be much higher, which is due to the presence of binder in the binder mat sample. The negative spectrum does not generate high resolution mass spectrum leading to low ion intensity but is still a useful tool in helping differentiate between glass mats with and without binder.

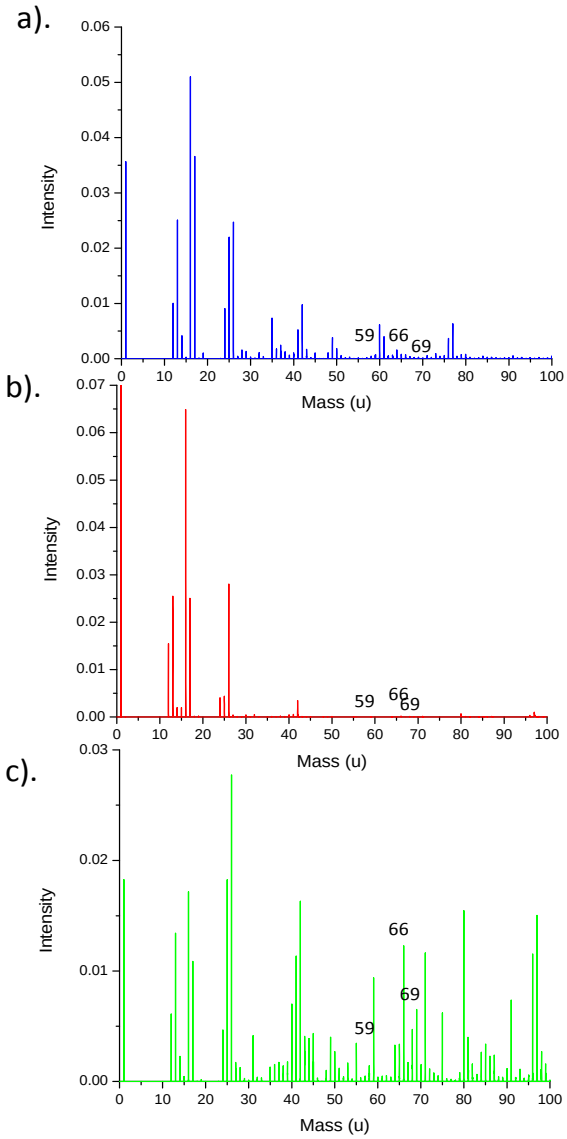

Figure 5. 9. TOF-SIMS negative ion spectra of surface of a). glass mat without binder, b). glass mat with binder and, c). binder coated on glass slide. The individual spectra help identify unique ions for each of glass fibers and binder to differentiate the binder from glass fibers.

Figure 5.10 shows the distribution of binder specific ions on the glass slide. The images are displayed in a heat scale which represents the ion concentration for each ion image. The darker areas (red color) represent regions with low ion concentration while the lighter areas (yellow color) represent regions with high ion concentration for each ion image. The $CH_3N_2O^-$ (59 amu) and $C_2N_3^-$ (66 amu) ions show higher total ion count with lots of uniform yellow spots indicating maximum coverage of these binder specific ions on the glass slide. The $C_2HN_2O^-$ (69 amu) ion has a lower total mass count and exhibits mixture of yellow and red spots with varied intensity but have uniform coverage. These ions can be useful for distinguishing the binder on the glass mat from the glass fiber surface.

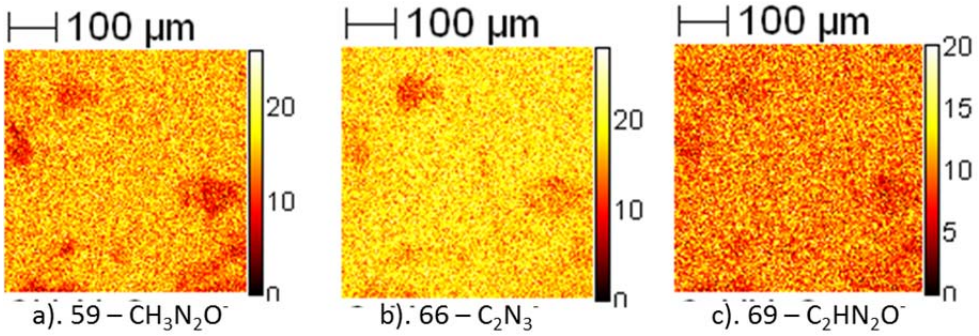

Figure 5. 10. Negative ion TOF SIMS mass spectral images of binder specific ions for binder coated on glass slide identified as a). $CH_3N_2O^-$ (59 amu), b). $C2N_3^-$ (66 amu) and, c). $C_2HN_2O^-$ (69 amu) showing intensity of these ions in binder.

Figure 5.11 shows the low spatial resolution negative ion images of the glass mat with binder. The specific ions belonging to the binder have been previously identified as $C_2HN_2^-$

(53 amu), $CH_3N_2O^-$ (59 amu), $C_2N_3^-$ (66 amu), $C_2HN_2O^-$ (69 amu). The intensity of these ions is relatively low, but they still are useful in studying the distribution of binder. Most of the glass fibers in the particular region of interest are not clearly visible due to low ion intensity. Some parts on the glass fiber surface displays yellow color, which represents presence of the particular ion in higher concentration. It appears the binder is coated non-uniformly on the surface of these glass fibers. The triangle shape shown in the upper left corner appears to be the cross-point between two glass fibers, which shows higher intensity of these ions indicating increased deposition of binder.

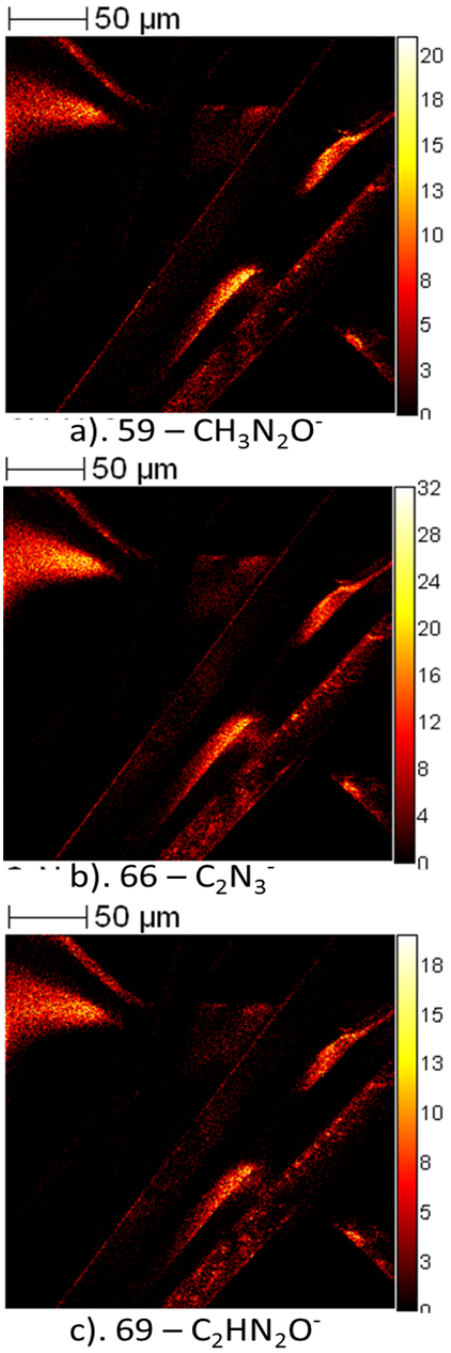

Figure 5. 11. Negative ion TOF SIMS mass spectral images of binder specific ions for glass mat coated with binder showing the regions of binder distribution.

5.3.4.2. Positive Spectrum

Figure 5.12 shows the comparison of positive ion mass spectra for glass mat with and without binder as well as glass slide coated with binder. The binder on the glass slide provides us with the binder specific peaks which can be used to differentiate between glass mats with and without binder. The peculiar peaks which can be seen in the binder on glass slide belong to CH_4N^+ (30 amu), $C_2H_4N^+$ (42 amu), $C_2H_2NO^+$ (56 amu), $C_2H_3N_2O^+$ (71 amu) and $C_3H_5N_2O^+$ (85 amu) ions. Most of these peaks are seen in the glass mat with binder while are completely absent or show some presence with much lower ion intensity in the glass mat without binder. The urea-formaldehyde (U-F) resin modified with acrylic polymer binder shows these prominent peaks consisting of nitrogen containing ions belonging mainly to highly cross-linked three dimensional network structure of U-F resin. Some other ions that are found in the binder can also be identified as $CH_5N_2^+$ (45) and $C_3H_3O^+$ (55) but are less prominent than the peculiar peaks. This confirms the presence of binder in the glass mat surfaces. The glass mat without binder acts as the control mat and shows distinct peaks for $C_3H_3O^+$ (41 amu), $C_2H_4N^+$ (42 amu), $C_2H_3O^+$ (43 amu), $C_2H_5O^+$ (45 amu), $C_4H_7^+$ (55 amu), $C_4H_9^+$ (57 amu) ions. These ions are originated from the previous processes of sizing, polyelectrolyte treatment which cover the inherent Si-O structure of the nascent glass fibers. Most of these peaks are absent or present with much lower ion intensity in the glass mat with binder indicating good coverage of the binder on the glass fiber surfaces.

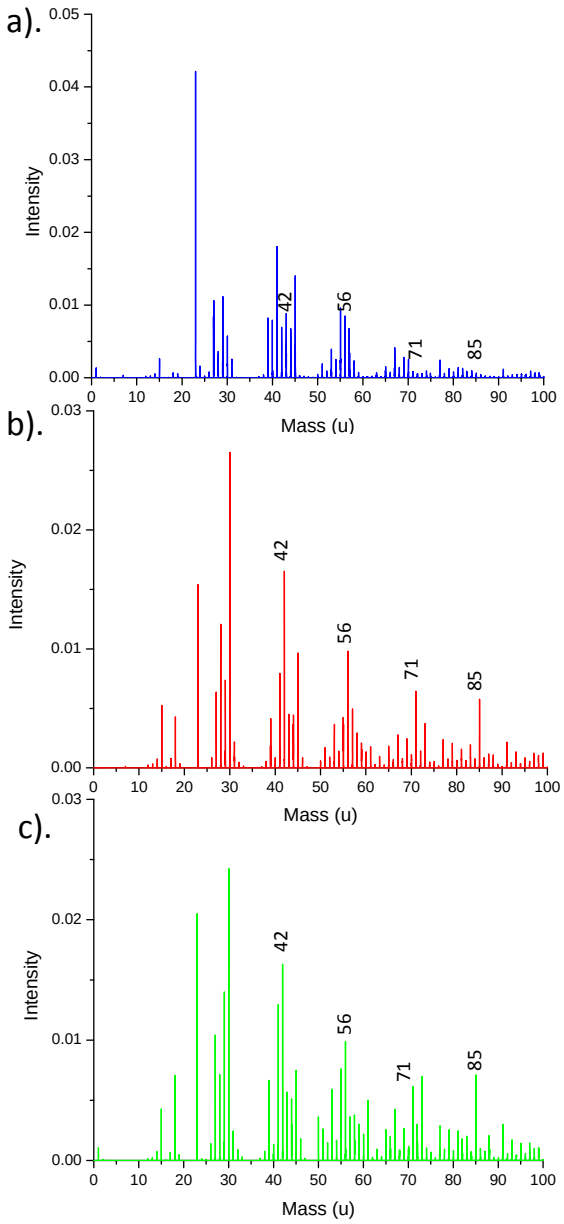

Figure 5. 12. TOF-SIMS positive ion spectra of surface of a). glass mat without binder, b). glass mat with binder and, c). binder coated on glass slide. The individual spectra help identify unique ions for each of glass fibers and binder to differentiate the binder from glass fibers.

The glass mat with the binder has a rough surface which causes the intensity to be low for some of the defined peaks. The absolute intensity is hence not used to compare surface coverage with each other as they are affected by a number of aspects including sample roughness, matrixes and analysis conditions. However, the relative intensities of different peaks can be used to determine surface modification. Since the information depth of TOF SIMS is only 1-2 nm, ions attributed from substrate will show much decreased intensities if the surface is successfully modified and covered. The difference for peculiar peaks can be mainly shown when looking at individual ion peaks. The specific ion peaks can be extracted and plotted separately to completely see the difference between various samples as shown in **Figure 5.13**.

Figure 5.13 compares the individual ion intensities of as $C_2H_4N^+$ (42 amu), $C_2H_2NO^+$ (56 amu), $C_2H_3N_2O^+$ (71 amu), $C_3H_5N_2O^+$ (85 amu) found in glass mat with and without binder and the binder coated on glass slide. To assist direct comparison, all ions are normalized to the total ion intensity. The y-axis shows the scaled intensity for each ion. The $C_2H_4N^+$ (42 amu) ion shows very high intensity (0.016) indicating distinct presence in the glass mat with binder but shows lower intensity (0.007) in glass mat without binder indicating reduced presence of this ion due to absence of binder. The $C_2H_2NO^+$ (56 amu) ion is a characteristic ion for the binder and shows high intensity (0.013) in glass mat with binder indicating strong presence and uniform coating of the binder. In glass mat without binder, this particular peak is completely absent and shows presence of a different species adjacent to the 56 amu fragment of $C_2H_2NO^+$. This comparison distinctly shows that the glass mat without binder doesnot contribute towards any of the binder peaks and the glass mat with binder shows very

similar peaks as the binder with matching frequencies. Similar observations are made for the $C_2H_3N_2O^+$ (71 amu) ion as well as $C_3H_5N_2O^+$ (85 amu) ion. In both cases, the binder peak is very sharp and prominent and can be seen prominently in the glass mat with binder while shows no presence in the control mat. These specific ions belong to the binder and can be used to confirm the presence of binders in the glass mat with binder and further to determine the distribution of binder across the fiber surface via TOF-SIMS imaging.

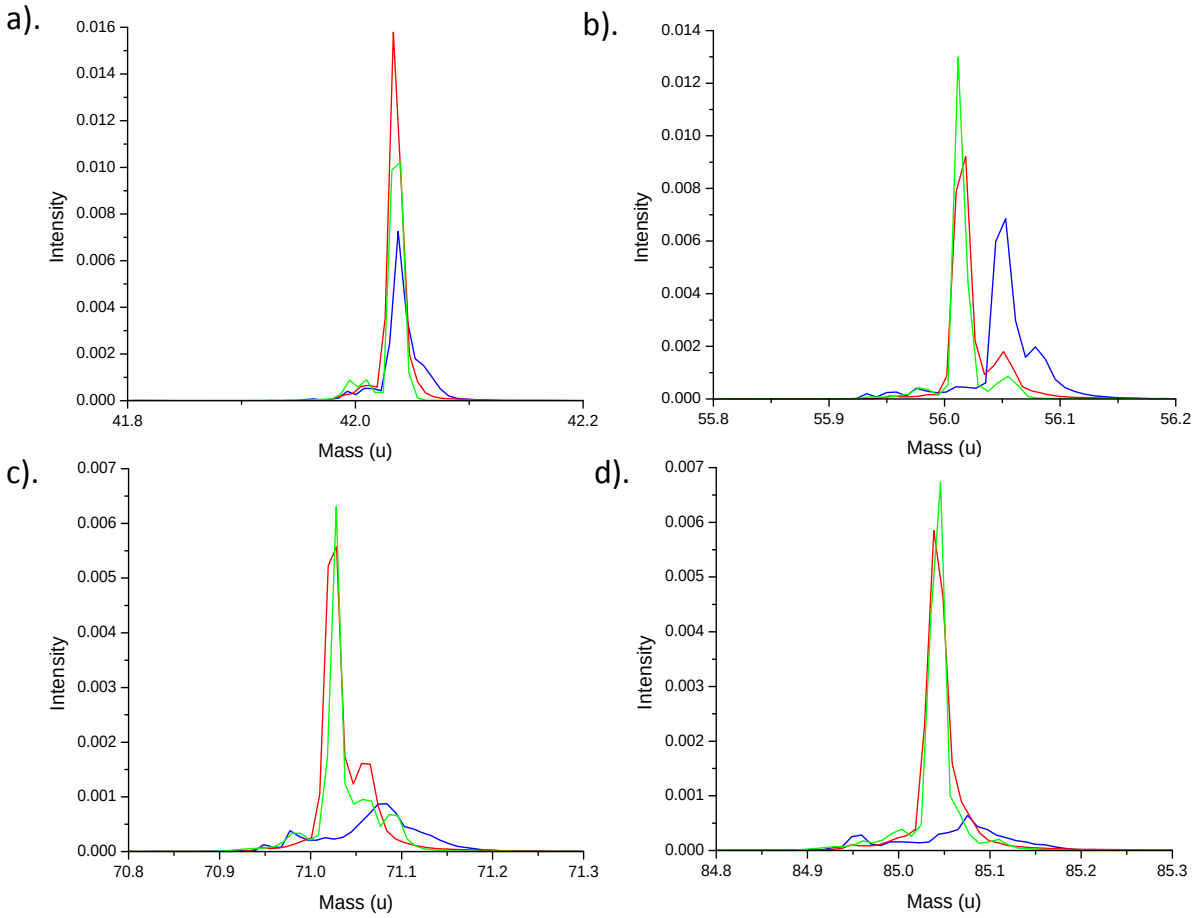

Figure 5. 13. Comparison of spectra of individual ions unique to binder identified as a). $C_2H_4N^+$ (42 amu), b). $C_2H_2NO^+$ (56 amu), c). $C_2H_3N_2O^+$ (71 amu) and, d). $C_3H_5N_2O^+$ (85 amu)) in glass mat without binder (blue--), glass mat with binder (red--)and binder on glass slide (green--) to confirm binder deposition

Figure 5.14 shows the low spatial resolution images of binder specific ions identified from the binder on glass slide. The $C_2H_4N^+$ (42 amu) and $C_2H_2NO^+$ (56 amu) ions contain higher total ion counts and show uniform yellow coverage with few red spots in the viewing area

indicating maximum coverage of these binder specific ions on the glass slide. The $C_2H_3N_2O^+$ (71 amu), $C_3H_5N_2O^+$ (85 amu) ions show a mixture of red and yellow spots indicating varying intensity but exhibit good coverage. The $C_3H_5N_2O^+$ (85 amu) ion shows more yellow spots as compared to the $C_2H_3N_2O^+$ (71 amu). All the four ions belong completely to the binder and can be used to distinguish the binder on the glass mat from the glass fiber surface.

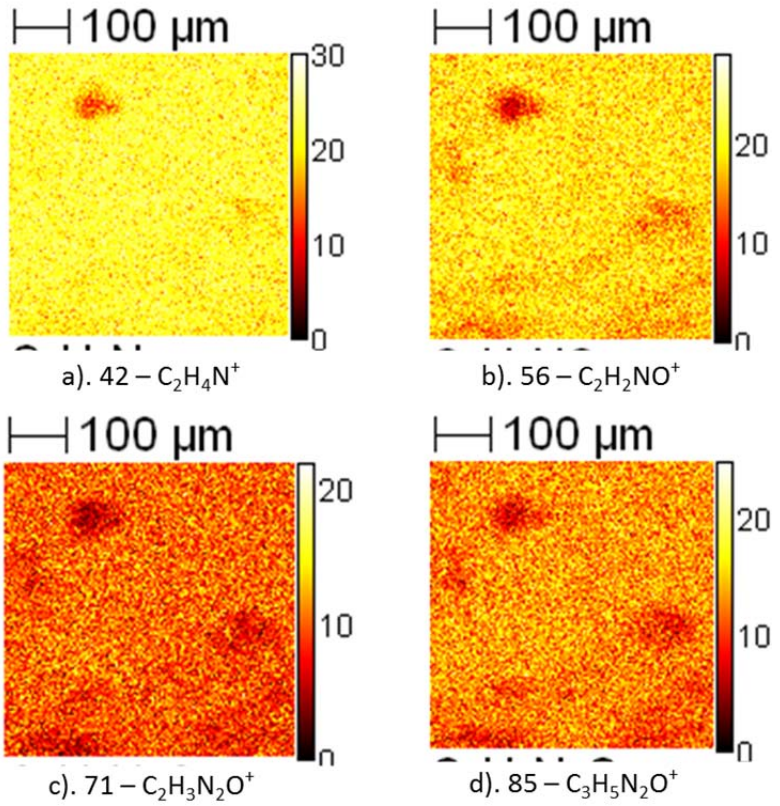

Figure 5. 14. Positive ion TOF SIMS mass spectral images of binder specific ions identified as a). $C_2H_4N^+$ (42 amu), b). $C_2H_2NO^+$ (56 amu), c). $C_2H_3N_2O^+$ (71 amu) and, d). $C_3H_5N_2O^+$ (85 amu) for binder coated on glass slide showing intensity of these ions in binder.

Figure 5.15 shows the high spatial resolution positive ion images of the glass mat with binder. The specific ions belonging to the binder have been previously identified as $C_2H_4N^+$ (42 amu), $C_2H_2NO^+$ (56 amu), $C_2H_3N_2O^+$ (71 amu), $C_3H_5N_2O^+$ (85 amu). The images from these ions show that the binder is present at the cross-points of glass fibers prominently as seen under confocal microscopy. The binder also seems to be present on the fibers at the back and also on the fiber going diagonally across. The intensity variation of fiber specific ions and binder specific ions is probably due to topography of the fibers. The yellow color at the cross-point and some of the fiber surface indicate higher amount of binder presence in these regions while others exhibit lower amount of binder deposition. This indicates that the binder treatment is non-uniform in nature. However, it is clear that the binder is present on both fiber surface as well as the cross-points.

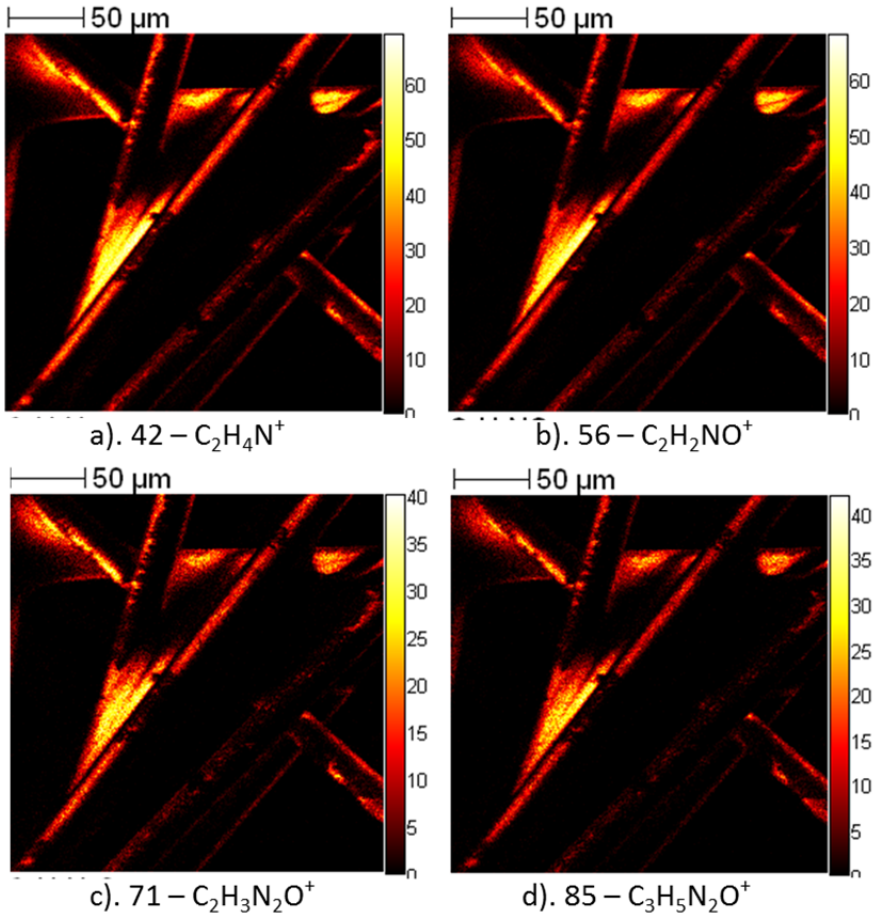

Figure 5. 15. Positive ion TOF SIMS mass spectral images of binder specific ions a). $C_2H_4N^+$ (42 amu), b). $C_2H_2NO^+$ (56 amu), c). $C_2H_3N_2O^+$ (71 amu) and, d). $C_3H_5N_2O^+$ (85 amu) for glass mat coated with binder showing the regions of binder distribution.

Figure 5.16 shows the distribution of binder ions on the glass mat at a different location in the glass mat with binder. The binder ions still show intensity variation due to fiber surface topography. The cross-point binder deposition is not as clearly visible as the fiber surface in these images. However, on the left side of the fiber cross-point, we see the slight deposition

at an angle to these fibers. There is a possibility of this binder being deposited at cross-point exactly below these fibers and hence cannot be seen. Some single fiber surfaces show varied colors indicating the binder treatment is non-uniform due to the variation of amount of binder deposited.

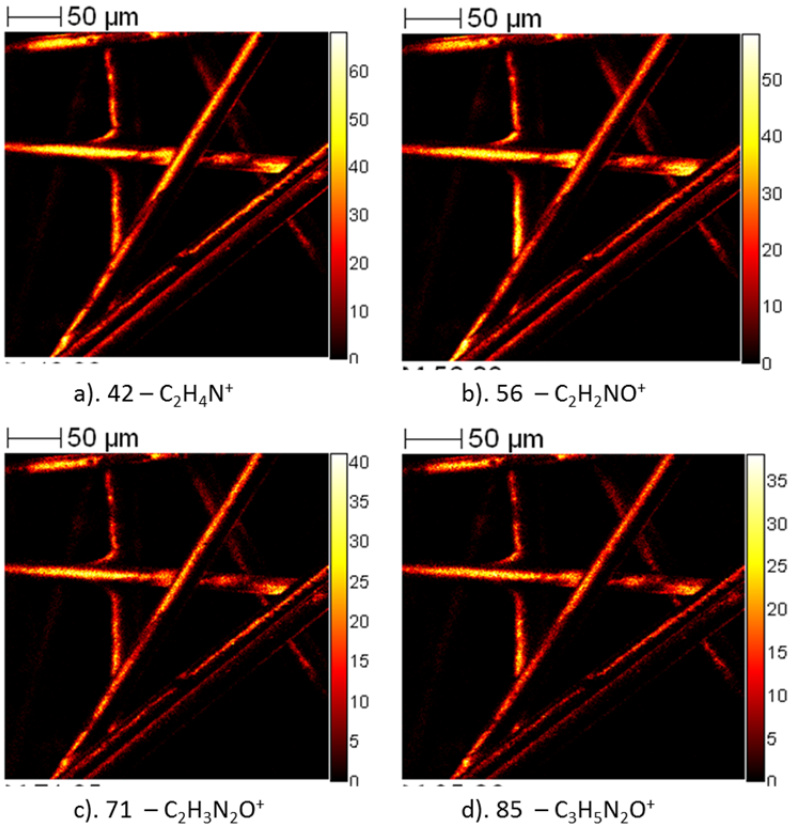

Figure 5. 16. Positive ion TOF SIMS mass spectral images of binder specific ions a). $C_2H_4N^+$ (42 amu), b). C_2H_2NO+ (56 amu), c). $C_2H_3N_2O^+$ (71 amu) and, d). $C_3H_5N_2O^+$ (85 amu) for glass mat coated with binder at different locations in the glass mat to confirm binder distribution.

Figure 5.17 shows the distribution of binder ions on the glass mat at higher magnifications specifically looking at the cross point of glass fibers. The binder deposition can be clearly distinguished from the glass fibers as the binder sits between the glass fibers as well as wets the glass fiber surface partially. All the binder specific ions show yellow color on the glass fiber surface as well as the binder deposited at cross point indicating presence of binder in high quantities in these regions. The single fiber seems uniformly coated with the binder on the surface. This indicates coverage of the previous treatments of sizing and polyelectrolyte with binder chemistry on the glass fiber surface.

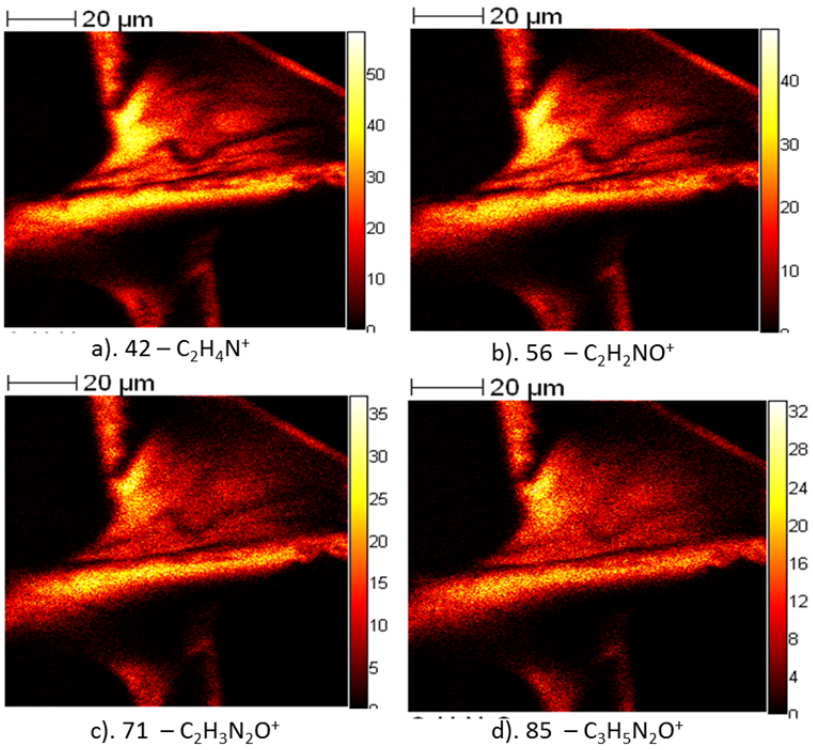

Figure 5. 17. Positive ion TOF SIMS mass spectral images of binder specific ions a). $C_2H_4N^+$ (42 amu), b). $C_2H_2NO^+$ (56 amu), c). $C_2H_3N_2O^+$ (71 amu) and, d). $C_3H_5N_2O^+$ (85 amu) for glass mat coated with binder at a particular cross point of glass fibers within the glass mat showing that binder is deposited in large quantities at the cross-point and is also present on the glass fiber surfaces which form the cross-point.

5.4. Conclusions

The glass mats with and without binder show different surface topography due to the binder deposition. The binder appears to be present at cross points between fibers as well as along the fibers but there is no evidence of the presence of binder on individual glass fiber surfaces under confocal microscopy. The glass mat with binder demonstrates a dynamically unstable

surface and exhibits slow hydrophilic interactions between binder and glass fiber surface. TOF-SIMS is an important surface characterization technique which provides useful information to identify binder adhesion and define binder distribution characteristics in glass mats. The binder deposits at the cross points between glass fibers and as a thin coating on the single glass fiber surface. The binder distribution is non-homogeneous in nature throughout the mat surface but when the binder is coated on the single glass fiber surface, it covers the fiber surface uniformly.

5.5. References

1. Tanoglu, M.; McKnight, S. H.; Palmese, G. R.; Gillespie Jr, J. W. The effects of glass-fiber sizings on the strength and energy absorption of the fiber/matrix interphase under high loading rates. *Composites Sci. Technol.* **2001**, *61*, 205-220.

2. Wu, H. F.; Dwight, D. W.; Huff, N. T. Effects of silane coupling agents on the interphase and performance of glass-fiber-reinforced polymer composites. *Composites Sci. Technol.* **1997**, *57*, 975-983.

3. Gao, S. L.; Mäder, E.; Plonka, R. Coatings for glass fibers in a cementitious matrix. *Acta Materialia* **2004**, *52*, 4745-4755.

4. Nishioka, G. M. Interaction of organosilanes with glass fibers. *J. Non Cryst. Solids* **1990**, *120*, 102-107.

5. Olmos, D.; González-Benito, J. Visualization of the morphology at the interphase of glass fibre reinforced epoxy-thermoplastic polymer composites. *European Polymer Journal* **2007***, 43*, 1487-1500.

6. Dong, D. IL, US Patent US 6,291,552 B1, 2001.

7. Mirous, G. Washington, USA Patent 5,656,366, 1997.

8. Klett, M. W.; Brown, N. E. MA, US Patent US 2012/0064295 A1, 2012.

9. Sims, G. D.; Broughton, W. R. In *2.05 - Glass Fiber Reinforced Plastics—Properties;* Kelly, A., Zweben, C., Eds.; Comprehensive Composite Materials; Pergamon: Oxford, 2000; pp 151-197.

10. Rodrigues, K. TN, US Patent US 20040082241 A1, 2004.

11. Samanta, B. C.; Maity, T.; Dalai, S. Influences of amine-terminated oligomers on glass fibre-epoxy composite. *Pigment & Resin Technology* **2008***, 37*, 3-8.

12. Hawkins, C. M.; Chen, L.; Hernandez-Torres, J.; Downey, W. E. US 20110021101 A1, 2011.

13. Chen, L.; Downey, W. E.; Hernandez-Torres, J. US 20110003522 A1, 2011.

14. Garcia, R.; Jaffee, A.; Scheerlinck, P.; Wang, L. US 20060099870 A1, 2006.

15. Wotier, E. In *In Selection Of U-F Modifiers For Glass Mat Membranes;* 1999 Nonwovens Conference; 1999; , pp 39-44.

16. Nedwick, P. Latex modification of urea formaldeyhde resins. *TAPPI Journal* **1998**, *81*, 181-184.

17. Andreevska, G. D.; Gorbatkina, Y. A. Adhesion of Polymeric Binders to Glass Fiber. *Product R&D* **1972**, *11*, 24-26.

18. Nandi, S.; Zheng, G.; Asrar, J.; Miele, P. F. US 7691761 B2, 2010.

19. Shooshtari, K. A.; Asrar, J. EP 1988066 A3, 2011.

20. Shooshtari, K. A.; Asrar, J. EP 2083021 A1, 2009.

21. Eckert, B.; Christensen, B.; Shooshtari, K. A.; Nandi, S.; Asrar, J.; Zhang, M. US 20120156954 A1, 2012.

22. Tamura, S.; Wu, Z.; Zhu, Y.; Nishino, Y. Cross-point Binders for glass fiber mat utilizing electronic ion effect . *http://extra.ivf.se/eccm13_programme/abstracts/1703.pdf*2011).

CHAPTER 6

Summary and Outlook

6.1. Summary

The overall objective of our work was to study and understand the surface interactions of different surface modification techniques on glass fibers and the glass-polymer composite interface. Studying these surface interactions has helped in combining the benefits of each of these interactions, understanding their synergistic effects and correspondingly tune and improve the processing and downstream properties of the composites. We have built upon past work and moved a step ahead in improving the fundamental understanding of interfacial properties.

We elucidated the important roles of each of the sizing components on the interface properties and its effect on the downstream composite properties. The effect of organofunctional silanes on the interface properties was well known, but the combined effect of different sizing interfaces was not well understood. We found that the sizing chemistry has a strong influence on the mechanical performance of these composites. We showed that the imidazoline component plays a key role in contributing to the mechanical performance of the composites. We also enhanced the knowledge on the electrokinetic properties of glass fibers as a function of the sizing chemistry formulation and how isoelectric point is an important parameter in predicting the dispersion properties of sized glass fibers.

The effect of surface treatments on the surface properties of glass fibers and their synergistic interactions were explored. The sizing, polyelectrolyte and binder treatments non-uniformly covered the surface of the glass fibers. We studied the dynamic wetting properties of these surface treatments and observed that sized glass fibers and the binder treated glass fibers are slightly hydrophilic in nature while the polyelectrolyte treated glass fibers are hydrophobic in nature. We also revealed that the in polyelectrolyte wets the sized glass fibers during dispersion. During the glass mat formation, there was very little attention given to the distribution of binder. We explored this area and found that the binder was present at the cross-points of glass fibers as well as was present on the surface of glass fibers. The distribution of binder was random and non-uniform but the surface coverage of deposited areas was good.

In summary, although the study of these interfacial properties has shown to reduce some of the gap in fundamental understanding of these glass fiber composites, there are various aspects and concepts of these interfaces which need to be thoroughly understood for the industry to gain control and improve the performance of composite properties.

6.2. Recommendations for Future Work

There seems to be huge scope for future work in this particular area. Throughout my dissertation, there have been various questions which remained unexplored. The findings of this work demonstrated that understanding surface interactions occurring between three components: 1) sizing distribution on glass fibers, 2) processing treatments for mat

formation, and 3). distribution of binder on surface of glass mats can provide greater control over composite properties. In the remainder of this chapter we discuss some recommended work which can help in providing improved control over properties for the manufacturers.

6.2.1. Influence of surface ageing on the interface properties

During our discussions with GAF, we understood that the sized glass fibers they obtain are generally kept for over a period of 20 days since the day of their formation. They found that the downstream properties like dispersion in polyelectrolytes, glass mat mechanical performance were poor if the sized glass fibers are used prior to that and were also different if kept for longer periods. This causes an increased inventory cost for them. To understand this behavior, we conducted a preliminary analysis by studying the electrokinetic behavior of these sized glass fibers over a period of 8 weeks as shown in **Figure 6.1**.

We selected one of the glass fibers from our own design of experiments from Chapter 3. The sizing treatment changes the IP from 2 to around 8 in the first week. After four weeks, the IP shifts from 8 to about 9. This would mean an increase in the basic nature of the surface. After 8 weeks, there is not significant change in surface as compared to after 4 weeks. These observations suggest that there is change in the surface chemistry over a period of time. The complex network found at the interface in the sizing may undergo some reorganization at the surface with time.

The change of surface chemistry with time, also known as ageing, is an important processing parameter. The glass-polymer interphase is a complex interpenetrating network between the sizing and matrix. However, the sizing treatment, which creates a fiber-size interface also is a complex network structure formed between the silane, imidazoline and other auxiliaries. If

any of these networks change with time, it may change the resulting downstream composite properties due to the changing surface and interfacial chemistries.

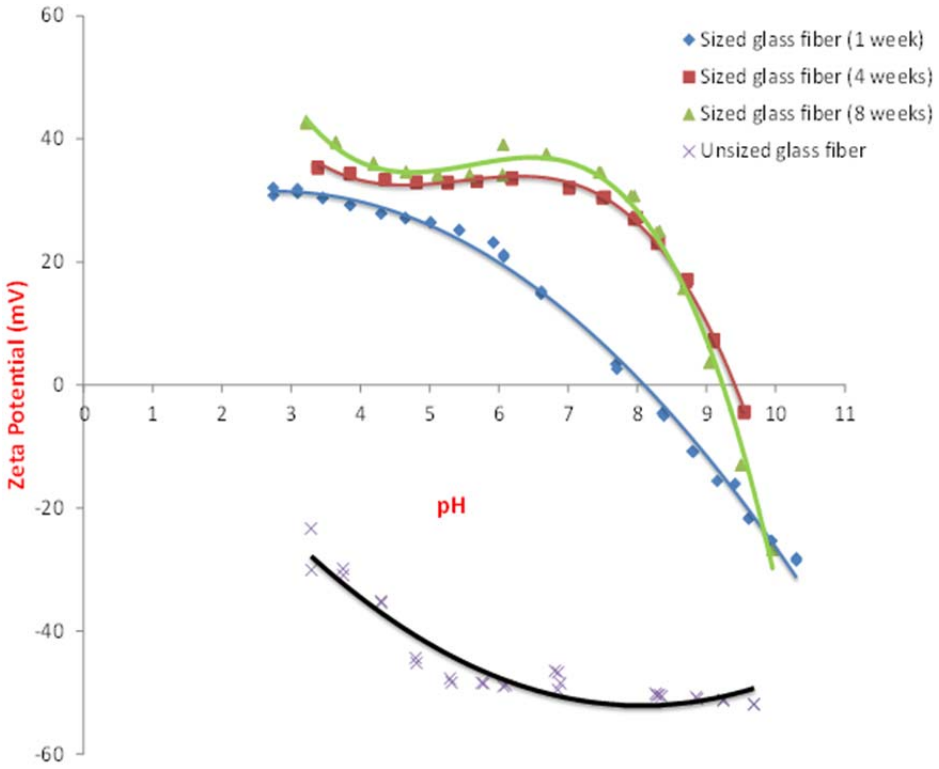

Figure 6. 1. Effect of surface ageing on the electrokinetic properties of sized glass fibers

The kinetics can be easily studied by zeta potential analysis and dynamic contact angle measurements. Therefore, if we can study these properties of sized glass fibers on a regular basis (every day or once in 2 days) since its formation, it may show us the slow change in the kinetics of surface reorganization. Also, if different sizing formulations are used, it can provide valuable information about synergistic interactions between sizing chemistry and

surface reorganization. This work can thus help in moving forward in path of reduction in the inventory costs.

6.2.2. Control of imidazoline distribution and its effect on mechanical performance of glass mats

In Chapter 3, we showed the importance of imidazoline within sizing on glass fibers in influencing the mechanical performance of the glass mats. An increase in the imidazoline concentration caused an increase in mat tear, dry and wet tensile strengths on the glass mat. We also showed that the imidazoline component distributes non-uniformly and shows agglomeration on the glass fiber surface. Silane component shows comparatively uniform distribution and causes a decrease in the mat tear and dry tensile strength.

If the imidazoline component is uniformly distributed on the surface of glass fibers, it may further increase the mechanical performance of these glass mats. There is a need to device methods to control the distribution of these sizing components on the glass fiber surface. Different manufacturing methods like two-stage sizing, different pick up rates during sizing and change in the preparation of the sizing bath can be studied to observe any change in distribution of imidazoline. Also, the silane is an important component for adhesion of binder to the glass surface and cannot be neglected during sizing.

Another method can be to understand the interaction of glass fiber surface with imidazoline using dynamic contact angle. This will reveal important information of the wetting characteristics of imidazoline towards the glass fiber surface. These interactions of imidazoline solution can be compared with that of the standard sizing solution interaction

with glass fiber surface. Also, the agglomeration characteristics of imidazoline can be studied using surface tension measurements, light scattering methods.

6.2.3. Targeted deposition of binder at cross-points in glass mats

In Chapter 5, we studied the distribution of binder on the surface of glass mats. We observed that the binder deposits non-uniformly in large chunks at the cross-points between the glass fibers as well as a thin coating on the surface of glass fibers.

In the glass mat industry, there is growing emphasis on the decrease in the basis weight of these mats and reduction in the material costs. The binder is responsible for holding these glass fibers together and is an important parameter in influencing the mechanical performance of these glass mats. An improved control of where and how the binder distributes on the glass mat surface will lead to improved control over the entire process. It is important to understand why the binder shows large depositions at the cross-points. We can then target the deposition of binder at the cross-points which will cause a reduction in the material costs and the basis weight of these mats. Also, it is important that the targeted distribution should not compromise the mechanical performance of these glass mats.

APPENDICES

Appendix A

Contact angle mapping on glass mats

The water contact angle mapping was done in order to understand the uniformity of the surface treatment of binder deposition. The mapping gives an idea which regions are similar or different in surface chemistry. The contact angle was measured in 5 different places throughout the mat as shown in Figures A.1 and A.2. For each location, the contact angle was measured in 7 different spots to get an average value and standard deviation. We also were able to track the contact angle over time to evaluate surface dynamics. A special distilled water syringe of 18 μL size was used to probe the surface with drop volumes set at 2μL. GAF's label on each mat was taken as the topside of the mat. All measurements were performed on this side. Mat A is the glass mat made from OC sized glass fibers while the Mat B is the glass mat made from JM sized glass fibers.

Mat A shows a greater variation in the contact angle distribution as compared to Mat B. Though the average contact angle is approximately 115 – 120^{o}, the standard deviation is greater than Mat B (thicker grey areas in Mat A) as shown in **Figure A1**. The contact angle has a large distribution around the mat especially the right top corner. This corner shows an exceptional increase in contact angle with time with a corresponding high standard deviation (the lowest contact angle reading is ~85^{o} while the highest is ~145^{o}). This is indicative of large non-uniformity in the surface chemistry. Further work is needed to confirm this is a change in binder distribution.

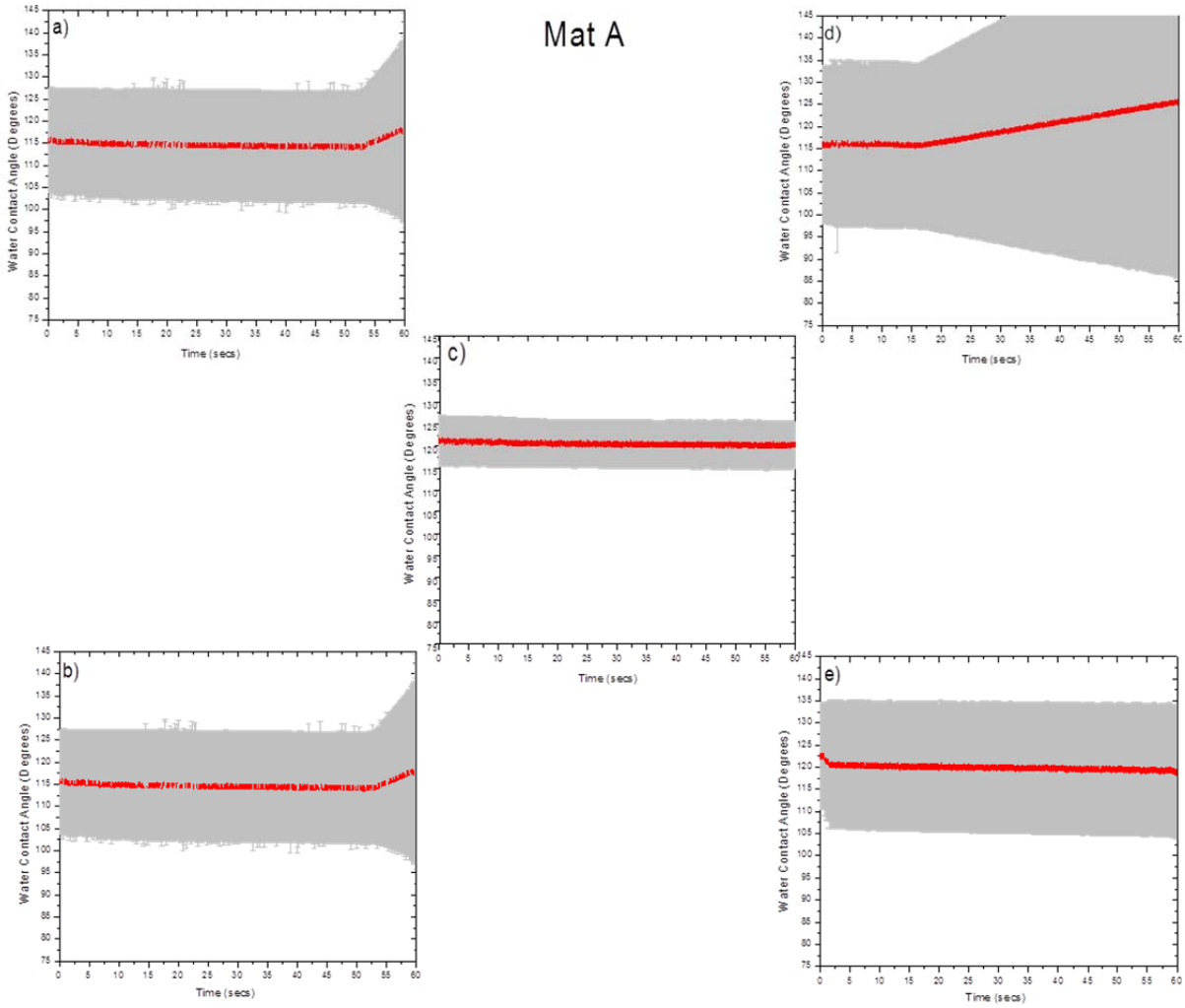

Figure. Appendix. A. 1. Water contact angle range (mean – red line; grey – standard deviation) for Mat A at different positions in the mat where a) is left top corner, b) is left bottom corner, c) is center, d) is right top corner, and e) is right bottom corner.

Conversely, Mat B has a lesser variation in the contact angle distribution for the regions tested (see **Figure A2**). Though the average contact angle changes from 120^{o} to 135^{o}, the key observation is the low standard deviation in contact angle values (the grey areas are small along the average line). The standard deviation only changes in some areas with time which

indicates the interaction of surface with water droplet. The right top corner once again shows angles varying from 75^{o} to 145^{o} with time. The average contact angle value reduces after 40 secs which indicates wetting behavior. In addition, the bottom right corner also exhibits greater variation than other regions on the mat after 55 secs. The processing parameters or coating protocols for this region of binder deposition should be evaluated.

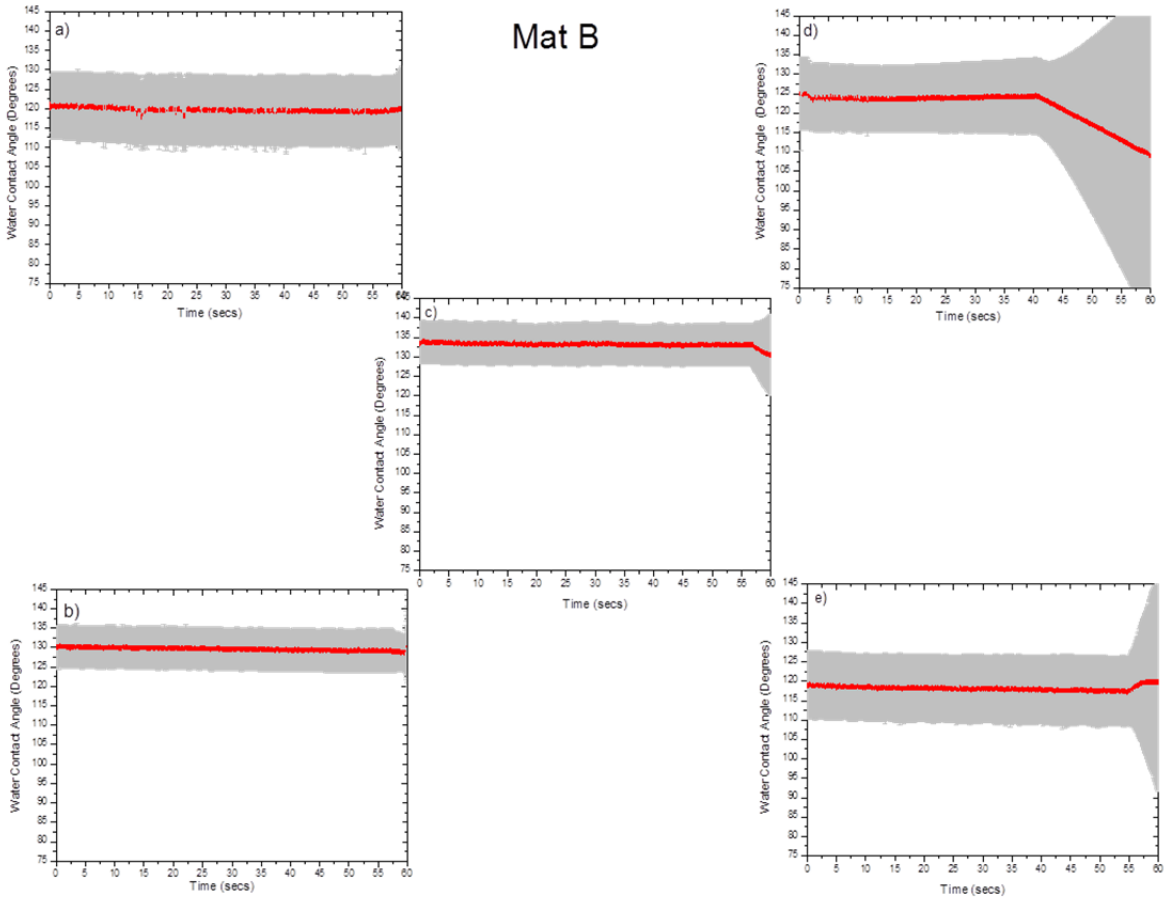

Figure. Appendix. A. 2. Water contact angle range (mean – red line; grey – standard deviation) for Mat B at different positions in the mat where a) is left top corner, b) is left bottom corner, c) is center, d) is right top corner, e) is right bottom corner.

Appendix B

The TOF-SIMS negative and positive ion spectra for both glass mat with binder and binder treated glass fibers were compared and showed very similar spectra. This indicated that binder treatment we did on glass fibers in our lab was closely related to the actual glass mat processing. This was helpful in studying the binder treatment process for glass fibers using TOF-SIMS and dynamic contact angle in Chapter 4.

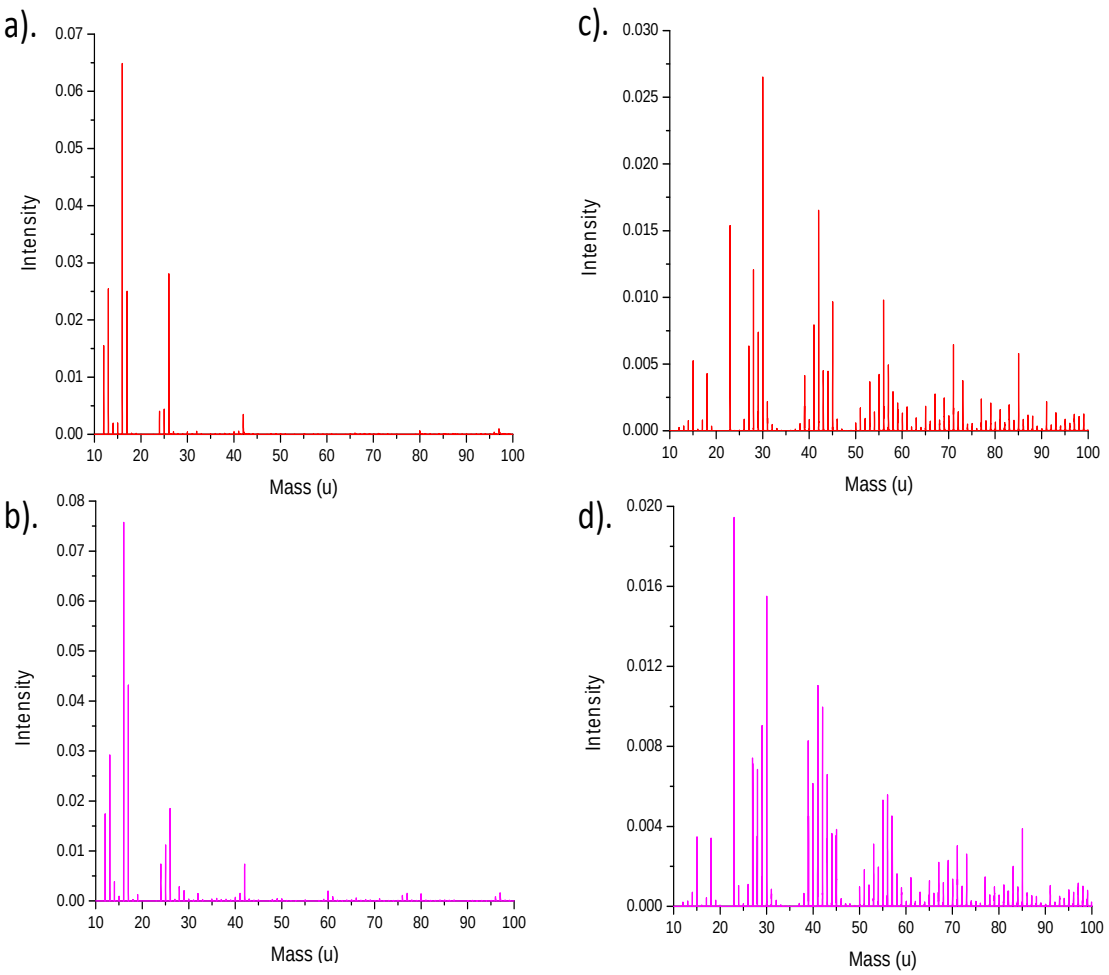

Figure. Appendix. B. 1. TOF-SIMS negative ion spectra of a). glass mat with binder and b). binder treated glass fibers; and TOF-SIMS positive ion spectra of c). glass mat with binder and d). binder treated glass fibers showing similar spectra to confirm the binder treatment of glass fibers with that of the glass mat processing.

Appendix C

Figures C.1, 2 and 3 shows that the side of the glass mat where vacuum suction was applied for removing excess binder did not dictate the surface chemistry. Both sides showed similar binder distribution under confocal microscope and contact angle data showed similar surface sensitivity.

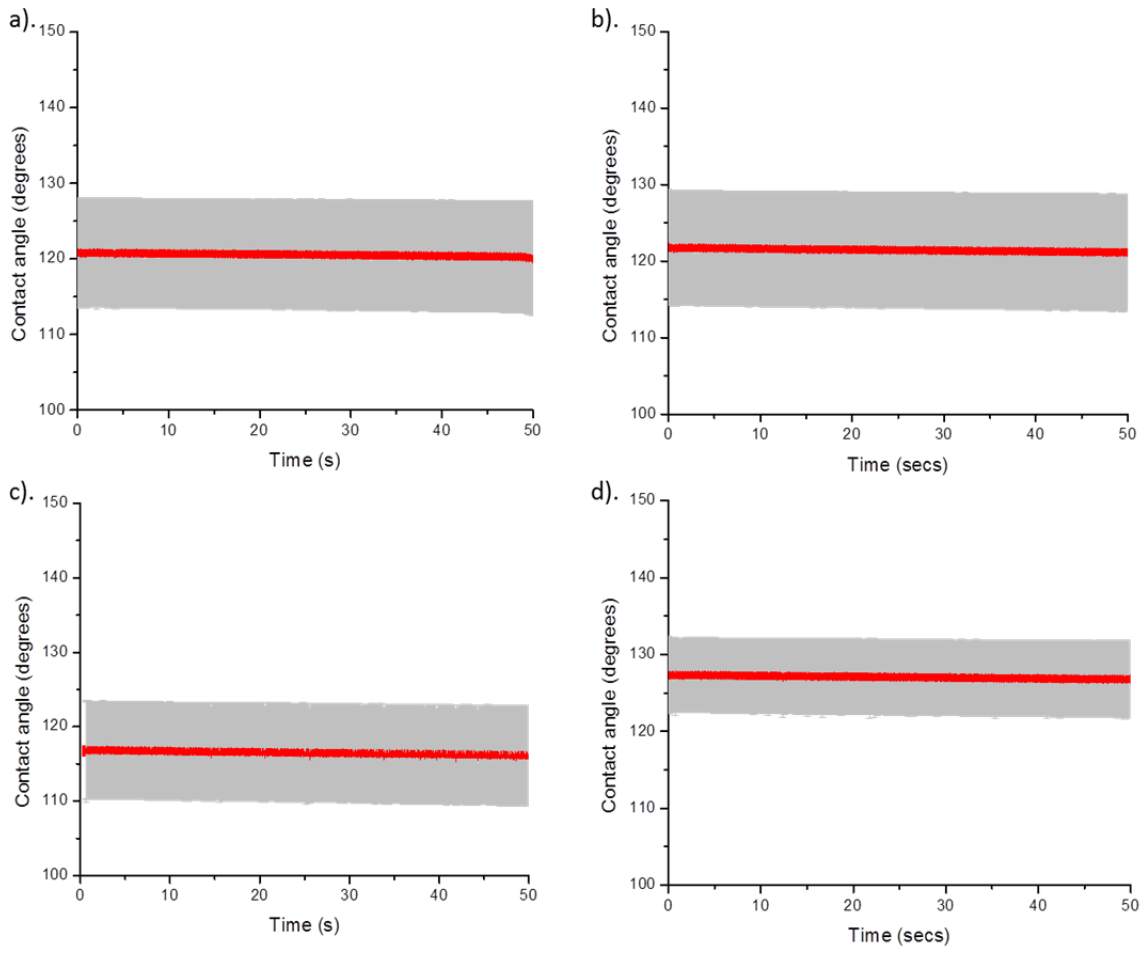

Figure. Appendix. C. 1. Water contact angle (mean – red line; grey – standard deviation) for JM mat with binder a). upper surface, b). bottom surface; and OC mat with binder c). upper surface, d). bottom surface exhibiting very similar contact angles.

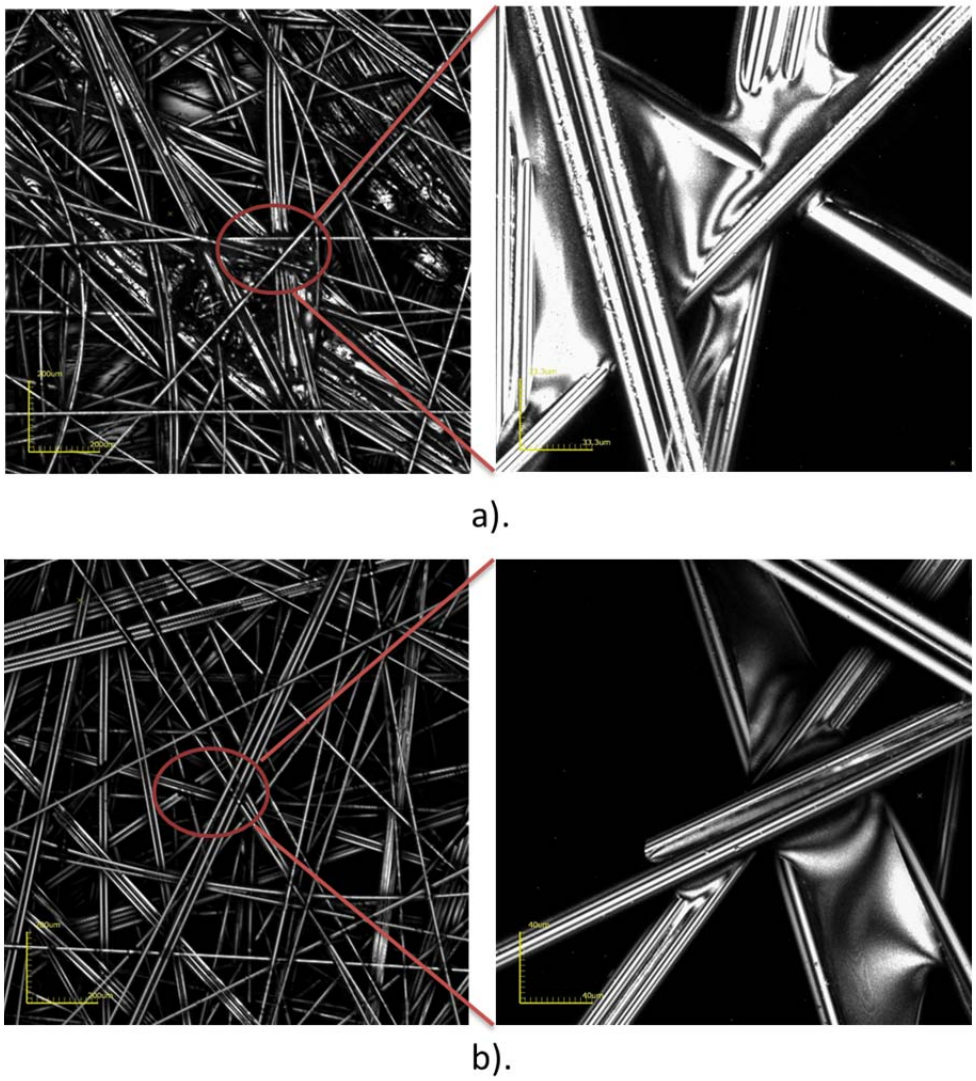

Figure. Appendix. C. 2. Confocal microscope images of OC glass mat with binder from a). upper mat surface and b). bottom mat surface exhibiting very similar binder distribution.

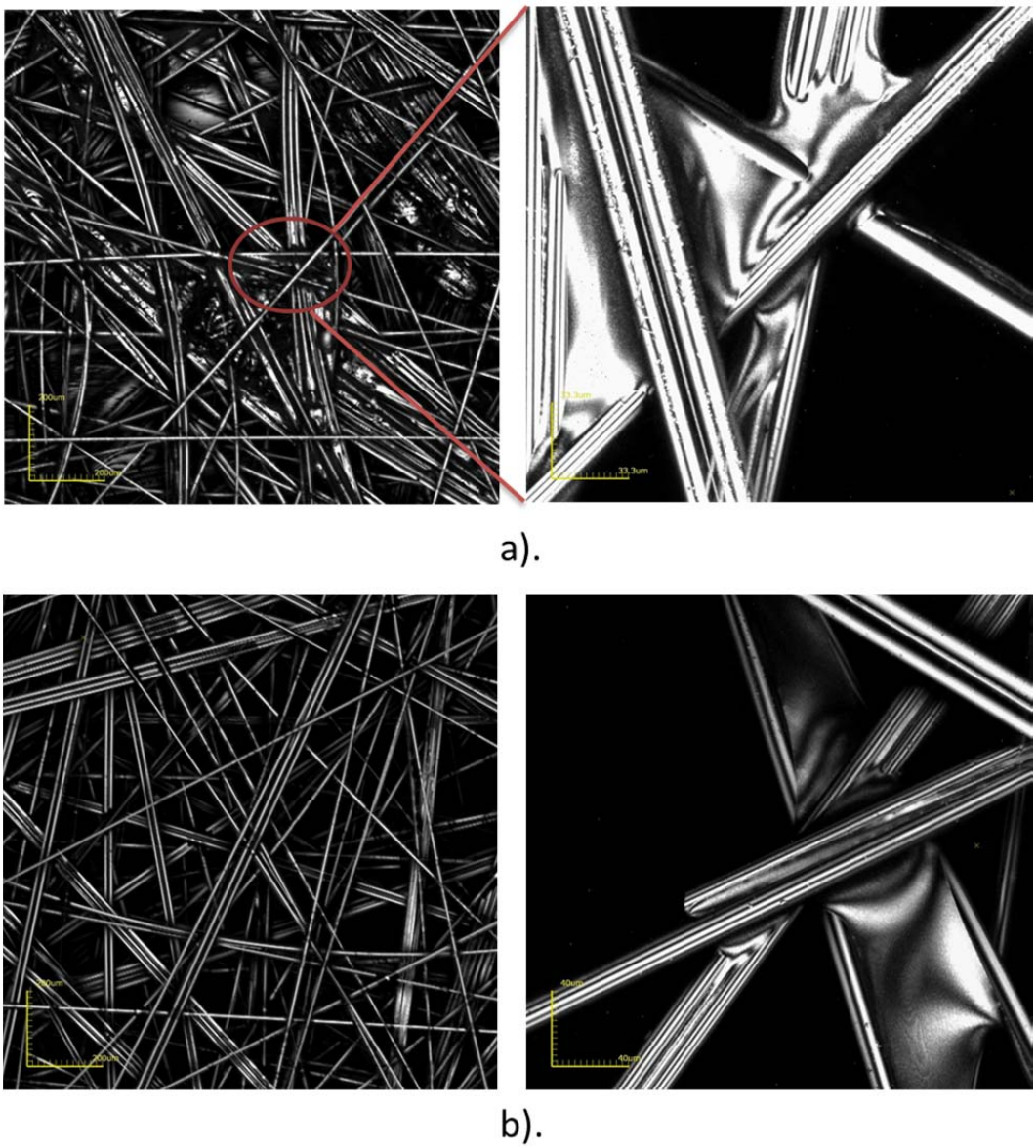

Figure. Appendix. C. 3. Confocal microscope images of JM glass mat with binder from a). upper mat surface and b). bottom mat surface exhibiting very similar binder distribution.